Integrated Modeling and Assessment of North American Forest Carbon Dynamics Technical Report

Tools for monitoring, reporting and projecting forest greenhouse gas emissions and removals

W.A. Kurz, R.A. Birdsey, V.S. Mascorro,
D. Greenberg, Z. Dai, M. Olguín, and R. Colditz

January 2016

Natural Resources Canada
Ressources naturelles Canada
CONAFOR COMISIÓN NACIONAL FORESTAL
FOREST SERVICE USDA DEPARTMENT OF AGRICULTURE
Fortalecimiento REDD+ y cooperación Sur-Sur México - Noruega
cec.org

Please cite as:

> W.A. Kurz, R.A. Birdsey, V.S. Mascorro, D. Greenberg, Z. Dai, M. Olguín, and R. Colditz. 2016. *Integrated Modeling and Assessment of North American Forest Carbon Dynamics Technical Report: Tools for monitoring, reporting and projecting forest greenhouse gas emissions and removals*. Montreal, Canada: Commission for Environmental Cooperation. 125pp.

This report was prepared by W.A. Kurz, R.A. Birdsey, V.S. Mascorro, D. Greenberg, Z. Dai, M. Olguín, and R. Colditz for the Secretariat of the Commission for Environmental Cooperation. The information contained herein is the responsibility of the authors and does not necessarily reflect the views of the CEC, or the governments of Canada, Mexico or the United States of America.

Publication Details

Publication type: Project Report
Publication date: January 2016
Original language: English
Review and quality assurance procedures:
Final Party review: January 2016
QA250

Project: 2013-2014/ Integrated Modeling and Assessment of North American Forest Carbon Dynamics and Climate Change Mitigation Options

Documento informativo, disponible en español

Document d'information disponible en français

Cover photo: US Forest Service

For more information:

Commission for Environmental Cooperation
393, rue St-Jacques Ouest, bureau 200
Montreal (Quebec)
H2Y 1N9 Canada
t 514.350.4300 f 514.350.4314
info@cec.org / www.cec.org

Natural Resources Canada | Ressources naturelles Canada | CONAFOR Comisión Nacional Forestal | Forest Service US Department of Agriculture | Fortalecimiento REDD+ y cooperación Sur-Sur México - Noruega | cec.org

Table of Contents

List of Tables

List of Figures

Abbreviations and Acronyms

AD	activity data
AGB	aboveground biomass
AVHRR	Advanced Very High Resolution Radiometer (NOAA)
Biome-BGC	BioGeochemical Cycles model
BL	baseline scenario
C	carbon
CBM-CFS3	Carbon Budget Model of the Canadian Forest Sector (Version 3)
CCMEO	Canada Centre for Mapping and Earth Observation
CCT	Carbon Calculation Tool
CEC	Commission for Environmental Cooperation
CFS	Canadian Forest Service
CH_4	methane
CL	cropland
CLCL	cropland remaining cropland
CO_2	carbon dioxide
CO_2e	carbon dioxide–equivalent
Conabio	*Comisión Nacional para el Conocimiento y Uso de la Biodiversidad* (National Commission for the Knowledge and Use of Biodiversity) (Mexico)
Conafor	*Comisión Nacional Forestal* (National Forestry Commission) (Mexico)
Corine	Coordination of Information on the Environment (European Union)
CRF	common reporting format
CRM	component ratio method
DBH	diameter at breast height
DL	disturbance losses
DM	disturbance matrix
DNDC	DeNitrification-DeComposition model
DOC	dissolved organic carbon
DOM	dead organic matter

DW	deadwood
EPA	United States Environmental Protection Agency
FAO	Food and Agriculture Organization of the United Nations
FCPF	Forest Carbon Partnership facility
FIA	Forest Inventory and Analysis Program (US Forest Service)
FL	forest land
FLFL	forest land remaining forest land
FMASK	Function of Mask – automated detection of clouds, cloud shadow, snow, water and no data in Landsat images
GDD	accumulated degree-days of plant growth
Gg	gigagram(s) (10^9 grams, or 10^3 megagrams, or one thousand tonnes)
GHG	greenhouse gas
GIS	geographic information system
GL	grassland
GLGL	grassland remaining grassland
GOFC-GOLD	Global Observation of Forest and Land Cover Dynamics (United Nations)
GPP	gross primary production
ha	hectare
HWP	harvested wood product
IR-MAD	Iteratively Reweighted Multivariate Alteration Detection algorithm
INEGI	*Instituto Nacional de Estadística y Geografía* (National Institute for Statistics and Geography) (Mexico)
INFyS	*Inventario Nacional Forestal y de Suelos* (National Forest and Soils Inventory) (Mexico)
InTEC	Integrated Terrestrial Ecosystem carbon-budget model
IPCC	Intergovernmental Panel on Climate Change
JPSS	Joint Polar Satellite System
kg	kilogram
Landsat	Earth-monitoring satellite (United States)
LC/LU	land cover / land use
LEDAPS	Landsat Ecosystem Disturbance Adaptive Processing System (NASA, United States)
LUC	land-use change

MAD-MEX	Monitoring Activity Data for the Mexican REDD+ Program
Mg	megagram(s) (10^6 grams, or one tonne)
MMU	minimum mapping unit
MODIS	Moderate Resolution Imaging Spectroradiometer (NASA, United States)
MRV	monitoring, reporting and verification
MS-D	multi-source, multi-scale disturbance assessment method
N	nitrogen
N_2O	nitrous oxide
n.a.	no data available, or not applicable
NALCMS	North American Land Change Monitoring System
NASA	National Aeronautics and Space Administration (United States)
NBP	net biome production
NCDC	National Climatic Data Center (United States)
NEE	net ecosystem exchange
NEP	net ecosystem production
NLCD	National Land Cover Database (United States)
NOAA	National Oceanic and Atmospheric Administration (United States)
NP	Nez Perce–Clearwater National Forest (United States)
NPP	net primary production
OCMS	organic carbon in mineral soil
OL	other land
OLOL	other land remaining other land
PDF	probability density function
Pg	petagram(s) 10^{15}g, or one billion tonnes
PG	Prince George region of British Columbia (Canada)
PRISM	Parameter Elevation Regression on Independent Slopes Model
Ra	autotrophic respiration
REDD+	Reducing Emissions from Deforestation and Forest Degradation (and Sustainable Forest Management) (United Nations)
Rh	heterotrophic respiration
RS	remote sensing

Sagarpa	*Secretaría de Agricultura, Ganadería, Desarrollo Rural, Pesca y Alimentación* (Ministry of Agriculture, Livestock, Rural Development, Fisheries and Food) (Mexico)
Semarnat	*Secretaría de Medio Ambiente y Recursos Naturales* (Ministry of the Environment and Natural Resources) (Mexico)
SL	settlement
SLSL	settlement remaining settlement
S-NPP	Suomi National Polar-orbiting Partnership
SOC	soil organic carbon pool
SOM	soil organic matter pool
SPOT	*Satellite pour l'Observation de la Terre* (Earth-monitoring satellite) (France)
SPU	spatial unit
TDF	tropical dry forest
TFI	Task Force on Greenhouse Gas Inventories, Intergovernmental Panel on Climate Change
Tg	teragram(s) (10^{12} g, or one million tonnes)
THF	tropical humid forest
UNFCCC	United Nations Framework Convention on Climate Change
US	United States
USAID	United States Agency for International Development
USFS	US Forest Service
VCT	Vegetation Change Tracker algorithm
VIIRS	Visible Infrared Imaging Radiometer Suite
WL	wetland
WLWL	wetland remaining wetland
YP	Yucatan Peninsula (Mexico)

Abstract

The forests of North America play an important role in the global greenhouse gas balance by removing carbon dioxide from the atmosphere, storing it in forest ecosystems and in products manufactured from harvested wood, and providing society with wood for construction, energy and other uses. The objective of this project was to improve and harmonize methods for assessing changes in carbon stocks and causes of change, among the three countries of North America, and to develop tools for the estimation, reporting and projection of past and future forest greenhouse gas balances as affected by natural disturbances, forest management, and land-use change. Such information lays the foundation for the development and quantification of policies and activities aimed at reducing carbon emissions and at enhancing carbon removal from the atmosphere by forests. Examples of such policies include the reduction of emissions from deforestation and forest degradation through sustainable forest management. A focus of this project was the demonstration and testing of computer models for the integrating of data from many different sources, such as forest inventories, ground plot measurements, and remotely-sensed time series of land cover and land-cover change. Two models, the Carbon Budget Model of the Canadian Forest Sector (CBM-CFS3) and the Forest DeNitrification-DeComposition model (DNDC) have been used in three representative landscapes (Yucatan Peninsula, Mexico; Nez Perce–Clearwater National Forest, US; and the Prince George region, Canada) to analyze past and future carbon budgets. The results of this study describe how different remotely-sensed data and processing algorithms affect the mapping and quantification of areas affected by activities such as natural disturbances and harvesting; how to use spatially referenced and spatially explicit data to drive the CBM-CFS3 model; and the capabilities of different models to assess the impacts of various disturbances on productivity and carbon stocks; as well as highlight the basic requirements for using models in assessments of carbon stocks, and make recommendations for future work based on the lessons learned in this project. The Commission for Environmental Cooperation (CEC) has coordinated and partially funded this collaborative project of scientists in Canada, Mexico and the US, involving the three national forest services, other agencies, and universities.

Executive Summary

W.A. Kurz, R.A. Birdsey, V.S. Mascorro, D. Greenberg, M. Olguín, and R. Colditz

Globally, forests are the largest land-based carbon sink, and over the past two decades have removed more than one-quarter of the emissions worldwide from the burning of fossil fuels (Le Quéré et al. 2015; Pan et al. 2011a). The projected future role of forests in the carbon cycle, and the potential impact of climate change mitigation by the forest sector remain highly uncertain (Friedlingstein et al. 2006; IPCC 2014a; Wieder et al. 2015). Therefore, we need a better understanding of the main drivers of forest carbon dynamics and their changes, which include human and natural disturbances, land use and land-use change, as well as climate and environmental changes (Birdsey et al. 2013).

As countries attempt to meet their commitments to greenhouse gas (GHG) emission reduction targets, governments seek to understand better how forests and the forest sector can contribute to climate change mitigation. This understanding is improved, first, by quantifying current drivers of emissions and removals, and, second, by identifying and quantifying which changes in human activities reduce emissions or increase forest sinks, relative to a baseline or a reference period (Lemprière et al. 2013).

This project was initiated by the three national forest services of North America, with support from the Commission for Environmental Cooperation (CEC) and other sponsors. The trilateral research cooperation involved experts from multiple agencies and institutions in the three countries. This research contributes to the development of science-based decision support models that quantify the impacts of alternative forest and land management options on the carbon balance of North American forests.

The fundamental principles of forest carbon dynamics apply to all forest ecosystem types but the responsible drivers and their impacts on GHG sources and sinks across diverse geographical regions and over time can differ greatly. Science-based models can inform policy by quantifying the past and future impacts of human activities on GHG emissions and removals and by assessing the effectiveness of climate change mitigation strategies designed to reduce GHG sources or increase sinks.

The primary focus of this project has been on improving forest-sector GHG assessments, through the use of analytical tools that integrate data from forest inventories, ground-plot measurements and intensive site studies, soil carbon measurements, and remote sensing of land-cover and its changes over time. We examined both empirical and process models and developed methods to use new remote sensing products, such as annual time-series analysis of land-cover change at 30-meter resolution, as spatially explicit input to models that estimate annual GHG emissions and removals. We demonstrate the use of such models in the analysis of past and projected future scenarios of GHG emissions. Finally, we provide examples of how these models can support the analysis of mitigation policies aimed at reducing GHG emissions or increasing GHG removals through changes in forest management, and reducing deforestation and forest degradation.

The approaches to estimating national GHG emissions and removals vary among the three countries of North America, because of differences in the available data, tools and other national circumstances. While all three countries follow methods defined by the Intergovernmental Panel on Climate Change (IPCC), this project seeks to harmonize the different scientific approaches. We demonstrate the use of IPCC Tier 3 methods that use empirical or process-based models to integrate data from a variety of sources, and apply these models to three selected regions: the Yucatan Peninsula (YP) in Mexico, the Nez Perce–Clearwater National Forest (NP) in Idaho, US, and the Prince George region (PG) of British Columbia, Canada. For the estimation of GHG emissions and removals, both modeling approaches clearly demonstrate the importance of "activity data," i.e., the information on area annually affected by natural and human disturbances, including harvesting and land-use change and in particular, deforestation, which is defined as the conversion of forest to non-forest land uses.

In this study, we predominantly used two forest carbon dynamics models to integrate data from many different sources for the estimation of GHG balances: the Carbon Budget Model of the Canadian Forest Sector (CBM-CFS3) and the Forest DeNitrification-DeComposition model (DNDC). The CBM-CFS3 relies heavily on empirical measurements obtained from forest inventories (to describe the initial distribution of forest types and their ages) and growth and yield (to quantify growth rates of different forest types). The CBM-CFS3 uses process-based modeling for the quantification of carbon dynamics in dead organic matter (litter and deadwood) and soil carbon pools (Kurz et al. 2009). The CBM-CFS3 can operate with spatially explicit (map-based) or spatially referenced (table-based) activity data. It is compliant with IPCC guidelines, reports on the five required carbon pools, and reports results that include the transitions among the land-use categories defined by the United Nations Framework Convention on Climate Change (UNFCCC). The model operates in annual time steps, and runs relatively fast, which enables the efficient analysis of multiple projected future scenarios and the exploration of mitigation options. Such scenarios can evaluate the impacts of changes in growth and decomposition rates, disturbance rates, forest management, and land-use change.

Process models such as DNDC simulate forest growth, as well as the dynamics of dead organic matter and soil carbon, by using information on soil, plant, climate and environmental conditions (Li et al. 2000; Stange et al. 2000). DNDC requires a very large amount of input data about the ecosystem, the tree species, and soil information for five vertical layers, as well as daily climate information. It operates in daily time steps and therefore individual runs can take many days to weeks, depending on the size of the landscape and the time period of the analysis. While it is not practical to use such a model at high spatial resolution for large geographic regions, we demonstrate here that the primary strength of process-based models, once calibrated and validated, is their ability to generate estimates of biomass carbon stocks that are in close agreement with observed values and that can then be used to simulate how different kinds of disturbances have affected or may affect forest carbon stocks. Another use of process models driven by climate and environmental variables (such as atmospheric CO_2 concentration) is their ability to simulate ecosystem responses to future climate changes, which are illustrated in this report.

Analyses of GHG emissions in forest ecosystems require detailed information on the initial conditions of the landscape, including the extent, type and age (or time since the last stand-replacing disturbance) of forest ecosystems. Equally important are empirical estimates of how forests grow after disturbances, including detailed accounting of the changes in different carbon pools. Tracking the different carbon pools and transfers among them is a critical element for accurately estimating past and future forest carbon budgets. These values are highly variable among different geographic regions, forest types, and type and intensity of various disturbances. A particular challenge in the tropical forests of the YP is that the forests are uneven aged and are often degraded as a result of recent non-stand-replacing disturbances, which are harder to detect and quantify than stand-replacing disturbances. Generating maps of the initial distribution of forest ages was a challenge in this study because it was difficult to distinguish from forest inventory information whether a plot with low biomass was a young forest or a degraded older stand. Further work will be required to improve the information on the initial forest conditions in these complex forest types, including the initial distribution of biomass and the associated growth rates.

Natural and human disturbances in forests are the key drivers of annual GHG emissions and removals in most forest ecosystems. Therefore, activity data that quantify the rate of natural and human disturbances are important information for the estimation of forest GHG budgets. Remote sensing products are increasingly becoming available that describe land cover at 250-meter, 30-meter or higher resolution, in annual time steps. Methods are being developed to calculate annual land-cover changes through these products (e.g., for Saskatchewan, Canada, see Hermosilla et al. 2015), from which activity data can be derived. Here we developed methods and a tool (Recliner) to use such remote sensing products of annual land-cover change as input to carbon budget models, and tested these in the three selected landscapes in Canada, Mexico, and the US.

We also used the CBM-CFS3 with input data for a single Landsat scene in the YP to evaluate the impacts on estimates of GHG emissions and removals of four different remote sensing and map-derived products of annual land-cover change, each with and without attribution of the changes to specific disturbance types. From the eight spatially explicit simulation runs with the CBM-CFS3 we concluded that uncertainties in GHG estimates can be reduced by:

(1) increasing the spatial resolution of remote sensing products from 250 to 30 meters, because at the higher resolution we can detect more small-patch disturbances common in the YP;
(2) increasing the temporal resolution of land-cover products to one year, because we can detect more disturbances that are followed by rapid regrowth; and
(3) attributing the land-cover change to the disturbance type, because this improves the estimation of the disturbance impact on GHG emissions, including, in the case of fire, non–carbon dioxide (CO_2) GHG emissions such as methane (CH_4) and nitrous dioxide (N_2O), which have much higher global-warming potentials than CO_2.

The large range of GHG emission estimates from the eight land-cover change products highlights that efforts to improve the accuracy of such products, including the identification of disturbance types, can yield substantial reductions in uncertainty of GHG estimates at the regional or national scale.

The study also explored the choice of timing of the remote sensing scenes (dry season vs. peak growing season) and the choice of change-detection algorithms, on the accuracy of land-cover change products. We tested a change detection algorithm (Vegetation Change Tracker—VCT) (Huang et al. 2010) that is well established and successful in temperate forest ecosystems. Unfortunately, due to cloud cover and lack of suitable imagery for some years, it failed to detect some significant disturbances particularly during the year 2009 of the simulation period, whereas the Hansen et al. algorithm (Hansen et al. 2013), which makes use of all available cloud-free pixels, was able to detect these disturbances. Results also showed that time series of land-cover changes derived from NASA's Moderate Resolution Imaging Spectroradiometer (MODIS) detected significantly fewer disturbances than the three other methods tested, all of which used higher-resolution Landsat imagery. Improved methods to remotely detect disturbances in persistently cloudy regions is a high-priority research issue for Mexico.

We examined the impacts on GHG estimates and trade-offs between the choice of spatially explicit and spatially referenced activity data. Spatially explicit approaches (IPCC Reporting Method 2, IPCC 2003, 2006) identify the location of every polygon (or pixel) in a landscape. In contrast, spatially referenced approaches (IPPC Reporting Method 1, ibid.) identify the geographic boundaries of land areas, such as management units, to which all data are referenced. Thus it can be known that a spatial unit contains X hectares (ha) of a particular forest type, but the exact location(s) of the forest type within the spatial unit is unknown. Spatially referenced input data, such as rates of firewood collection or other activities that are not readily mapped, require rule-based information in order to allocate these activities to the appropriate polygon or pixel.

Process-based models such as DNDC currently cannot use spatially referenced data, and the CBM-CFS3 is limited to using either spatially referenced or spatially explicit data sources—it cannot combine the two types of input data in one simulation. Spatially referenced approaches greatly reduce the volume of input data, and are more conducive for analyses of future scenarios as they do not require spatially explicit forecasts of the location of future disturbances or human activities such as deforestation.

We evaluated the differences of GHG estimates derived from spatially referenced and spatially explicit simulations. We compared cumulative GHG emission estimates, obtained from a single spatially explicit simulation, with several sets of 400 spatially referenced simulations, for the NP forest in Idaho, US. The uncertainties in GHG estimates obtained from spatially referenced simulations decreased when there were increasing constraints on the eligibility of forest stands for selection, by each disturbance type. However, with increasingly stringent rules, the number of stands that were repeatedly disturbed increased. These repeat disturbances in the spatially referenced simulations introduced a bias in estimates compared to the spatially explicit simulations because emissions resulting from second and subsequent disturbances in the same stands are lower. Adding a rule to prevent repeat disturbances in the spatially referenced simulations reduced the bias, but changed the sign of the bias because in reality, a few repeat disturbances were observed in the spatially explicit simulations. Thus, rule sets that are used to implement spatially referenced data in simulations of GHG estimates need to consider both the eligibility of stands and the amount of repeat disturbances in the same stands. The study demonstrated that, with the appropriate rule sets, spatially

referenced activity data can be used in the CBM-CFS to quantify past GHG emission and removal estimates and to simulate scenarios of future forest management and land-use change scenarios.

We used the process model DNDC to estimate the impact of different kinds of disturbances on carbon stocks of different pools. After calibrating and validating DNDC using independent data from field observations, we simulated the effects of fire, hurricane, harvest, and combinations of these disturbances. At each site, these disturbances showed significant losses of stored carbon immediately following the event, after which stocks began to recover quickly. In the YP, the simulated category 4 (severe) hurricane caused a significant loss of about 86% of the live biomass, 70% of which was assumed to be salvaged and the remainder added to woody debris and soil carbon pools. Biomass added to dead organic matter pools decomposed quickly in the tropical climate of the YP. Disturbances in temperate and boreal forests also have profound effects that last for decades. For the NP, harvests during 1991–2011 removed about 763.5 Gg C from the aboveground biomass; however, other disturbances caused a larger loss of live trees than harvest in the same period—about 4131 Gg C of live, aboveground biomass were lost to fires and insects, and most of the live biomass was transferred to deadwood pools. These disturbances also left a large amount of dead roots in the soils of the forest, which produced a subsequent increase in soil CO_2 flux due to decomposition (heterotrophic respiration). Fires caused significant loss of litter carbon, over 10 Mg C ha^{-1} at the locations where canopy fires occurred.

We also used DNDC to simulate the expected effects of selected climate changes and increases in atmospheric CO_2 concentrations, which may affect future forest productivity and significantly affect projected changes in carbon stocks. In the YP we found significant relationships between biomass stocks and both temperature and precipitation. Based on climate variability in the last 33 years (1981–2013), DNDC projected that carbon storage in moist forests could increase with an increase in temperature in the YP. However, biomass carbon storage in dry forest could decrease with an increase in temperature. Biomass carbon could increase by a large amount with an increase in precipitation in moist forests, and by a much smaller amount in dry forests. In the NP forest, DNDC suggested that biomass increases with increasing temperature, and decreases with increasing precipitation, although these relationships were inconsistent for different forest types.

Using the CBM-CFS3 in a spatially referenced approach, we conducted analyses of the historic and projected future carbon balance for the entire Yucatan Peninsula, stratified into six spatial units. We used the spatial framework that was developed for national-scale analyses in Mexico (94 spatial units) and simulated six spatial units in the YP which result from the intersection of the boundaries of three states and two ecoregions (Level 1, CEC 1997). We developed estimates of annual activity data from land-use change matrices that were derived by comparing land-cover maps for the periods 1993–2002, 2002–2007 and 2007–2011. We estimated the contribution of disturbances (fires) and land-use change to the GHG balance of the entire YP and the results showed a small annual carbon sink that diminished over time as the total forest area decreased due to net deforestation, the growth rate of the remaining forests decreased with age, and the emissions per hectare deforested increased with increasing forest age. We also documented the contribution of the three main land-use categories to the overall GHG balance of the peninsula. We estimated the average GHG fluxes from 2001 to 2010 to be: Forest Land remaining Forest Land (a big sink; -52 Tg CO_2e yr^{-1}), Forest Land converted to

Other Land (a medium source; 27 Tg CO_2e yr^{-1}), and Other Land converted to Forest Land (a small sink; -8 Tg CO_2e yr^{-1}). However, it is likely that the overall GHG balance of the peninsula will approach zero as additional more-complex and finer-scale disturbances (i.e., degradation) are included in the analysis (Olguín et al. 2015).

Future mitigation efforts, including the reduction of emissions from REDD+ (Reducing Emissions from Deforestation and Forest Degradation [and Sustainable Forest Management]) activities, are evaluated against a reference level or baseline. We evaluated two possible methods to define such a baseline: the average emissions over the past decade, or the emissions resulting from average activities over the past decade. We demonstrated that the results differ greatly. In the first approach the annual sink is assumed to remain the same, while in reality (as represented by the second approach) the sink decreases as the cumulative impacts of deforestation reduce the forest area and thus reduce the capacity of the overall area to absorb atmospheric CO_2.

We also demonstrated the use of the CBM-CFS3 for the estimation of changes in emission resulting from changes in future deforestation rates in the YP. The annual gross deforestation rate is estimated to be about 0.6% yr^{-1} from 2001 to 2010 and we simulated a second scenario in which that rate was reduced by 2.5% yr^{-1}. We estimated that, relative to the REDD+ baseline defined by average activity data, net GHG emissions from deforestation can be reduced by 16% in 2020 if the gross deforestation rate is reduced by 25% in 2020, or these emissions can be reduced by 41% in 2030 if deforestation can be cut in half by 2030. It is important to note that selecting the REDD+ baseline defined by past average emissions would result in an accounted increase in emissions (relative to the baseline) even when the deforestation rates are reduced.

We compared selected results from the different modeling approaches with each other and with available data sets, to improve understanding of the ecosystem responses to perturbations and to highlight some uncertainties about how forests will respond in the future, as a result of anthropogenic or natural factors. In practice, empirical models are well suited to representing carbon stock changes of the different carbon pools due to impacts from management activities, fires, insects, and land-use change; to quantifying the uncertainty of directly measured carbon pools; and to validating the independent estimates from process models. Process models are more useful for simulating forest ecosystem response to changes in climate or the concentration of atmospheric CO_2, and may be used to make estimates or projections outside the spatial and temporal boundaries of the data used for parameterization. It is important to validate models with independent data sets before attempting to use them outside the range of parameterization data.

Comparing results of the two models revealed that a high level of analytical skills may be required to use empirical and process models, since both classes of model usually require significant efforts for acquiring and managing the input data—which may not be readily available, representative of the region or forest type of interest, or properly prepared for the model. As a general rule, empirical models are easier to understand whereas process models usually involve detailed representation of mechanisms and their responses to environmental drivers, which should be well understood by the modeler. Model comparisons are exceedingly difficult to perform. Different models have different data requirements, may or may not be spatially explicit, may include representation of different environmental drivers, and may use different definitions of variables. Estimates of key variables, such

as net primary production (NPP), net ecosystem production (NEP) and net biome production (NBP), are significantly different among modeling approaches, and the causes of these differences are hard to interpret. Sorting out these differences is labor-intensive, and was beyond the scope of this project.

We concluded that Tier 3 models are powerful and flexible tools for the integration of data from multiple sources. They can generate the data required for regional and national estimates of GHG emissions and removals in the forest sector: the CBM-CFS3 has been used since 2006 to generate the input data for Canada's national GHG inventory report (Stinson et al. 2011; Environment Canada 2015) and it has been used to estimate reference emission levels for Mexico's submission to the Emission Reductions Program Idea Note, of the Forest Carbon Partnership Facility (FCPF 2013). We also demonstrated some of the abilities of process models to enhance the analysis of, validate results of, and estimate ecosystem responses to climate change.

Conclusion

The results of this study contribute to the desired outcome of improved design and assessment of climate change mitigation activities aimed at sustainable forest management and REDD+ activities in the forest and land-cover change sector in North America. This study revealed some issues and opportunities in data availability and modeling applications that could improve results, and these lessons learned will help guide additional work to improve forest greenhouse gas assessment at different scales. Future CEC-funded work will focus on the use of these tools for the analysis of climate change mitigation options in the forest sector in representative landscapes of North America. Analyses of mitigation options will require that additional analytical capabilities and supporting data are developed, because such analyses require an assessment of changes in forest carbon stocks, changes in harvested wood product carbon stocks, and the changes in emissions in other sectors resulting from the substitution of emissions-intensive products such as concrete, steel and plastics with harvested wood products (Lemprière et al. 2013), as demonstrated for national-scale analyses in Canada (Smyth et al. 2014). Work will also continue on the development and testing of approaches to improving remote sensing products of land-cover change and the integration of such products with models of GHG emissions and removals.

Acknowledgments

The success of this project is the result of the cooperation of many experts in key institutions in Canada, Mexico and the United States. We thank the Commission for Environmental Cooperation (CEC) for project funding and for its assistance in administration, coordination and organization of the work: Karen Richardson, Itzia Sandoval, and Sarah Heiberg provided great support.

We thank the three North American Forest Services (*Comisión Nacional Forestal (*Conafor), Canadian Forest Service, and US Forest Service) for in-kind support of the project and we thank remote sensing and other governmental agencies including *Comisión Nacional para el Conocimiento y Uso de la Biodiversidad* (Conabio), Canada Centre for Mapping and Earth Observation, United States Geological Service and the US National Aeronautics and Space Administration). Many other programs and institutions contributed to this work. From Mexico we acknowledge the collaboration and support from Conafor's project Reinforcing REDD+ and South-South Cooperation, and the *Colegio de Postgraduados*. From the U.S., we greatly appreciate the substantial contribution of funds from the Agency for International Development, the US Forest Service International Program Office, and the SilvaCarbon program, all of which supported participation by scientists and technicians from agencies and institutions in the US and Mexico.

We also acknowledge the contributions of the following individuals:

Graham Stinson, Sally Tinis, Dennis Paradine and Don Leckie (Canadian Forest Service) developed the land-cover change datasets that supported the modeling of the Prince George region in Canada. Alexa Dugan (US Forest Service) provided datasets, information about US forests, and process model results for the US forest used in the case study. Craig Wayson (US Forest Service) provided support in the development of activity data and estimating the impacts of activities on forest carbon. Shannon Franks and Jeff Masek (NASA) contributed the data on forest disturbances for Mexico. Gregorio Ángeles-Pérez (*Colegio de Postgraduados*) helped to estimate the impacts of different activities on forest carbon.

1. Introduction

W.A. Kurz, R.A. Birdsey, and V.S. Mascorro

Globally, forests are the largest land-based carbon sink and over the past two decades have removed more than one-quarter of the emissions from the burning of fossil fuels. However, the projected future role of forests in the carbon cycle remains highly uncertain (Friedlingstein et al. 2006; IPCC 2014a; Wieder et al. 2015), and there are opportunities for countries to engage in activities that can help sustain or increase the global forest carbon sink (Canadell and Schulze 2014). Therefore we need a better understanding of the main drivers of forest carbon dynamics, and in particular we need a better understanding of the main drivers of change—which include human and natural disturbances, land use and land-use change—and the future responses of forests to climate and global environmental changes (Birdsey et al. 2013).

As countries attempt to meet their commitments to greenhouse gas (GHG) emission reduction targets, governments seek to understand better how forests and the forest sector can contribute to climate change mitigation. This understanding is improved, first, by quantifying current drivers of emissions and removals, and second, by identifying and quantifying which changes in human activities reduce emissions or increase forest sinks relative to a (projected or historic) baseline (or reference level) (Lemprière et al. 2013). Examples of activities that can contribute effectively to reductions in net GHG emissions include reducing rates of deforestation (the conversion of forest to non-forest land uses), reducing or eliminating forest degradation, increasing removals of atmospheric carbon by forests through land management (e.g., reforestation or afforestation), and increasing use of harvested wood products to retain carbon and to substitute for other emissions-intensive materials such as concrete, steel and plastics (Pérez-García et al. 2005; Schlamadinger and Marland 1996; Skog 2008; Smyth et al. 2014; Werner et al. 2010).

This project was initiated by the three Forest Services of North America and supported by the trinational Commission for Environmental Cooperation (CEC). It contributes to the development of science-based models, data, and tools that can quantify the impacts of alternative forest and land management options on the carbon balance of North American forests. Such tools are developed with the goals to improve the understanding of forests' contribution to regional and national GHG budgets and to support future policy and management decisions about climate change mitigation activities. The project is part of the Climate Change–Air Quality cluster of CEC projects that supports work on measuring emissions and quantifying carbon sinks, mapping ecosystem carbon, and developing approaches to mitigating black carbon. The CEC funded large parts of this research, and additional financial and in-kind contributions came from United States Agency for International Development (USAID) bilateral and SilvaCarbon programs, Conafor's Reinforcing REDD+ and South-South Cooperation project, the Canadian Forest Service, and other collaborating agencies and institutions in the three countries. The CEC also played an additional important role by assisting the coordination of the research across the three countries.

The fundamental principles of forest carbon dynamics apply to all forest ecosystem types, but the responsible drivers and the distribution of GHG sources and sinks across diverse geographical regions and over time can differ greatly. For example, degradation and conversion of forests to other land uses is the largest contributor to carbon emissions from forests in Mexico; natural disturbances cause large sources in

some regions of the US and Canada; and actively growing young forests contribute to carbon sinks in all of North America.

Science-based models can inform policy by quantifying the past and future impacts of human activities on GHG emissions and removals and by assessing the effectiveness of climate change mitigation strategies designed to reduce GHG sources or increase sinks. Such tools can be used to simulate alternative scenarios of mitigation activities. The results of such scenario analyses can identify and evaluate the potential of various forest-sector activities to contribute toward national GHG emission reduction targets in Canada, the US and Mexico, including initiatives aimed at reducing emissions from deforestation and degradation—e.g., REDD+. (The "+" identifies additional components added in 2010 to represent conservation of forest carbon stocks, sustainable management of forests, and enhancement of forest carbon stocks.)

This report synthesizes results and the improved understanding of forest carbon dynamics rising from trilateral research cooperation among experts from the three North American Forest Services and from associated agencies. The authors' focus has been on advancement of methods for monitoring and reporting forest-sector GHG emissions, and the development of approaches to integrate large amounts of data from a variety of sources and disciplines into systems that can then be used for the quantification of past GHG emissions and the simulation of future scenarios. We do not seek to develop national-scale estimates, as these are the responsibility of the respective national agencies. Instead, through our research in selected landscapes in Mexico, the US and Canada, we seek to improve the coordination and integration of activities and the resulting products in support of forest-sector GHG estimation in North America. Of particular interest has been the development of methods to use newly available remote sensing products as input to ecosystem and carbon-budget models that estimate GHG emissions and removals in response to land management activities as well as to natural and human disturbances. The CEC also supports the North American Land Change Monitoring System (NALCMS), which produces time series of land-cover change products for North America (< http://www.cec.org/tools-and-resources/north-american-environmental-atlas/land-cover-and-land-cover-change >). These and related products from other agencies provide new opportunities to reduce uncertainties in North American forest carbon dynamics estimates. However, at the start of this project, tools that can use these remote sensing products to improve GHG estimates did not exist or were in the early stages of development. Examples describing the approaches and the application of these tools in Mexico, the US and Canada are included in this report.

The report provides an overview of the approaches to forest GHG estimation and reporting and outlines the importance of an integrated systems approach that combines data, methods and models from multiple sources, to derive estimates of forest GHG balances, their changes over time, and the main drivers of change. It provides examples of regional applications of tools to develop GHG emissions and removal estimates, and highlights the new opportunities and challenges arising from remote sensing-derived land cover-change products. The results of this study contribute to the desired outcome of improved design and assessment of climate change mitigation activities aimed at sustainable forest management, and REDD+ activities in the forest and land-cover change sector in North America.

2. General Concepts of Forest Carbon Estimation and Reporting

W.A. Kurz, V.S. Mascorro and R.A. Birdsey

2.1 Brief overview of the basic principles

The Intergovernmental Panel on Climate Change (IPCC) Task Force on Greenhouse Gas Inventories (TFI) has developed a series of reports and supporting tools for the preparation of GHG inventories (IPCC 2003, 2006, 2014a, 2014b). These include a set of fundamental principles: transparency, consistency, comparability, completeness, accuracy, verifiability and efficiency (IPCC 2000, Table 2.1, <www.ipcc.ch/ipccreports/sres/land_use/index.php?idp=59>). Inventories are also expected to neither over- nor under-estimate GHG emissions and removals, as far as can be judged. Moreover, countries are expected to identify, quantify and reduce, as far as practicable, the uncertainties in their GHG estimates. This requirement encourages a continuous improvement process in the preparation of inventories, which can only be achieved through dedicated programs and sustained teams of experts responsible for the preparation of GHG inventories, using models and other tools to integrate and analyze relevant data from many sources.

Table 2.1 Core principles of an accounting system

Principle	Description
Transparency	The assumptions and methods used in the accounting system should be clearly explained, to facilitate the replication and assessment of the information by its users.
Consistency	The accounting system should be consistent with the scientific principles of carbon processes and the institutional context in which the system is applied (e.g., objectives driving the need for the system), including carbon coverage over space, pools, and time.
Comparability	The information produced should be comparable across Parties and over time. Differences in methods and data should be made transparent so that the numbers are as consistent and comparable as possible.
Completeness	All the sources and sinks that are "applicable" should be accounted for and defined by the provisions of the Kyoto Protocol.
Accuracy	The reported numbers from an accounting system should be valid and accurate. Accurate estimates should be unbiased and should not systematically under- or overstate the true number.
Verifiability	The reported numbers in the accounting system should be verifiable by a third party. They should be built on proper data collection, measurement, and reporting procedures; and based on substantiated data, models, and methods. The location and extent of the land on which the claimed carbon sequestration took place should also be clearly identified, preferably using a consistent geographic information system that would facilitate identification of possible double-counting and the overlay of information used for verification (e.g., remotely-sensed data).
Efficiency	An efficient accounting system should operate at the point where the marginal costs of increased accuracy, precision, and verifiability just equal the marginal benefits of achieving the improvements. When resources are not available to obtain an efficient system, the objective should be to obtain the most effective system given the available resources.

Source: Derived from the IPCC Core Principles (IPCC 2000).

There are three steps in the preparation and use of GHG inventories: *estimating*, *reporting*, and *accounting*.

- Estimating GHG emissions and removals involves the preparation of estimates and their associated uncertainties.
- The reporting of these estimates follows internationally agreed-upon formats such as the common reporting format (CRF) tables.
- Accounting involves the determination of credits and debits, and the assessment of achievements relative to GHG emission reduction targets.

2.2 Five carbon pools in ecosystems (plus harvested wood products)

The IPCC (IPCC 2003, 2006) defines five carbon pools in terrestrial ecosystems: aboveground biomass and belowground biomass, which together make up the biomass pool; litter and deadwood, also called the dead organic matter (DOM) pool; and the soil organic carbon pool (SOC), also known as the soil organic matter (SOM) pool. The five pools are explained more detail in Table 2.2.

Table 2.2 Five ecosystem carbon pools defined by the IPCC

	Pool	Description
Biomass	Aboveground biomass	▪ Includes all the living plants and woody forms above the soil (i.e., trees, shrubs, herbs, stems, stumps, branches, and foliage).
	Belowground biomass	▪ Comprises all biomass of live roots. Live fine roots of less than (suggested) 2 mm diameter are often excluded because they are difficult to measure, but roots can be included in the soil organic matter pool.
Dead Organic Matter (DOM)	Litter	▪ Includes all non-living biomass with a size greater than the limit for soil organic matter e.g., 2 mm) and less than the minimum diameter chosen for deadwood (e.g., 10 cm) downed dead, in various states of decomposition above or within the mineral or organic soil, e.g., detritus of leaves, fruits, flowers, twigs and small branches.
	Deadwood	▪ Comprises all woody debris not included in the litter pool. ▪ Includes all the deadwood on the forest surface, standing dead trees, stumps, dead logs, coarse woody debris and dead roots that have a diameter larger than or equal to 10 cm (suggested).
	Soil organic matter	▪ Includes all organic carbon in mineral soils at the depth of the soil profile limit chosen by the country according to their national specifications. ▪ Live and dead fine roots with diameters less than the suggested limit for belowground biomass (2 mm) can be included when they cannot be distinguished empirically.

Note: mm = millimeter(s); cm = centimeter(s).
Source: Derived from the IPCC guidelines for GHG inventories (IPCC 2006).

Guidelines for the estimation of carbon stocks and stock changes also exist for harvested wood products (HWPs) (IPCC 2006, 2014a). Harvested wood products, including sawn timber, panels, pulp and paper, and related products can store carbon for years to centuries. Understanding carbon storage in and releases

from HWPs is also important for the assessment of forest-sector mitigation options (Lemprière et al. 2013; Smyth et al. 2014). However, carbon stocks in HWPs were beyond the scope of this study.

2.3 Gain-loss and stock change methods for estimating carbon emissions and removals

There are two methods suggested by the IPCC to estimate carbon emissions and removals. The gain-loss (or default) method and the stock change method are briefly described in this section. For both methods, the calculations have to be conducted for each pool, year, and land category. Depending on the size and complexity of the area analyzed, and the level of reporting detail desired, large numbers of calculations have to be made and their uncertainties estimated. Such calculations can be assisted by spreadsheets or models or other forms of analytical frameworks that enable the integration of large amounts of data from a variety of sources.

Gain-loss method

This is the default method provided by the IPCC (IPCC 2003, 2006) and is ideal for situations where an initial inventory is established at the starting year or period for reporting. It calculates the annual balance of carbon stock gains and losses for each pool, and sums across the pools. This method can report interannual variability of emissions and removals, and it allows for attribution of cause of change and of calculation of non–carbon dioxide (non-CO_2) GHG based on activity-specific emissions—e.g., methane (CH_4) and nitrous oxide (N_2O) correlated with area burned. Implementation requires a starting inventory, activity data, and information on ecosystem carbon dynamics, including: growth and mortality rates, stratified by species and forest types; rates of litterfall and biomass turnover; and decomposition rates. The calculation (Figure 2.1) is iterated in annual (or other) time steps.

Figure 2.1 Gain-loss method for estimating carbon emissions and removals

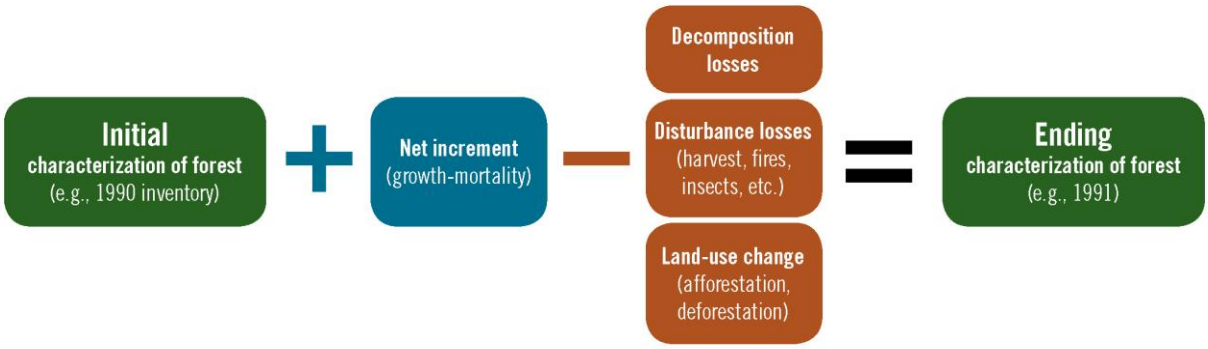

Stock change method

In this method, the difference in carbon stocks between two points in time is calculated, based on starting and ending inventories (Figure 2.2). It requires estimates at both ends of the time series, which is both an advantage for and constraint against the use of this approach in countries that do not have well

established, continuous forest inventories. The main advantage is that an inventory at two (or more) points in time provides an unbiased estimate of the rate of change in carbon stocks over the period. The observed rates of change and the net carbon balance are then averaged over the period of measurements, which leads to the disadvantage that there is no direct calculation of interannual variation in emissions and removals over the observation period, i.e., that the variation over time is necessarily presumed to be linear. Attribution of cause of changes may be limited to variables observed in the inventory process, such as harvesting or mortality, and estimating interannual variability and non-observed causes of change are only possible if additional activity data are available and calculations of gains and losses are made, similarly to the requirements for the gain-loss method.

Figure 2.2 Stock change method for estimating carbon emissions and removals: The difference of carbon stocks between two points in time

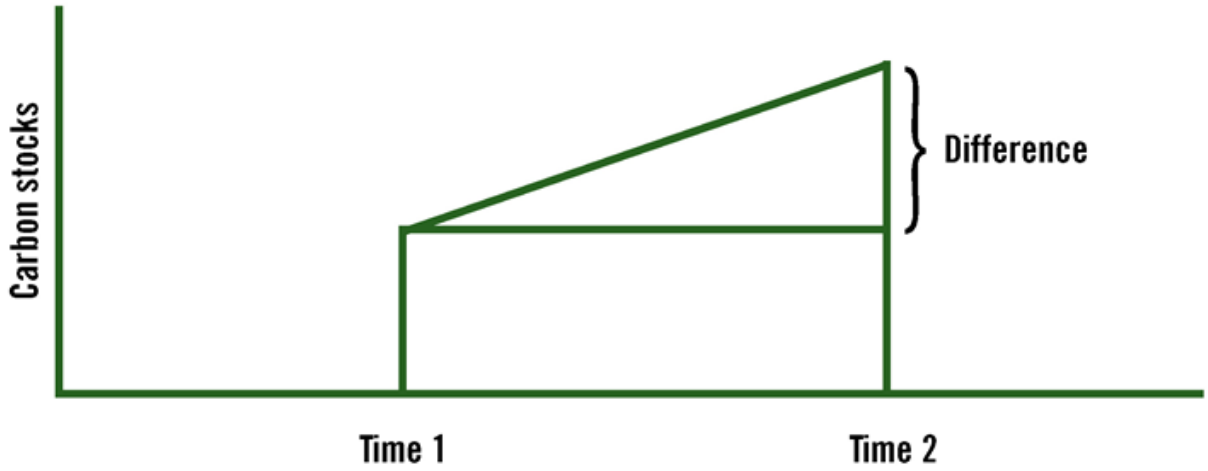

The combined use of both methods allows for further improvements to the estimates. Where repeated inventory measurements are available, these can be used to validate the results obtained with the gain-loss method, and conversely the estimates of annual gains and losses can be used to inform the stock change method about interannual variation in emissions and removals and to improve identification and quantification of the causes of observed changes.

2.4 Carbon budget models

Models of carbon dynamics for terrestrial ecosystems can improve the precision and accuracy of estimates of carbon stocks and stock changes for the forest sector and their response to management, disturbances or climate (GOFC-GOLD 2011; Huntzinger et al. 2012; Kurz et al. 2009). Models enable the quantification of forest carbon dynamics though the synthesis and integration of data from many different sources, including forest inventories, ground plots, and remote sensing (Birdsey et al. 2013; Kurz et al. 2009; Lemay and Kurz 2008; Wulder et al. 2008), and the process of modeling improves understanding of the mechanisms controlling carbon exchanges between the land and the atmosphere. Models may also be used to generate emissions factors, to develop a forward-looking baseline, or to analyze scenarios (e.g.,

management, land-use change, natural disturbances). Models may also help identify gaps in information, and guide future research or monitoring to fill in these gaps in a cost-effective manner (Huntzinger et al. 2012; IPCC 2011; Liu et al. 2011).

Generally, models can be divided into two broad groups: *empirical models*, which use data typically obtained in national forest inventories or other field surveys; and *process models*, which use detailed ecophysiological relationships between plants, soil and atmosphere. However, process models also require information on forest type and distribution, and other data similar to those used in empirical models. The distinction between the two modeling approaches is often blurred, and *hybrid models* that rely on both empirical data and process modeling are common. For example, the CBM-CFS3 model used in this study uses empirical relationships to represent tree growth and mortality, and process modeling to represent the dynamics of dead organic matter and soil for which inventory information is much more limited.

Empirical models

Empirical models use observed variables, such as wood volume and tree biomass, from sample plots and relate these quantities to classification variables, such as stand age and forest type, using an empirically estimated functional relationship, such as described by a regression equation or yield curve. It is relatively straightforward to estimate the uncertainty of estimates from empirical models as long as the data represent the population of interest. Empirical models may not require data of environmental conditions, although the landscape may be partitioned or stratified into domains that represent a range of environmental factors, forest types, activities, or disturbance types. The quality and quantity of observations will have a strong influence on the accuracy of empirical modeling results.

Process-based models

Process-based models simulate the main biophysical and biogeochemical processes in forests, using equations that represent phenology and data describing environmental conditions. Process-based models need a large amount of data related to forest environmental conditions, climatic variability, and soil conditions (Landsberg and Waring 1997; Ojima et al. 1990; Thornton et al. 2005). Like empirical models, process models require information about the domain of interest, such as stand age and forest type. Field observations are always needed to evaluate models and to determine whether they are performing well and the model inputs are proper, especially those parameters related to phenology. The extent to which the simulated processes and the data informing these simulations capture the real-world behavior of the ecosystem will determine the accuracy of process-modeling results.

Some models have both empirical and process characteristics and are considered hybrid models. In order to make more-reliable projections of carbon exchanges between vegetation and the atmosphere, and to determine the magnitude and direction of the response of forest ecosystems to global change, the combination of both modeling approaches may be necessary, taking advantage of the strengths of each (Luo et al. 2011; Stinson et al. 2011).

Models used in this study

In this study, we predominantly used two forest carbon dynamics models. The Carbon Budget Model of the Canadian Forest Sector, version 3 (CBM-CFS3), and the Forest DeNitrification-DeComposition model (DNDC). CBM-CFS3 is a hybrid model that uses empirical data (yield curves derived from forest inventories) to represent tree growth and mortality, activity data on natural and human disturbances to represent drivers of carbon stock changes, and process simulation to link the dynamics of dead organic matter and soil carbon pools to the dynamics of biomass pools (Kurz and Apps 1999; Kurz et al. 2009). The CBM-CFS3 uses forest inventories to describe the initial distribution of forest types and their ages. The CBM-CFS3 primarily operates with spatially referenced (table-based) activity data, but it can and has been used here to operate with spatially explicit (map-based) time series of activity data. The model reports on the five required carbon pools, and reports results that include the transitions among the UNFCCC land-use categories. The model operates in annual time steps, and runs relatively fast, which enables the efficient analysis of multiple projected future scenarios and the exploration of mitigation options.

DNDC is a spatially explicit process model simulating forest growth, carbon and nitrogen dynamics, and emissions of trace gases, based on the balance of water, light, and nutrients in forest ecosystems (Li et al. 2000). It simulates forest growth, as well as the dynamics of dead organic matter and soil carbon, from information on soil, plant, climate and environmental conditions. The model requires a very large amount of input data about the ecosystem, the tree species, and soil information for five vertical layers, as well as daily climate information. The model operates in daily time steps and therefore individual runs can take many days to weeks, depending on the size of the landscape. While not practical to use such a model at high spatial resolution for large geographic regions, we demonstrate in this study that the primary strength of process-based models, once calibrated and validated, is their ability to generate estimates of biomass carbon stocks that are in close agreement with observed values, and then use the model to simulate how different kinds of disturbances have affected or may affect forest carbon stocks. Another use of process models driven by climate and environmental variables (such as atmospheric CO_2 concentration) is their ability to simulate ecosystem responses to future climate changes, which is also illustrated in this report.

2.5 IPCC guidelines for Tiers 1, 2, and 3

The IPCC methodological guidance has introduced three tiers, representing different approaches and methodological complexity that allow countries to prepare GHG inventories according to their national circumstances, such as available data, tools and expertise. Along with the concept of multiple tiers, the IPCC recommends that the development of GHG inventories be a continuing improvement process, in which uncertainties are identified, quantified and reduced as far as is practicable (IPCC 2003). Here we present a brief overview of the main characteristics of the three tiers (IPCC 2006).

Tier 1 methods are designed to be the simplest to use by any country. They deploy simple methods and default parameters provided by the IPCC. Many simplifying assumptions facilitate the development of initial estimates. While it is recommended that country-specific activity data are used, global default values (e.g., for carbon densities of different forest types) can be used when national data are missing.

Tier 2 methods and assumptions are often similar to those of Tier 1 but will always be used with country- or region-specific parameters, emission factors and activity data. Tier 2 methods use higher temporal and spatial resolution activity data that are more disaggregated—for example, to represent a variety of forest types.

Tier 3 methods typically include models and inventory systems tailored to national circumstances and that integrate data from many sources, such as: forest inventory data collected at regular time intervals, data from GIS-based systems, age data, forest productivity data, soils data, and land-use and management activity data. For Tier 3 methods, the IPCC does not specify the details of how these are implemented but provides guidelines for "good practice" in the development, testing and validation of the methods used, (IPCC 2003, 2006, 2011, 2014a). While Tier 3 methods are more complex and expensive to implement, they are expected to yield estimates with lower uncertainties.

2.6 Carbon cycle indicators and activity data

A variety of approaches exists to measure and monitor ecosystem carbon stocks and fluxes at different spatial and temporal scales. It is therefore necessary to define the different components and indicators included in the measurements. To facilitate communication and understanding, here we provide an overview of terms and of components considered in the terrestrial carbon cycle (see Table 2.3).

Carbon stocks define the quantity of carbon in a pool, such as biomass, deadwood, litter or soil, and are usually measured in units of megagrams per hectare (Mg ha^{-1}), or grams per square meter (g m^{-2}). Carbon fluxes are the transfers of carbon between pools, or between pools and the atmosphere or the forest product sector. Fluxes (or transfers) are measured in units of megagrams per hectare per year (Mg ha^{-1} yr^{-1}) or grams per square meter per year (g m^{-2} yr^{-1}). One fundamental principle in developing carbon budgets is the need for conservation of mass, which means that the sum of the fluxes that are reported must be equal to the stock changes over the same time period.

Table 2.3 Overview of indicators considered in the terrestrial carbon cycle

Indicator		Description
GPP	Gross primary production	Carbon (C) uptake during plant photosynthesis
Ra	Autotrophic respiration	Respiration of primary producers (i.e., trees—leaves, stems, roots—released as CO^2 into the atmosphere)
NPP	Net primary production	NPP = GPP - Ra Plant photosynthesis minus the autotrophic respiration of primary producers—the sum of all organic matter produced
Rh	Heterotrophic respiration	Respiration of heterotrophic organisms (animals and microorganisms)
NEP	Net ecosystem production	NEP = NPP – Rh Net change in ecosystem C stocks prior to disturbances
DL	Disturbance losses	Carbon (including CH^4) losses from fires, harvest, and land-use change (activity data)
NBP	Net biome production	NBP = NEP – DL Net change in ecosystem C stocks

GPP - Ra = NPP NPP - Rh = NEP NEP - DL = NBP

Source: Based on Chapin et al. 2006; IPCC 2006; and Schulze and Heimann 1998.

Activity data

Estimates of GHG, inventories, and REDD+ require information about the rates at which natural and human disturbances (DL in Table 2.3) affect the terrestrial carbon cycle. Such observations of the drivers of terrestrial ecosystem change are referred to as activity data. Activity datasets can be map-based (spatially explicit) or table-based (spatially referenced) summaries of observations of natural or human disturbances, changes in forest area, or land conversions between categories. Since natural and anthropogenic disturbances are one of the main drivers that alter the forest structure over time (Lorenz and Lal 2010; Turner 1989), it is critical to characterize land-cover change observations and their agents of change, to accurately quantify their impact on the forest carbon dynamics (Kurz 2010a; Spalding 2009).

2.7 UNFCCC land-use categories and transitions between them

To promote adequate, consistent, complete, and transparent data in order to estimate carbon fluxes and GHG emissions, the IPCC has developed a set of guidelines to represent different land-use categories and conversions between them (IPCC 2006) (Table 2.4).

Table 2.4 Land-use categories

Land-use category		Description
Forest land	FL	Includes all land with woody vegetation consistent with thresholds used to define FL in the national greenhouse gas inventory.
Cropland	CL	Includes cropped land, including rice fields, and agro-forestry systems where the vegetation structure falls below the thresholds used for the FL category.
Grassland	GL	Includes rangelands and pasture land that are not considered CL. ▪ systems with woody vegetation and other non-grass vegetation such as herbs and brushes that fall below the threshold values used in FL ▪ grassland from wild lands to recreational areas, as well as agricultural and silvi-pastural systems, consistent with national definitions
Wetland	WL	Includes areas of peat extraction and land that is covered or saturated by water for all or part of the year (e.g., peatlands) that is not in the FL, CL, GL or SL. ▪ reservoirs as a managed sub-division and natural rivers and lakes as unmanaged sub-divisions
Settlement	SL	Includes all developed land, including transportation infrastructure and human settlements of any size
Other land	OL	Includes bare soil, rock, ice, and all land areas that do not fall into any of the other five categories

Source: IPCC 2006.

According to the IPCC (IPCC 2006), three approaches can be used to estimate activity data for the quantification of GHG emissions and removals, which can be combined for different regions according to the country circumstances:

1. Estimating total area of land categories, without quantifying changes among them.
2. Tracking land conversions between categories (e.g., land-cover change matrix).
3. Spatially explicit monitoring of changes in area or changes between categories, commonly via satellite imagery.

Note that it is often necessary to subdivide these land-use categories in order to reduce uncertainty of estimates or to facilitate reporting requirements. For example, "forest land" may be divided into forest types, ecoregions, and/or administrative regions.

Categories of land-use conversion

- FLFL = forest land remaining as forest land
- GLGL = grassland remaining as grassland
- CLCL = cropland remaining as cropland
- WLWL = wetland remaining as wetland
- SLSL = settlement remaining as settlement
- OLOL = other land remaining as other land

In addition, transitions between land-use categories are also possible, e.g., CLFL = cropland converted to forest land, FLSL = forest land converted to settlement, and so on. The IPCC guidelines further define that after 20 years, lands in a transition category transfer to the main reporting category. For example, afforested cropland (CLFL) will transition to FLFL after 20 years, provided that no further land-use change has occurred.

2.8 Estimating uncertainty and validating results

Two critical steps in providing quantitative estimates of carbon stocks and stock changes are to estimate the uncertainty and to validate results. Although these steps usually require some substantial additional effort, they are important for conveying a sense of accuracy to decision-makers, for assessing confidence in monitoring and modeling that may be used to assign a value to carbon credits, for determining the best ways to improve future estimates, and for quantifying gains from improvements.

Some common sources of uncertainty stem from natural variability, measurement errors, the use of sampling statistics, lack of representativeness and model form, use of parameter estimates, and human errors in data processing. It may be difficult or impossible to quantify and characterize completely all the uncertainties, but measurement error and natural variability (sampling error) are the most rigorously quantified in ecology (Lehrter and Cebrian 2010; Yanai et al. 2010).

It may be challenging to estimate uncertainty even for basic components of the forest carbon budget, such as biomass stock (Wayson et al. 2014); nonetheless, the IPCC strongly encourages countries to pay special attention to estimating uncertainties, including conducting a qualitative assessment of the improvements that can be made in the estimation process, along with potential reductions in uncertainty (IPCC 2000).

A few definitions are important to keep in mind because they may be improperly used. The following definitions of a few common terms are adapted from IPCC (IPCC 2003, 2006):

- **Uncertainty** – A general and imprecise term which refers to the lack of certainty resulting from any causal factor—such as an unidentified source or sink, lack of transparency, or lack of knowledge of the true value of a variable—that can be described as a probability density function (PDF) characterizing the range and likelihood of possible values. Uncertainty depends on the analyst's state of knowledge, which in turn depends on the quality and quantity of applicable data as well as on knowledge of underlying processes and inference methods.
- **Accuracy** – Agreement between the true value and the average of repeated measured observations or estimates of a variable. An accurate measurement or prediction lacks bias; that is, it neither over- nor under-estimates the true value.
- **Precision** – Agreement among repeated measurements of the same variable. Better precision means less random error. Precision is independent of accuracy.

The main approaches to estimating uncertainty for supporting monitoring, reporting and verification (MRV) are described in Birdsey et al. (2013), and include expert opinion, classical, Monte Carlo, and Bayesean methods. Error propagation of the individual component uncertainties is part of the process of

estimating the overall uncertainty in an estimate, and can be done through statistical error propagation—which is only possible if the error structure of the individual components is known—or through the use of Monte Carlo analyses, whereby many model runs or repeat analyses are conducted, with input parameters varied to represent the uncertainty in individual input data. The distribution of results from the repeated model runs or analyses provides a measure of the uncertainty of the estimates (Yanai et al. 2010).

Validation is an important aspect of applying models and assessing their accuracy. Model validation involves comparing the model results with an independent data set representing local conditions. The independent data source is different from the data used to develop or parameterize the model. This step can be very important, especially when the uncertainty analysis does not fully and explicitly account for all of the sources of possible error, which is common when estimating forest carbon budgets because of the many variables and combinations of approaches that are typically used. An example of a validation of the CBM-CFS3 against a large number of completely independent ground plot measurements across Canada was recently completed (Shaw et al. 2014). It demonstrated that overall bias was very low: the model-derived estimate of total ecosystem carbon stocks was within 1% of the observed value but accuracy decreased considerably when the results were examined by ecoregion, tree species or carbon pool.

3. Integrating Data from Multiple Sources into GHG Emissions and Removal Estimates

W.A. Kurz, R.A. Birdsey, V.S. Mascorro, and M. Olguín

In the preceding sections, we outlined the approaches, key input data requirements, and the expected outcomes of greenhouse gas estimation and reporting activities. Here we describe specific examples of the integration of data from multiple sources into internally consistent estimates and time series of GHG emissions and removals.

Central to the successful integration of data for the purpose of estimating GHG emissions and removals are tools that provide a common and transparent framework to integrate data and information across space and time (see Figure 3.1). These tools need to operate within a common spatial framework to ensure that all relevant land areas are included, without gaps or overlaps.

Figure 3.1 Carbon dynamics model: Integrating data from multiple sources, using input requirements of CBM-CFS3 as example

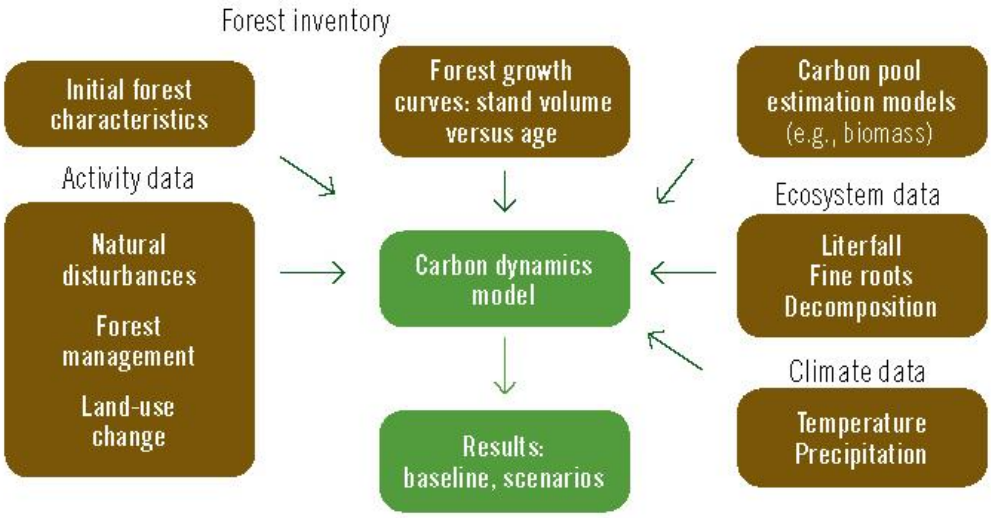

3.1 Spatial framework

In terrestrial carbon budgets, the stocks and fluxes at the regional and national scale are the sum of the stocks and fluxes at smaller spatial levels. Thus, national-scale estimates of forest GHG emissions and removals can be calculated as the sum of entity-level, state-level or province-level stocks and fluxes, which in turn are the sum of fluxes of the counties or management units within states or provinces, which again are the sum of the estimates at the stand, polygon or pixel levels (Figure 3.2).

Figure 3.2 Spatial hierarchy for estimation of terrestrial carbon dynamics

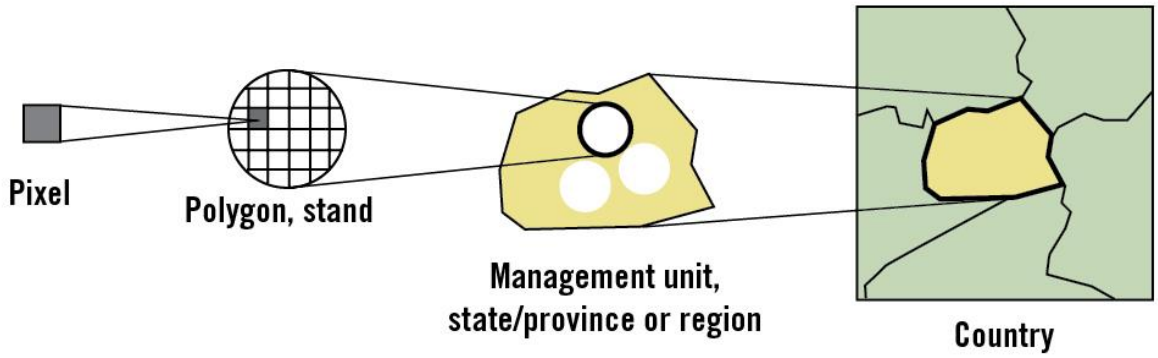

Note: Areas in the hierarchy should provide complete, non-overlapping coverage. Depending on data availability, either spatially explicit or spatially referenced approaches can be developed.

Spatially explicit approaches (see IPCC reporting method 2, IPCC 2003, 2006) identify the location of every polygon (or pixel) in a landscape. In contrast, spatially referenced approaches (reporting method 1) identify the geographic boundaries of land areas, such as management units, to which all data are referenced. Thus, it is known that a spatial unit contains X ha of a particular forest type, but the exact location of such forest within the spatial unit is unknown. Spatially referenced input data, such as rates of firewood collection, or other activities that are not readily mapped, require rule-based information in order to allocate these activities to the appropriate polygons (stands) or pixels.

Spatially explicit and spatially referenced approaches to the estimation of forest carbon dynamics have different requirements for the type and volume of input data. In a spatially explicit approach, all required data layers need to be provided in map form, using a common reference system. Pixel (grid) and vector-based approaches are readily converted from one form to the other. In a spatially referenced approach, spatial units are defined by their geographic boundaries and could be forest management units or other administrative or ecological entities. All information about the forest, other land categories, and activity data is summarized for each spatial unit. However, the location of each polygon or disturbance event within the spatial unit is not known. Existing, spatially explicit information can be re-processed and summarized into spatially referenced information, but the inverse is not possible. Therefore, spatially referenced summary information about past (or projected future) disturbances, such as the number of hectares burned per year and spatial unit, cannot be spatially-distributed to individual polygons or pixels without additional information. A rule-based approach can be used to allocate the known disturbances to the polygons in the forest inventory. Examples of such rule-based approaches include specifications of which polygons are eligible for harvest, insect disturbances, or fire. Rules could be species- and age-specific (harvest, insects) or they can be random (fire), provided that some minimum criteria of fuel load have been met (see section 5.2).

National-scale spatial frameworks are typically based on the intersection of administrative boundaries (Provinces or Territories in Canada, States in the US and Mexico) and ecological classification (ecological regions of North America, CEC 1997; or country-specific forest type classifications). In Canada, the National Forest Carbon Monitoring, Accounting and Reporting System (NFCMARS) (Kurz

and Apps 2006; Stinson et al. 2011) includes 60 reconciliation units (intersection of administrative and ecological boundaries), and over 600 spatial units defined by the boundaries of forest management units, parks or other entities that are recognized as spatial units and for which forest inventory information is compiled and spatially referenced to the geographic boundaries of these spatial units. For the work conducted by this project in Mexico, we intersected the administrative boundaries of 32 states with the ecological boundaries of terrestrial ecological zones level I (CEC 1997) to obtain a total of 94 spatial units (see Figure 7.1). Greenhouse gas inventory statistics in the US are developed and reported by state boundaries, forest types, and ownership categories, such as federal, state, and private (US EPA 2014). Spatially explicit estimates are developed for specific projects, such as a silvicultural treatment of a particular area in a national forest, or a project that participates in a greenhouse gas registry such as the Climate Action Reserve in California (Climate Action Reserve 2013).

In this study, we demonstrate the use of IPCC Tier 3 methods that use carbon budget models to integrate data from a variety of sources, and apply these models to three selected regions: the Yucatan Peninsula (YP) in Mexico, the Nez Perce–Clearwater National Forest (NP) in Idaho, US, and the Prince George region (PG) of British Columbia, Canada (see Figure 3.3).

Figure 3.3 Selected regions for this study: The Yucatan Peninsula in Mexico, the Nez Perce–Clearwater National Forest in Idaho, US, and the Prince George region of British Columbia, Canada

Note: Yellow area corresponds to the entire Yucatan Peninsula, and the blue shows the study area corresponding to the Landsat scene path/row 20/46.

3.2 Initial forest conditions (forest area, by stratum, forest age)

Both the stock change and gain-loss methods for estimating GHG emissions and removals in forests require an initial forest inventory. The model used to conduct the analyses determines the input data requirements. For the CBM-CFS3, the analysis area is first stratified into spatial units (see previous section), and within each spatial unit the forests are further stratified using a set of up to 10 classifiers defined by the user. These classifiers typically include forest type, leading species, site productivity class, and other categories required to select the appropriate yield curve (see next section). Other classifiers can be used to refine rules for the allocation of disturbances, such as whether or not land is eligible for timber harvest (managed, parks, private) or for reporting purposes (ownership, county). Conceptually similar stratifications are used in the US or are being developed for use in Mexico.

Stand-level carbon dynamics are strongly affected by the time since last disturbance. In even-aged forests that regrow following a stand-replacing disturbance such as harvest or fire, growth curves can define biomass increment over time (see next section). In uneven-aged stands, the relationships between forest growth and stand age are less well defined, but disturbances and post-disturbance recovery do affect carbon dynamics of different carbon pools in similar ways. Therefore, time since last disturbance, and where available, type of last disturbance, are important data in support of forest carbon modeling.

Developing maps (or tabular information) on the distribution of forest ages and disturbance types (including uneven-aged stands) for the analysis area can be challenging. Forest carbon dynamics at the landscape scale are particularly sensitive to the assumptions about recent disturbances, because of the large changes in ecosystem carbon fluxes in the initial years after disturbance. Maps of stand-age distributions can be generated using air-photo interpretation, satellite-derived time series of recent stand-replacing disturbances, or other statistics (e.g., hurricane tracks or harvesting statistics; see Pan et al. 2011b). An alternative approach is to derive stand age (or time since disturbance) estimates from biomass estimates, and to estimate, using yield curves, the time required to reach the observed biomass. However, in regions with forest degradation or non-stand-replacing disturbances, a low biomass can be associated with a young stand or an older but degraded or disturbed stand. Because a young regrowing stand and an older degraded stand can have very different stand-level carbon dynamics, uncertainties in GHG estimates can result from uncertainties in stand-age distributions.

In some cases the available forest inventory does not coincide with the intended start year of the carbon budget analysis. If the start year is prior to the year of the inventory, it is possible to "roll back" the inventory to the start of the simulation. For example, if the available inventory is for 2003, but the analysis is supposed to start in the year 2000, then it is possible to decrease the age of all stands by three years. Stands that are assigned negative ages require special treatment, because these have been subject to a stand-replacing disturbance during the rollback period. Assumptions or auxiliary information will be required to determine the year and type of disturbance, as well as the stand conditions prior to the disturbance. After inventory rollback, the simulation can start in the year 2000, using the information on stand-replacing disturbances between 2000 and 2003 to simulate forward to the year 2003. A comparison of the initial inventory for 2003 against the 2003 inventory obtained after rollback to 2000 and forward simulation to 2003 can be used to verify that the rollback process did not materially alter the 2003 inventory conditions.

3.3 Biomass dynamics, growth rates, and productivity

Live biomass is typically the most dynamic of forest carbon pools (Figure 3.4) and so it is critical to have accurate and precise estimates of rates of biomass change for the representative strata described in the previous section. A significant effort may be required to develop estimates of biomass dynamics that are specific for the area of interest, since the data requirements may be large and the available data within the area of interest may be limited to variables that are related to live biomass, such as volume or basal area. In such cases, equations that relate biomass to these data may be used but the availability of equations for the specific area of interest is often limited. Because age and time since disturbance are key factors that determine biomass and are usually part of the stratification, data on biomass dynamics are usually compiled as growth curves or yield curves, and these curves are then used as input to empirical carbon budget models. Process models often require similar information to validate the predictions of biomass growth rates derived from environmental and other variables.

Figure 3.4 Carbon dynamics for different carbon pools after insect, fire, and clear-cut disturbance events

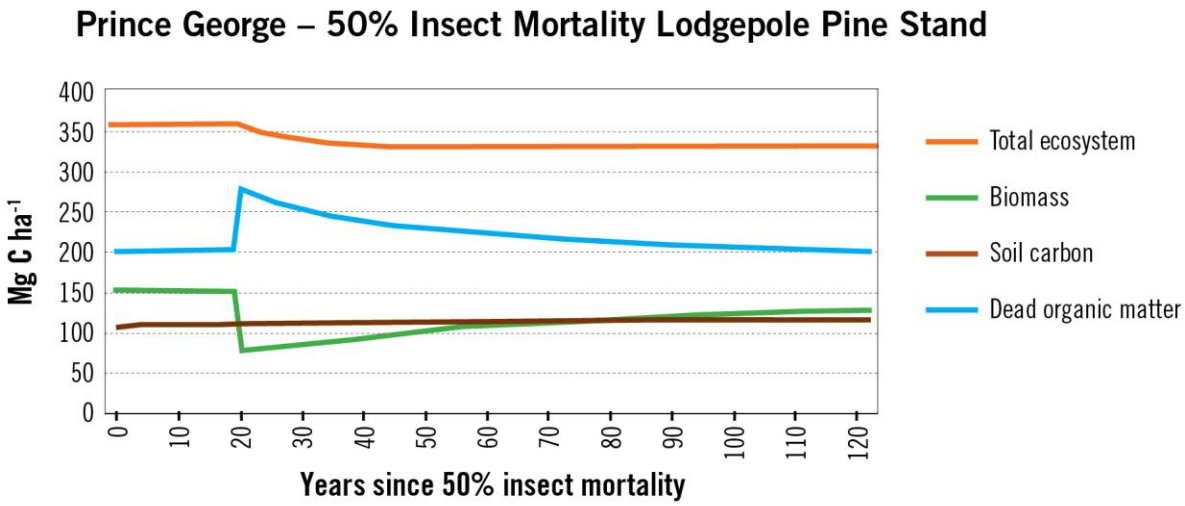

Note: MgC ha^{-1} = megagrams of carbon per hectare

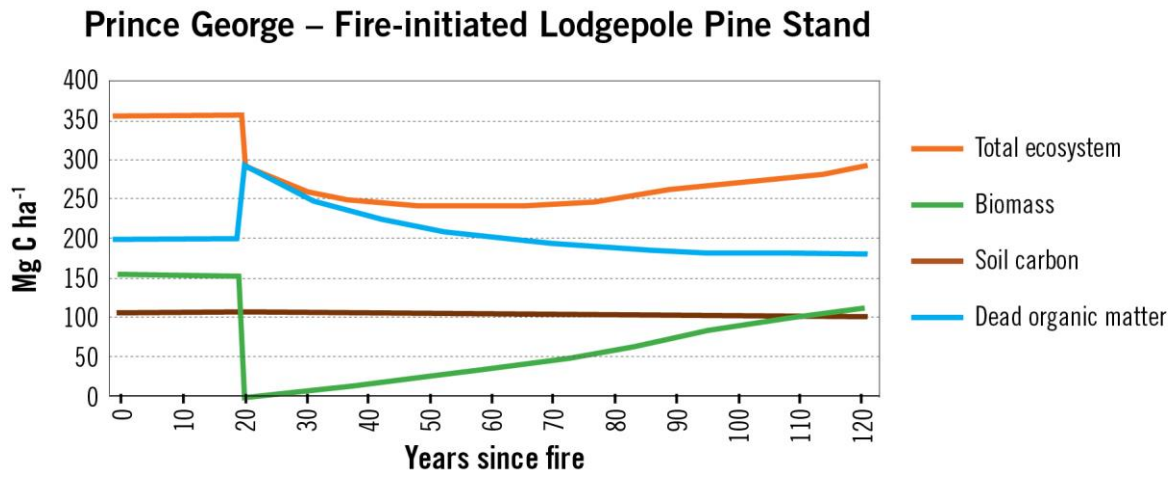

Note: MgC ha^{-1} = megagrams of carbon per hectare

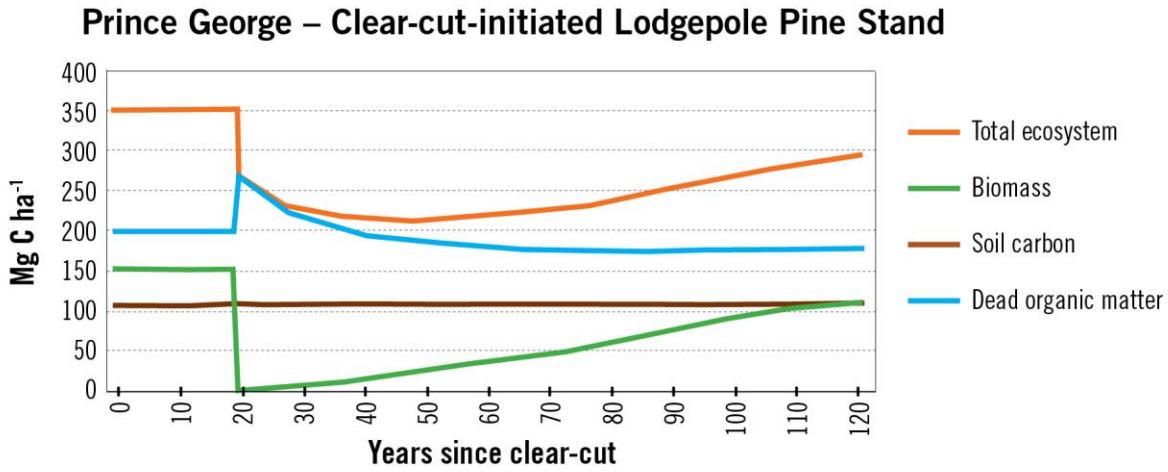

Note: MgC ha^{-1} = megagrams of carbon per hectare

CBM-CFS3 accepts volume estimates by age classes, and then uses a series of stand-level volume-to-biomass equations (Boudewyn et al. 2007) to convert volume to aboveground biomass components (Kurz et al. 2009). These conversion factors can be calibrated to the area of interest. Belowground biomass of fine and coarse roots is predicted from empirical regression equations stratified for softwood and hardwood species (Li et al. 2003). Stand-level volume and biomass estimates are derived from tree-level measurements of diameter and/or height. Species-specific biomass equations are then used to predict tree-level biomass. Hybrid approaches are also possible. For example, in the US forest inventory, biomass is estimated for individual sample trees by converting volume to biomass and then using biomass equations to account for the biomass of tree components (such as branches) that are not represented by the volume estimate (Chojnacky 2012).

Sources of data for generating growth or yield curves are typically from forest inventories, intensive monitoring sites, or special studies such as measurements on a chronosequence of time since disturbance. The data are partitioned according to the determined stratification, and then a statistical procedure such as regression analysis is used to develop a relationship between the variable of interest (volume or biomass) and age or time since disturbance. In practice, a library of such curves will be needed to estimate the carbon dynamics of different strata in the inventory. In the CBM-CFS3, such libraries can be simple and contain only a small number of curves for few forest strata or they can contain thousands of curves to represent large and ecologically complex landscapes.

It may be difficult to determine the age of a sample plot in tropical or subtropical areas such as found in Mexico, where trees do not exhibit distinct growth rings, and disturbances are not typically "stand-replacing" but may affect only a portion of the trees. In such cases, yield curves can still be used to characterize the increment in volume or biomass. However, conceptually, "age" then becomes the pointer to the current stand volume (or biomass) on the growth curve. "Age" or time since disturbance can be assigned by comparing the observed stand biomass or volume with an expected value on a yield curve. One problem that can arise from this approach is that a low biomass stand can either be a young stand or an older stand that has been subject to a partial disturbance or degradation event. Auxiliary data (such as tree diameter distributions, stand density, or disturbance history) can sometimes be used to distinguish young stands from disturbed stands. Ideally, plot measurements should be available to quantify growth rates of young and of disturbed stands to determine whether they need to be assigned different yield curves. Data on post-disturbance recovery are, however, rarely available for all of the types and intensities of disturbances for the different forest types.

3.4 Dead organic matter and soil dynamics

The carbon dynamics of dead organic matter and soil are significant following ecosystem disturbance, though it is often the case that the size of these carbon pools and their magnitude of change are not as great as those of biomass (Figure 3.4), with important exceptions for carbon-rich soils such as found in peatlands, and for high-biomass forests that experience severe disturbances after which deadwood is not removed. Data about dead organic matter and soils are almost always less available than data for live biomass; therefore, approaches to estimation tend to rely more heavily on modeling than on empirical data analysis.

The IPCC guidelines suggest that the representation of dead organic matter and soil carbon dynamics be closely linked to the dynamics of the biomass pools. For example, models that simulate the transfer of biomass to dead organic matter pools during windthrow or during insect outbreaks that kill trees may be better able to capture carbon dynamics than empirical relationships that predict dead organic matter pools as a function of the size of the biomass pools or other inventory information but without consideration of disturbance history. Moreover, by explicitly accounting for the transfer of biomass to dead organic matter pools associated with disturbances, conservation of carbon mass can be ensured. Unfortunately for the soil carbon pool, these transfers are difficult to measure or model.

In the absence of inventory or ground measurements of dead organic matter and soil carbon stocks, the initialization of these carbon pools can be challenging. The CBM-CFS3 uses a spin-up procedure that takes into consideration climate, tree productivity, decay rates and historic disturbances, and the type of and time since the last stand-replacing disturbance, to initialize dead organic matter pools. In Canadian forest ecosystems this approach works reasonably well in many ecosystems (Shaw et al. 2014) but not in ecosystems where mosses contribute substantially to the organic layer carbon stocks (Bona et al. 2013). Mosses are currently only included in a research version of the CBM-CFS3. Process models such as DNDC also make use of spin-up procedures to initialize the different carbon pools.

Initialization of dead organic matter and soil carbon pools can also be challenging in ecosystems with a long or intensive history of human land-use. Long periods of land use may affect soil carbon stocks, and whenever possible, the results of model initialization should be compared against ground plot measurements.

3.5 Activity data (primary drivers between the three countries and within countries)

Almost all forests are recovering from past human and natural disturbances. Forest disturbances profoundly affect carbon stocks and fluxes in forest ecosystems for decades, yet it has been a challenge to assess disturbance impacts in estimates of forest carbon budgets over landscapes or regions. Forest inventories can be used to generate tables of age-class distributions of forest types in different regions and such information has been used to simulate the carbon dynamics of Canadian forests (Kurz and Apps 1999; Stinson et al. 2011) and US Forests (Heath et al. 2011; Smith et al. 2007). Maps of forest age (or time since disturbance) are effective ways to summarize the status of forest recovery and can be used along with data about how different carbon pools change over time to assess carbon dynamics and project future trends. Pan et al. (2011b) compiled the first continental-scale forest age map of Canada and the US (Figure 3.5), by combining forest inventory data, historical fire data, optical satellite data and the dataset from NASA's Landsat Ecosystem Disturbance Adaptive Processing System (LEDAPS) project for the US (Masek et al. 2008), and showed how such information can be used with inventory data to analyze carbon management opportunities. The age map for the US became a key input to several advanced analyses of forest carbon dynamics and the effects of main drivers (Lu et al. 2015; Zhang et al. 2012). By combining geographic information about forest age with estimated carbon dynamics, by forest type, it is possible to conduct a simple but powerful analysis of the net CO_2 uptake by forests, and the potential for increasing (or decreasing) this rate as a result of manipulating forest age class distributions through management activities.

Figure 3.5 Stand age of forests of North America

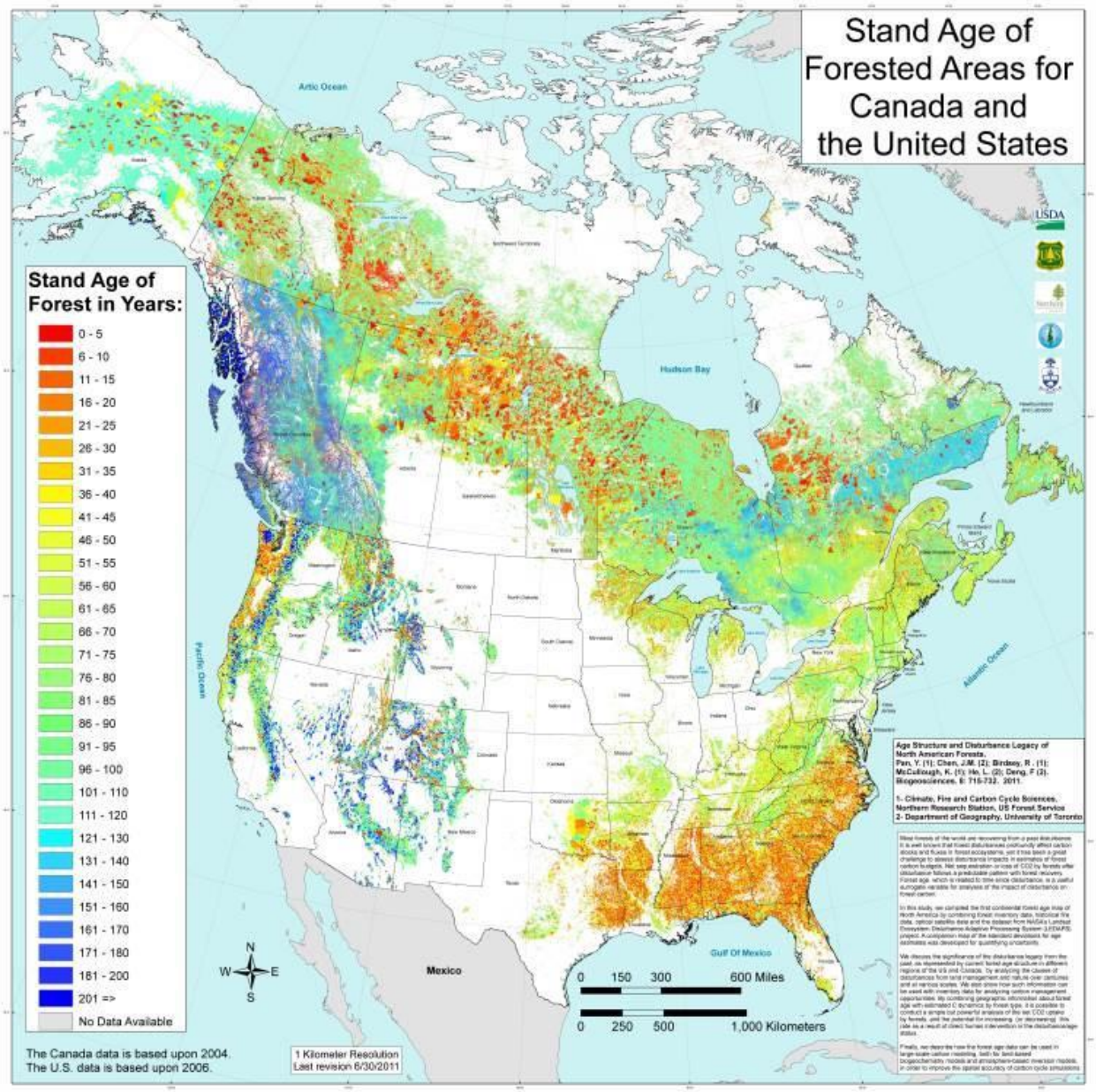

Note: Work is underway to develop a comparable map for Mexico.
Source: Updated from Pan et al. 2011b.

Canada, US, and Mexico have different disturbance histories and outlooks for future disturbances and impacts, related to land management, climate variability and change, and other factors. Table 3.1 summarizes the area of forests recently affected by selected disturbances in Canada, US, and Mexico. The estimates reveal that almost 19 million ha, or 2.6%, of the forest area of North America is affected by some level of disturbance each year. Insects damage the largest area, followed by tree harvesting for wood products, wildfire and deforestation. The impacts of disturbance types vary greatly, with

deforestation resulting in complete removal of forests and conversion to other non–forest land uses. In contrast, the impact in areas affected by insects can range from growth reduction and small amounts of mortality to high levels of tree mortality (Kurz et al. 2008).

Table 3.1 Area of forest (1000 ha yr^{-1}) affected by recent disturbances (during ~2000–2008) for countries of North America

Type of disturbance:	Canada	United States	Mexico	Total
Harvesting – clearcut[1]	878	1,721	n/a	2,599
Harvesting – partial cut[1]	90	2,658	780	3,528
Deforestation[1]	45	355	228	967
Degradation[2]	n/a	n/a	411	411
Wildfire[3]	1,980	1,352	270	3,602
Insects[4]	5,337	2,744	38	8,119
Wind	n/a	n/a	n/a	n/a
Total of disturbances	8,330	8,830	1,727	18,887
Total forest area (revised)[5]	348,000	310,084	69,600	727,684
Percent of forest area disturbed annually	2.4	2.8	2.5	2.6

Note: n/a = not applicable.*Sources:*
[1]Masek et al. 2011, with De Jong et al. (2010) for Mexico.[2]Masek et al. 2011.
[2]Kasischke et al. 2011 for Canada and Mexico; US EPA 2010 for US.
[3]USFS 2010 for US—includes areas of mortality only, excludes defoliation without mortality. Stinson et al. 2011 for Canada—includes areas of mortality and defoliation, for managed forest area only. FAO 2010 for Mexico.
[4]Natural Resources Canada 2014; Oswalt et al. 2014; De Jong et al. 2010.

The three countries have different disturbance profiles, especially with respect to the relative influence of direct human and natural factors (Figure 3.6). The main forest disturbances of Canada include insects, wildfire, and harvesting. Areas affected by insects in Canada increased significantly after 2000 (Kurz et al. 2008; Stinson et al. 2011), and now are the largest area of any disturbance type in North America. The area of wildfire has been decreasing in the last decade (Stinson et al. 2011). Harvesting in Canada increased between 1990 and 2005, after which the area harvested declined significantly during the global economic crises (National Forestry Database, <http://nfdp.ccfm.org/data/graphs/graph_21_a_e.php>). In Canada less than 0.02% of the forest area is affected by deforestation (45 kha yr^{-1}) (Environment Canada 2015).

In the US, the main forest disturbances include harvesting (including deforestation), insects, and wildfire. Historically, harvesting has been the most significant disturbance to forests of the US. Timber production has been relatively stable for about two decades, and more area is partially harvested than clearcut (Table 3.1). Areas damaged by fire and by insects have been increasing, though, on average, each is still less than the area harvested (Table 3.1). The area of deforestation has been significant (Table 3.1), though the

loss of forest area is not noticeable in estimates of total forest area because afforestation has affected an even larger area, resulting in a net increase in forest area in recent decades (Smith et al. 2009).

The main disturbances of Mexico's forests include harvesting, deforestation, forest degradation, and wildfire, with partial-cut harvesting the largest among these. Data on timber production in Mexico suggest an overall 50% reduction in harvest from 1986 to 2004 (Masek et al. 2011). Estimated areas of deforestation and forest degradation in Mexico have varied widely, with example estimates of 228 kha yr^{-1} and 411 kha yr^{-1}, respectively, used in Table 3.1. Trends in area affected by wildfire are not known but generally affect less than half of the area marked by other disturbances.

Figure 3.6 Percentage of total area of disturbed land per year, in Canada, US and Mexico

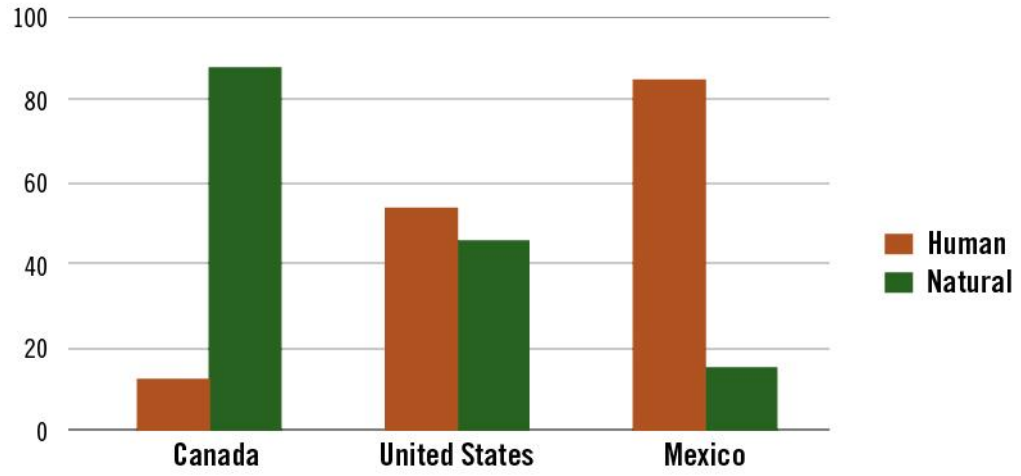

Note: General types of disturbances (not including indirect human-induced disturbances).

3.6 Impacts of disturbances and post-disturbance dynamics

Depending on their severity, forest disturbances can have a minor and non-stand-replacing impact, or a stand-replacing impact. Stand-replacing disturbances generally result in severe alteration to the forest structure, killing all or most of the trees in the stand, and bringing the forest back to the initiation stage. Following this, the forest becomes a net carbon source for a period until the removals from the regrowing vegetation exceed the emissions from decomposition of dead organic matter, and soil organic carbon and NEP returns to positive values. The time to reach this compensation point depends on the type and severity of the disturbance impact; the degree and speed of regrowth; stand density; as well as decomposition and regeneration rates (see Figure 3.7).

Figure 3.7 Generalized schematic of the dynamics of stand-level net primary production (NPP), heterotrophic respiration (Rh), and their net balance, net ecosystem production (NEP), following a fire disturbance

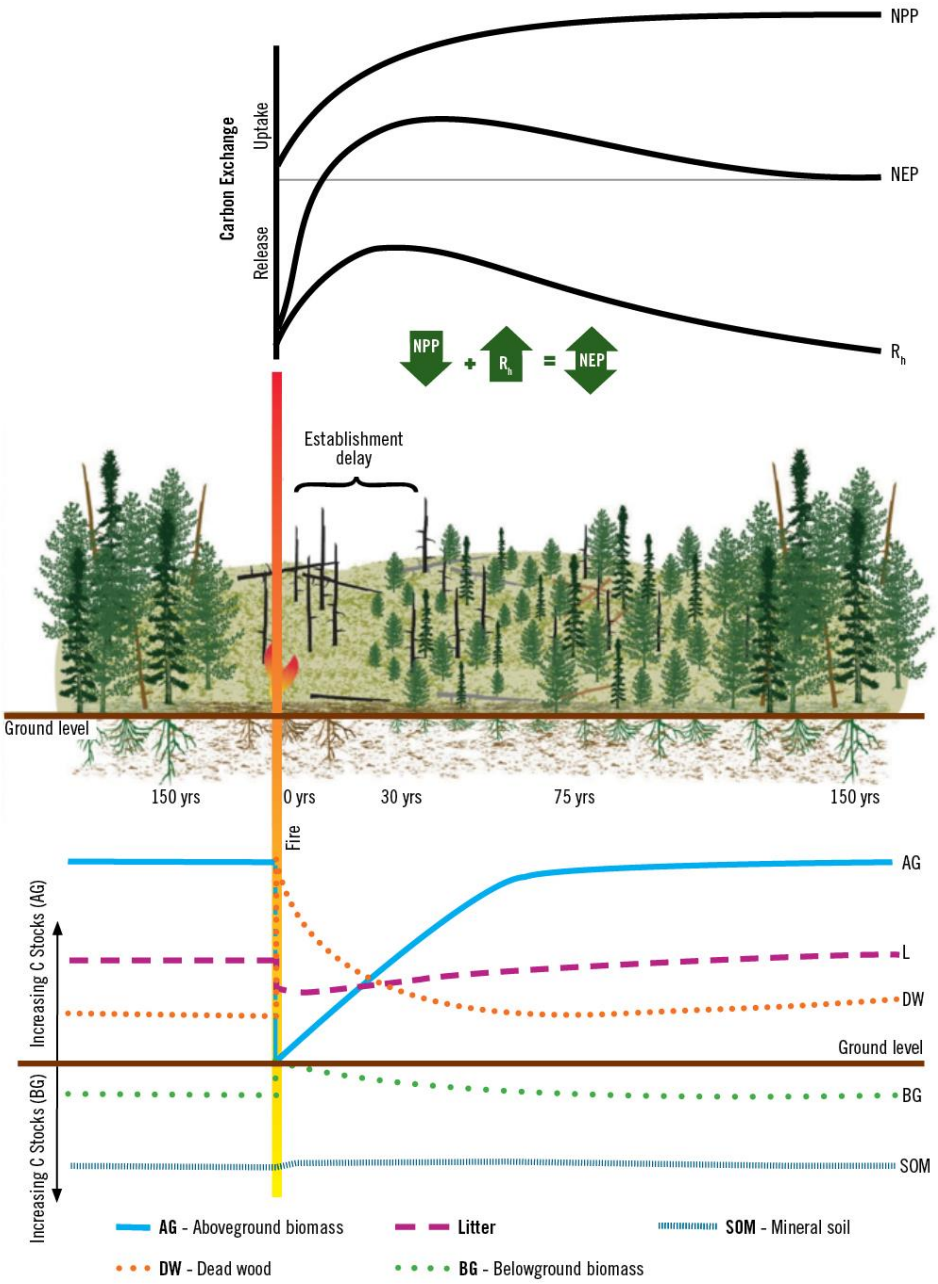

Note: Heterotrophic respiration (Rh) is shown here as a negative flux and includes in this graph large, direct fire emissions in the year of the disturbance. The generalized carbon stock dynamics following a fire disturbance are shown in the lower graph. For simplicity, dead belowground (coarse root) wood is included in the aboveground deadwood (DW) pool.
Source: Kurz et al. 2013.

Non-stand-replacing or minor disturbances (e.g., low-intensity fires, low-level insect or disease infestations, or selective logging) affect forested landscapes at a finer spatial scale, damaging or killing individual trees or small groups of trees, or in the case of firewood collection, removing carbon from both live and dead organic matter pools such as downed wood. Non-stand-replacing disturbances reduce the overall forest productivity and thus carbon uptake; however, they result in a smaller proportion of the ecosystem's carbon being returned into the atmosphere compared to stand-replacing events, and the existing forest often remains a carbon sink in the years following such disturbances unless there are many repeat disturbance events, such as annual insect mortality or illegal timber harvesting.

Following a disturbance, regenerating forests typically experience a period of rapid growth during which they remove large quantities of CO_2 from the atmosphere through photosynthesis, whereas in old forests the overall uptake of CO_2 has typically slowed because ecosystem losses through respiration have become high enough to offset carbon uptake through photosynthesis. The buildup of carbon in dead organic matter pools that is common after most disturbances will be gradually released through decomposition over a period of a few years to decades, depending on the climatic conditions, on whether deadwood is standing or down, and on the size of dead trees or branches.

To better quantify the disturbance impact on the different carbon pools, we need to know what, when, how and where the disturbance occurred. As each disturbance type affects the landscape in a unique way, knowledge of the type, location, and extent of disturbances, ideally with annual statistics, can improve the characterization of disturbance impacts and post-disturbance carbon dynamics.

The impacts of disturbances on the amount, composition and distribution of carbon in the ecosystem can be characterized by a disturbance matrix (DM) (Kurz et al. 1992) or a set of equations (Raymond et al. 2015). For each disturbance type and intensity, the DM or equations define the proportion of carbon in each pool that will remain in that pool, be transferred to another pool, released to the atmosphere, and transferred to the forest product sector as a result of the disturbance. For example, clear-cut harvest will transfer merchantable-size trees to the forest-product sector and leave behind slash and dead roots. In contrast, a crownfire may consume foliage and forest floor carbon, release large amounts of carbon to the atmosphere as CO_2 and methane, as well as kill most trees.

Post-disturbance carbon dynamics of dead organic matter pools can be estimated by direct measurement (Domke et al. 2013) or by simulating decomposition losses and additions to dead organic matter pools from the regrowing stand, or fall rates of dead standing trees (e.g., after a wildfire), using empirical or process models (Russell et al. 2015).

Regeneration of stands following disturbance can be represented using empirical yield curves or process simulation. In some cases, disturbances affect succession, and after the disturbance event new forest types or species grow.

Tier 2 methods rely on "emissions factors" to quantify the release of carbon resulting from disturbances and to quantify the carbon uptake from forest regrowth. Emission factors assume constant (linear) rates of change and represent a simplification of the complex non-linear carbon dynamics during and following disturbances. Where data are available to quantify disturbance impacts and post-disturbance regrowth, Tier 3 models of carbon dynamics are a substantial improvement over the simplified emission factor assumptions used in Tier 2 approaches.

3.7 Integration

In previous sections we have outlined the stand- and landscape-level drivers of change and how the information on carbon dynamics of individual stands can be calculated and summarized as tables of coefficients, emissions factors, or yield curves. Figure 3.8 shows an example of different stand-level carbon dynamics based on forest inventory information, disturbances (activity data) and information about forest growth and mortality (defined in yield curves). Conceptually, every stand in a landscape can be represented by one (or more) records in the model database and refer to a group of stands with similar conditions (spatially referenced) or to a polygon or pixel that can be mapped. Once the carbon dynamics of individual stands (pixels) are known, the carbon dynamics of a region can be estimated as the sum of the carbon dynamics in individual stands (Figure 3.9).

Figure 3.8 Simplified examples of two forest stands that experience different carbon dynamics due to different patterns of disturbance, growth, and dead organic matter (DOM) decomposition

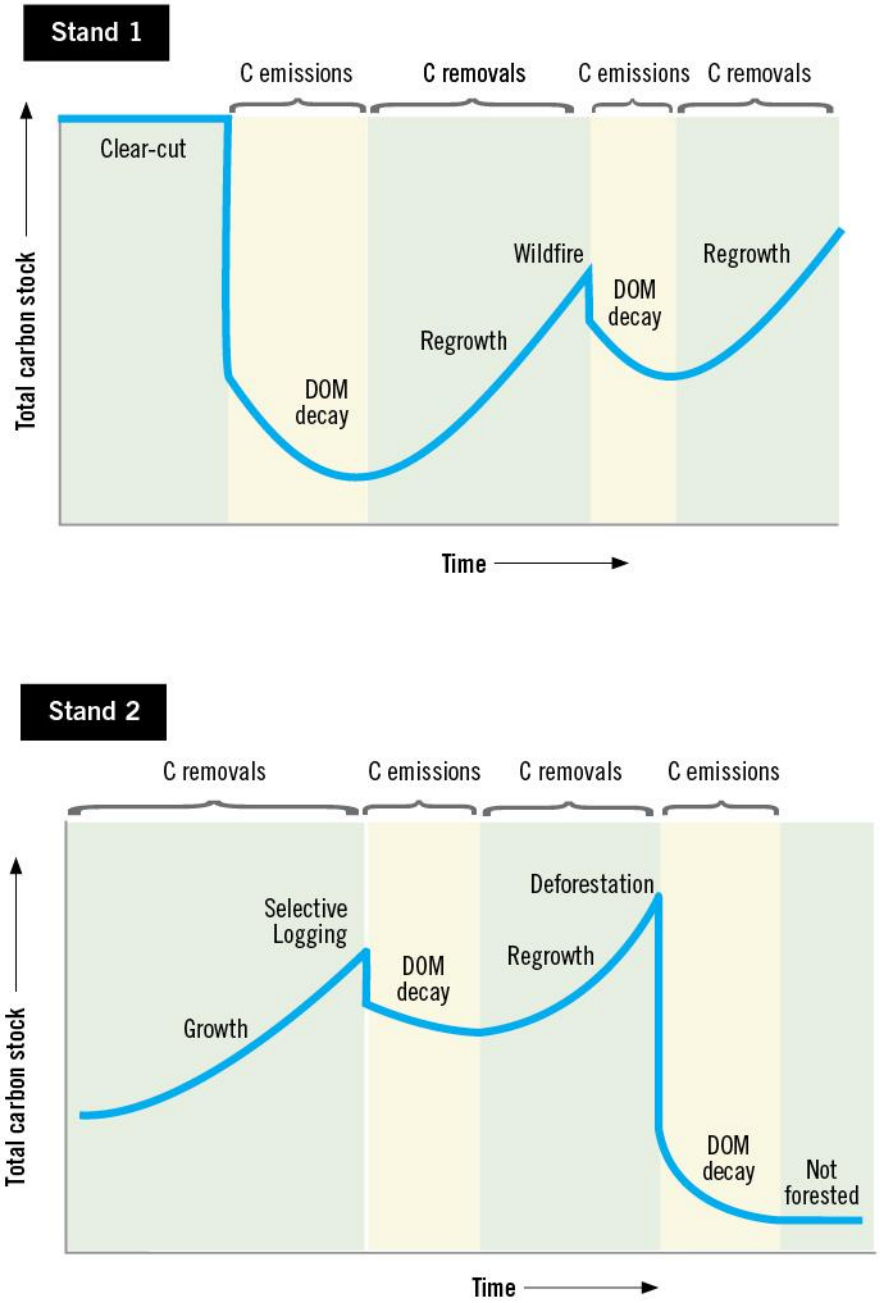

Note: The resulting differences in GHG emissions and removals over time, due to the different patterns of disturbance, growth, and dead organic matter (DOM) decomposition, can be considerable. C = carbon.

Figure 3.9 Example of a hypothetical landscape, with multiple pixels and carbon dynamics for individual pixels

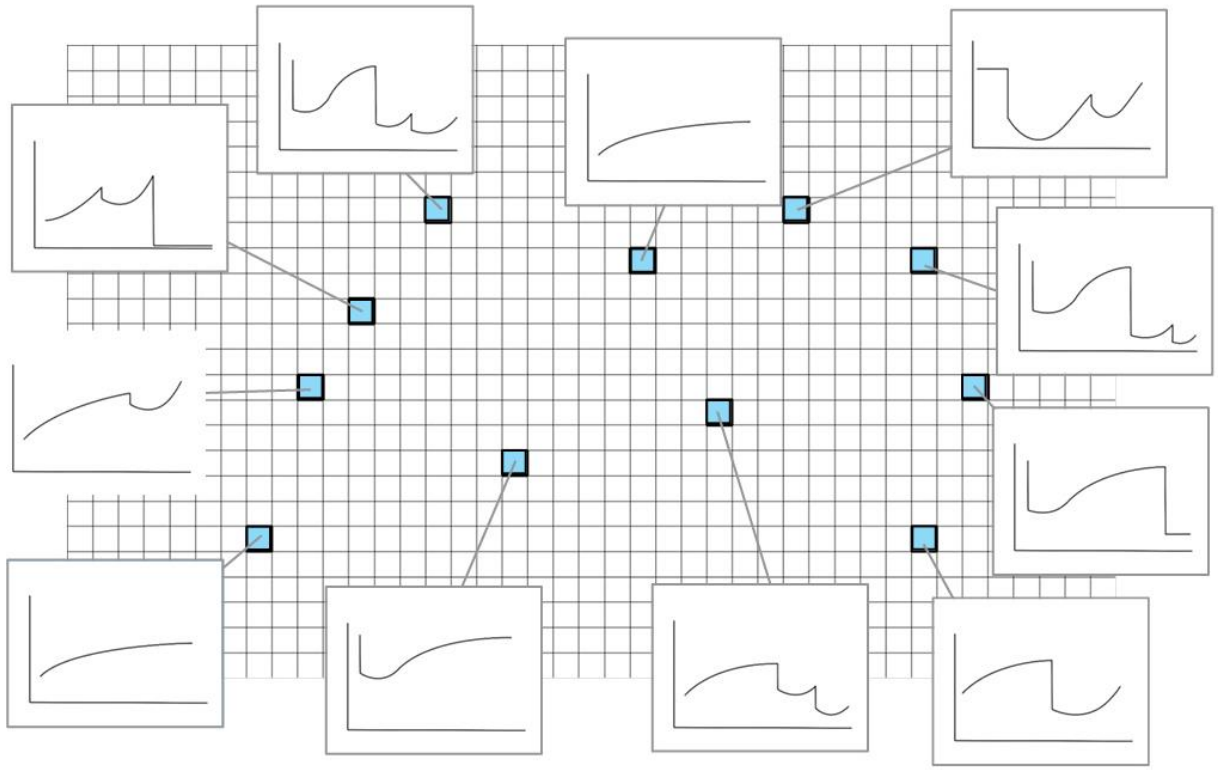

Note: The carbon dynamics are summed up by the model into dynamics at the landscape scale, with each stand experiencing different dynamics owing to different patterns of disturbance, growth, and dead organic matter decomposition. The squares within the grid represent individual stands, the ones highlighted in bold represent particular stands for which the carbon dynamics are being illustrated, and the rectangles pointing to those individual stands depict variation in carbon per hectare over time (as in Figure 3.8). Large landscapes can experience significant spatiotemporal variation in GHG emissions and removals, and therefore carbon budget simulations require detailed information about the types, timing, and impact of individual disturbances at specific locations.

4. Approaches to Generating Land-Cover and Land-Cover-Change Data

R. R. Colditz,R. Llamas, S. Gebhardt, T. Wehrmann, J. Equihua, R. Ressl, and M. Schmidt

This chapter qualitatively and quantitatively explores data sets of different spatial and temporal scales and compares selected change detection methodologies. A test site on the Yucatan Peninsula was selected, namely the area of Landsat 5TM and 7ETM$^+$ path-row 020-046 (World Reference System, WRS2) which covers the western side of the northern Yucatan Peninsula south of the City of Merida (see Figure 3.3 in Section 3). The study site has an area of 31,746.7 km^2. This section discusses four main issues that affect change detection: legends and translations of land cover maps; the spatial resolution of the input data, including levels of map generalization; temporal data availability; and selected methods for change detection.

4.1 Legends, translations and land cover maps

Figure 4.1 illustrates the difficulties of land-cover mapping, using data sets for circa 2005. For visual purposes, all maps were recoded to the NALCMS (North American Land Change Monitoring System) legend. In Figure 4.1, (a) and (b) depict two interpretations of the INEGI Series III vegetation map for the NALCMS and MAD-MEX (Monitoring Activity Data for the Mexican REDD+ Program) projects (Gebhardt et al. 2014). The maps (c) and (d) show the land cover maps classified from MODIS for NALCMS and Landsat for MAD-MEX for the year 2005. There are notable differences—for instance, using INEGI's series III vegetation map generalized to the NALCMS classification scheme (Figure 4.1a), the study area is dominated by the following land cover classes: Tropical or subtropical broadleaf evergreen forest (36.1%), Tropical or subtropical broadleaf deciduous forest (23.2%), Tropical or subtropical shrubland (23.6%), and Cropland (11.3%). In the NALCMS 2005 land cover map from MODIS (Figure 4.1c), the areas categorized Tropical or subtropical broadleaf evergreen forest increased by 11%, mostly at the expense of Tropical or subtropical broadleaf deciduous forest, and the area of Cropland doubled, diminishing the area of Tropical or subtropical shrubland. The recode of the INEGI vegetation map to MAD-MEX (Figure 4.1b) results in a completely different spatial pattern with a more than three-times higher proportion of Tropical or subtropical broadleaf deciduous forest (77.25%), and there is no Tropical or subtropical shrubland. The reason for that dramatic difference in baseline maps is that NALCMS considers semi-deciduous forests as evergreen, whereas they are classed deciduous in MAD-MEX, and the successional stage of shrubby forests was translated from tropical forests, in MAD-MEX, to shrubland.

MAD-MEX maps from Landsat (e.g., Figure 4.1d) appear to have a closer match with their baseline from INEGI; minor confusions exist between Cropland and Tropical or subtropical grassland. The striped patterns at the edge of the map are the result of fewer available data of Landsat 7ETM+ due to scan-line errors in imagery past May 2003. The reasonable match for MAD-MEX is due to a translation of not-specified "Secondary vegetation"—shown in black in Figure 4.1d, mainly in the northeastern quadrant

and central-western area—as Tropical or subtropical broadleaf deciduous forest. A translation to Tropical or subtropical broadleaf evergreen forest would have resulted in a 21% difference.

A similar exercise aggregating all maps to the 6-class IPCC legend results in the spatial distributions of Figure 4.1e–g. The reduced number of classes, in particular aggregated forest classes, results in a much higher agreement of maps. Still, there are differences, which in some cases may depend on the actual translation of classes. For instance, whether managed grasslands are considered grassland or cropland may depend on the particular translation. The overestimated cropland area in NALCMS (which in the original data included grasslands used for grazing) is still reflected in the final maps.

In summary, there is a need for consistent land-cover definitions, as translations from individual sources may lead to very different maps. Changes to the initial state of land cover will affect estimates of carbon stocks and emission. It should be noted that although protocols for land cover harmonization exist, e.g., the FAO land cover classification system (LCCS) (Di Gregorio 2005), there remains a lot of room for interpretation of what specific land cover classes may mean and how they should be assimilated into a carbon measurement, reporting and verification system.

Figure 4.1 Land cover maps for selected site in Yucatan Peninsula

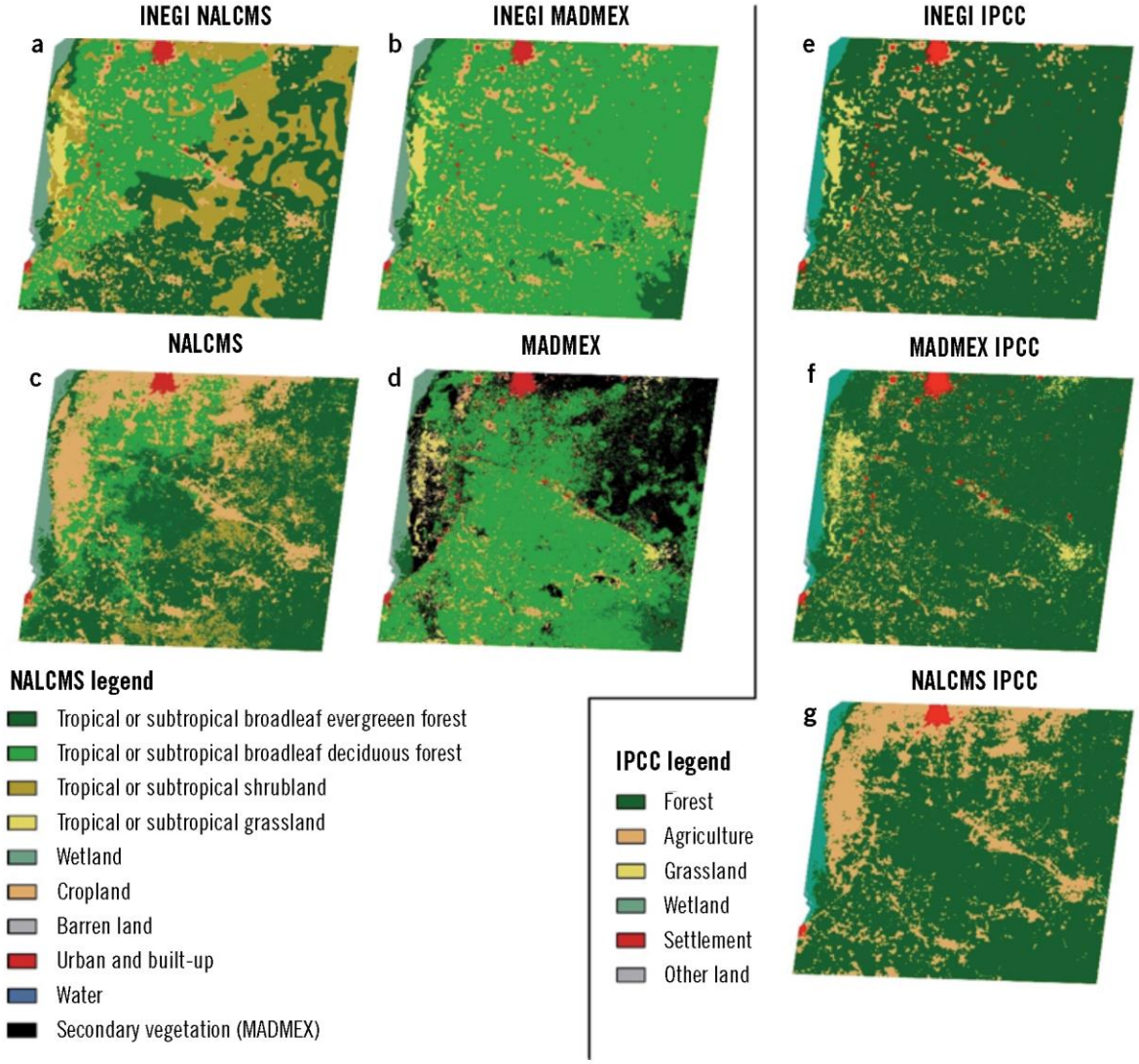

Note: Only NALCMS classes that exist in this area are shown.

Sources: These are maps or translation (recodes to the NALCMS and IPCC legend) of maps we have generated in Conabio. For institutional abbreviations see list of acronyms.

There are three base-line maps:

[1]INEGI Vegetation map: INEGI (2005). Conjunto de datos vectoriales de la carta de uso del suelo y vegetación, Escala 1:250,000, Serie III (CONTINUO NACIONAL). Instituto Nacional de Estadística y Geografía—INEGI. : Aguascalientes, Ags., México.

[2]NALCMS: Land cover map of the North American Continent for the year 2005.

[3]MAD-MEX: Land cover maps of Mexico for the year 2005.

4.2 Spatial issues

The spatial resolution of remote sensing data is a primary criterion for their use in applied studies. Figure 4.2 illustrates the resolution of data from three different sensors commonly used for forest carbon monitoring: RapidEye resampled to 5m (nominally 6.5 m at the sensor), Landsat with 30 m, and MODIS with 250 m. Most desirable is a higher spatial resolution; however, this comes at the expense of a less frequent area coverage (see next section), which may limit mapping and, in particular, change detection.

The pixel size may affect what can be detected in a land-cover or change map, as a continuous image is transformed to a discrete set of classes assigned to each pixel. The general assumption is that the characteristic with the largest area proportion in the pixel will be assigned as class; however, this may be modified by the particular algorithm. For change detection, algorithms may be adjusted to minimize omission or commission errors (Olofsson et al. 2014)—that is, to report all potential changes or to only report changes which are highly certain.

Figure 4.2 Spatial resolution and minimum mapping units for selected sensor data

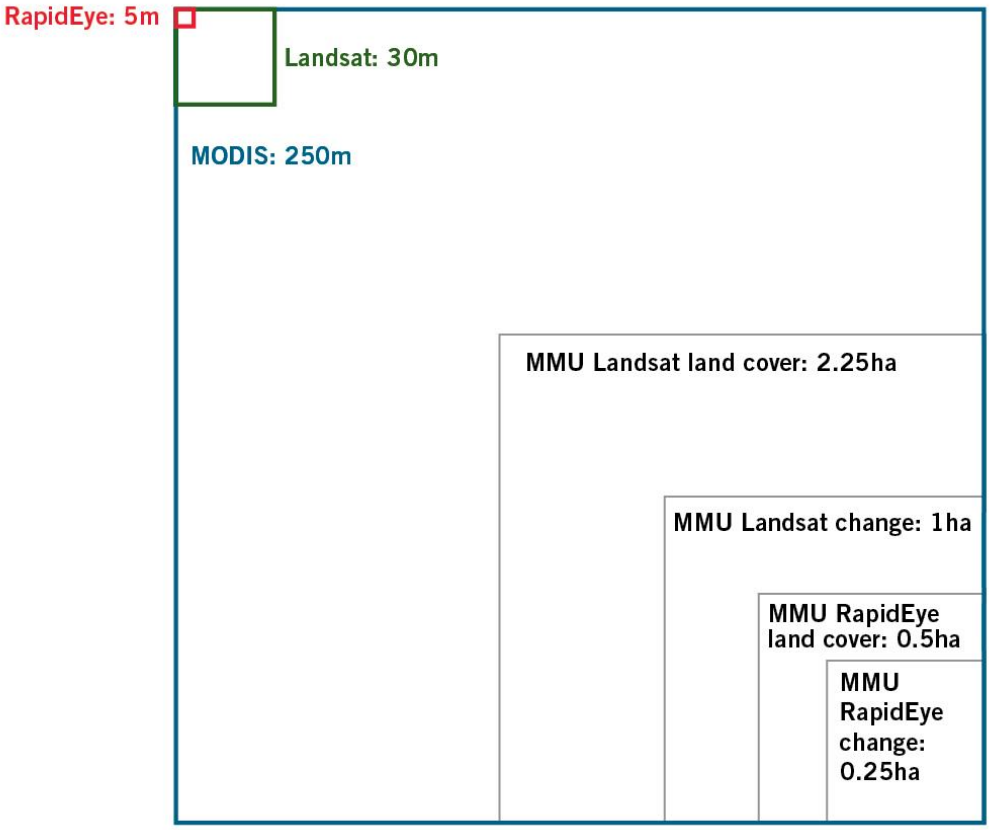

Note: Rapid Eye, MODIS and Landsat are satellite monitoring systems. MMU = minimum mapping unit; m = meters; ha = hectares.

In addition to spatial resolution, another often-overlooked aspect is the level of generalization at which maps are provided to the user community. For instance vector data are provided for certain scales—e.g., INEGI vegetation map at 1:250,000—which clearly limits the spatial detail of the data set, as only larger spatial features can be represented. For raster maps a minimum mapping unit (MMU) is applied, which indicates the smallest area of connected pixels of the same class retained in the map, that area being also known as a patch or region. Most land cover maps are generalized; for example, the European Union's Corine land-cover dataset only depicts polygons of at least 25 ha in area (Feranec et al. 2010), and the National Land Cover Database (NLCD) of the US contains a class-specific MMU, with 0.45 ha for urban, 2.88 ha for pasture and cropland, and 1.08 ha for all other classes (Fry et al. 2011).

Figure 4.2 shows 4 MMUs which are applied to RapidEye and Landsat data for forest carbon mapping in Mexico; the MMU for NALCMS MODIS maps is 25 ha (4 connected MODIS pixels of 250m spatial resolution, or four times the area of the blue box in Figure 4.2). MMUs for change are generally smaller than MMUs for land-cover mapping for instance circa 1ha (11 pixels) for Landsat, and 0.25ha (100 pixels) for RapidEye (Figure 4.2). The shape of the patch may have any form (not necessarily square as shown here) with the smallest instance being the resolution of the pixel.

Although these differences cannot be observed from a distance, the local modifications have an effect on area statistics and thus on change detection. In general terms, classes that form large patches, which usually also have the higher area proportions, will gain in area at the expense of classes with generally smaller area proportions and scattered patches of smaller size (Blanco et al. 2013; Fisher 2010).

4.3 Temporal issues

Data availability is a key issue for change detection, and even more so for forest carbon monitoring, for which the year, and in some cases the approximate day of change, plays an important role. From the remote sensing point of view there are three considerations: availability of historical data, data continuity in the future, and intervals between image acquisition.

Availability of historical data is important for monitoring forest recovery over longer time periods. The need for historic data is also related to policy or reporting requirements. For example, UNFCCC reporting of GHG emissions and removals starts in 1990, and activity data thus are needed starting in that year. Therefore many more-recent sensor systems (e.g., RapidEye) are not able to provide these activity data for the entire reporting period. However, they can play a role in mapping the recent and future changes, because the data quality is better and the spatial resolution is higher. An effective assessment of past changes can only be accomplished by taking the long-term records of the 30-m Landsat TM/ETM+ data (from 1982) and extrapolating them back to 1972 by using the data from the limited coverage of the 60-m Landsat MSS; or by taking the 250-m MODIS data (from 2000) and extrapolating them back to 1981 with various 1-km 4-km, 8-km or 0.05° products derived from NOAA-AVHRR.

Data continuity is at least as critical as historic data availability as sensor calibration or inter-calibration is still a challenging field in remote sensing science. Some satellites, like the NOAA-AVHRR series, underwent considerable relative and absolute (inter-)calibration campaigns but in some cases still exhibit minor variations not related to reality. Integrating data from different sensor systems that have different

spatial and spectral resolutions, which have an effect on what changes may be detected, is even more complicated. Processing systems need to be carefully designed, robust and invariant to changes in the data stream, otherwise observed changes may merely show the alterations in data sets and not in activities on the ground. Data continuity is assured for all historical sensor systems like Landsat (today with Landsat 8's Operational Land Imager) as well as AVHRR/MODIS (today S-NPP and JPSS in the future). The European Space Agency Sentinel satellites, in particular optical systems of Sentinel IIA/B and III will complement and play a major role by providing new products in the near future. Several commercial satellite data providers also ensure longer-term data availability but are more focused on exploring new applications and markets, which sometimes hinders continuity of spectral bands for long-term data streams.

The interval between image acquisitions and the capacity to obtain wall-to-wall coverage for a large study area is an important criterion for selecting data from a specific satellite. Pointability, which focuses the satellite to a specific area off-nadir, is important for reducing the risk of obtaining cloudy imagery and helps to obtain frequent coverage, which can be augmented even more by satellite fleets such as RapidEye, but pointability limits frequent wall-to-wall coverage. Therefore nadir-looking instruments become useful, as they ensure consistent area coverage at defined intervals, e.g., Landsat every 16 days. At higher latitudes, paths start to converge significantly and pixels of neighboring paths may be used to build a denser time series for overlapping areas (Griffiths et al. 2013; Roy et al. 2010).

However, not all Landsat data were actually acquired, stored or made available to the public. Figure 4.3a shows image data availability of Landsat 5TM/7ETM+ over Mexico, with less than 10% cloud cover, according to image metadata for the year 2000. There is a significant gradient from North to South because in tropical regions fewer images are available in general and cloud cover is more frequent.

Focusing on Landsat path-row 020-046 (black circle), Figure 4.3c shows the annual image data availability, independent from cloud cover, for the period 1 January 1985 to 31 December 2013. It can be noted that only in some years was the maximum availability achieved, and that the average availability was 36.7% for Landsat 5TM (1985–2011) and 63.9% for Landsat 7ETM+ (2000–2013). Noticeable are data gaps for Landsat 5TM during 1988–1991, when Landsat 4TM images were acquired, and 2002–2008, due to a discontinuation of Landsat 5TM data acquisition for southern Mexico.

However, the data availability at pixel level is much lower, due to clouds, haze, sensor problems, etc. Figure 4.3b shows the percentage of invalid pixels as defined by FMASK (Zhu and Woodcock 2012) for all 434 available images of Landsat 5TM and 7ETM+. At least 40% of all images show invalid data. The number of invalid data increases toward the edge of the image mainly because of the scan-line error in Landsat 7 data. However, there is also a regional difference in the study area, with the eastern side and mainly the southeastern quadrant having fewer available pixels due to cloud and shadow issues.

Figure 4.3 Availability of images over Mexico in 2000, distribution of invalid data, and availability of images during 1985 to 2013

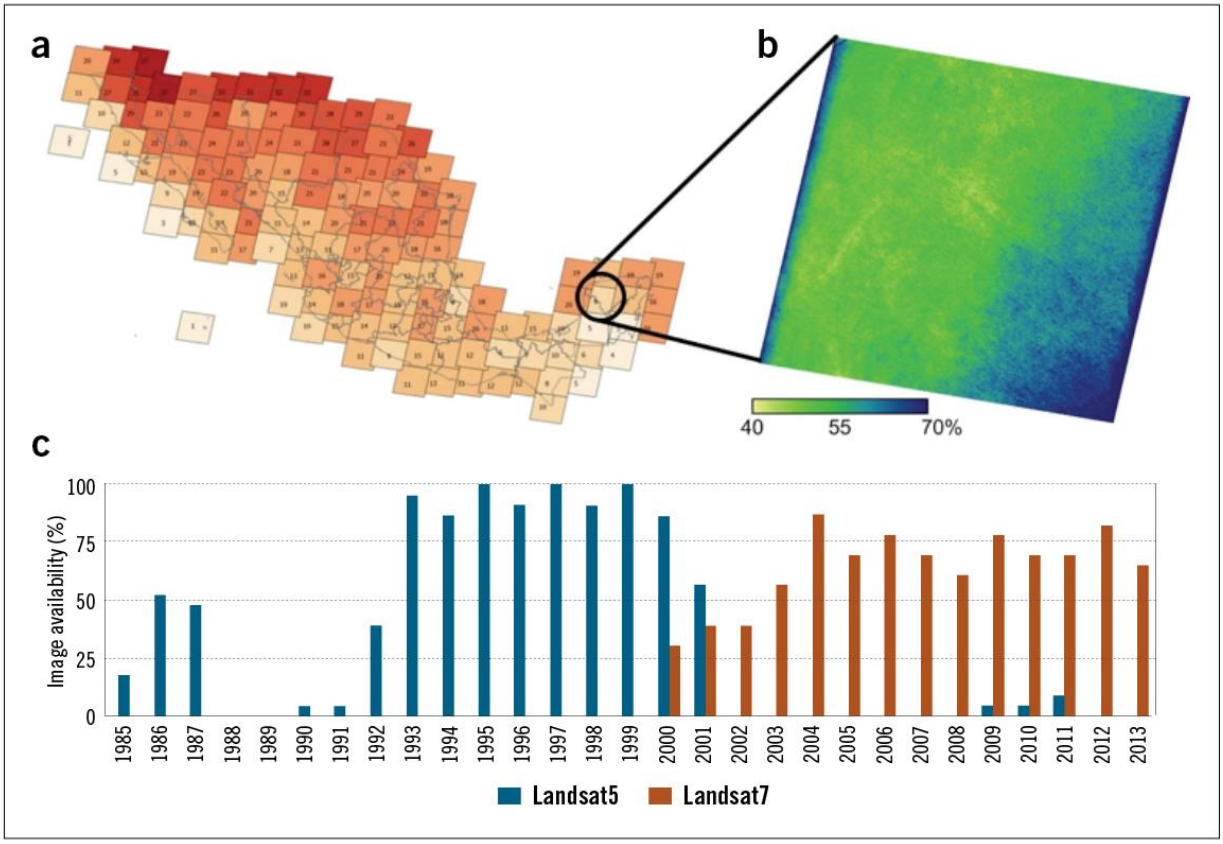

Note: a) Availability of Landsat TM/ETM+ image data over Mexico, with less than 10% cloud cover, for the year 2000. b) Spatial distribution of invalid data according to FMASK, from available images in path-row 020-046 (black circle), in percent. c) Availability of Landsat 5TM and ETM+ images for path row 020-046 from 1985 to 2013.

For the sake of comparison, Figure 4.4 shows results from 250 m spatial resolution 16-day MODIS NDVI data for Mexico (MOD13Q1 from 1 January 2000 to 31 December 2014), which are based on daily MODIS image acquisitions. The MODIS product quality layer was used and pixels with good and acceptable quality, no clouds, no shadow and no snow/ice, as well as good or marginal reliability were included. Figure 4.4a shows the expected spatial pattern for invalid pixels, with more invalid data toward the South, along the coast, and in mountainous regions. Particularly noticeable is the gradient of less valid data in the eastern Yucatan Peninsula; where upward of 50% of observations were invalid. Temporally there are fewer valid data during the rainy season in summer (Figure 4.4b). The number of invalid observations, however, is only one part of temporal analysis. Frequent but short temporal gaps are easier to close by interpolation than are long data gaps. The length of the longest data gap indicates the worst-case scenario. Figure 4.4c indicates that in the entire country the shortest data gap was three composites, one composite corresponding to 16 days, because of the missing first three composites at the beginning of the year 2000. The longest data gaps occurred in southeastern Yucatan, where there were prolonged periods of no data during half a year.

Figure 4.4 Analysis of MODIS Terra NDVI composites (MOD13Q1) for Mexico, 2000–2014

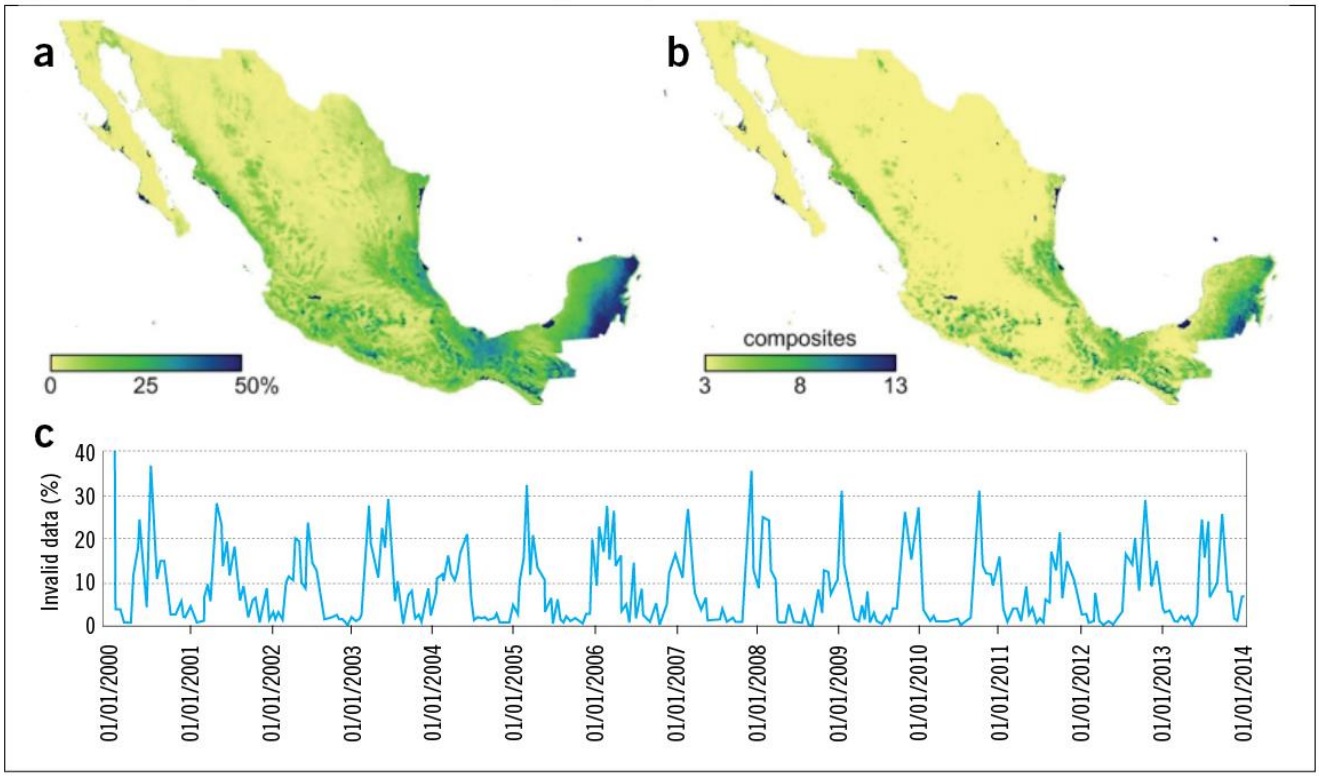

Note: a) Spatial pattern of invalid pixels, by percent. b) Spatial pattern of maximum gap length, represented by number of missing composites (one composite corresponds to 16 days). c) Percent of invalid temporal pixel data.

4.4 Change detection algorithms

The success of implementing a change detection method depends on several factors (Kennedy et al. 2009), such as:

- available resources,
- time for completing the study,
- image availability,
- access to ground observations,
- access to ancillary data,
- availability of and experience with change detection algorithms,
- area of expertise, and
- intended use of the product, etc.

Moreover, one needs to define "what is change," as many aspects from the above list depend on this definition (Coppin et al. 2004; Mayaux et al. 2008):

- Change may be the conversion of land cover to another class (forest clear-cut) or the modification of that class (e.g., forest thinning).
- Change may be abrupt (forest fire) or a gradual process over many years (e.g., bush encroachment).
- Change may be reversible in a short or medium-length time (e.g., forest regrowth) or permanent for many decades (e.g., reservoir).

Many well-explored change detection algorithms (for reviews, see Coppin et al. 2004 and Lu et al. 2004) can be applied to remotely sensed data. Post-classification may be the most widely known approach: the analyst generates independent maps for different points in time and then calculates the difference between those maps. The inherent simplicity of this approach is at the same time its weakness, as the error of such change detection products is the product of the error between the maps. This approach may work for small, well-known study areas where the analyst visually generates or corrects the independent land cover maps, but it can be disregarded for wall-to-wall change detection of large areas.

More effective are strategies that focus on updating a baseline map and time series (Huang et al. 2010; Kennedy et al. 2009; Pouliot et al. 2014; Verbesselt et al. 2010). Also, limiting detection to specific change types, e.g., forest disturbance or forest cover change, may result in higher accuracies.

For the study area of Landsat path-row 020-046, the Vegetation Change Tracker (VCT) algorithm was applied; this method was previously successfully employed in other forest change studies in temperate regions. The algorithm builds on a Disturbance Index (Healey et al. 2005) and applies additional rules mainly focusing on temporal persistency of change. The use of images at the peak of growing season maximizes the difference between a healthy forest and no vegetation in the next image. The peak of growing season in temperate regions coincides with less cloud cover during the summer season, but in tropical regions this corresponds to the rainy season. Therefore, significantly fewer clear images (i.e., free of cloud cover or atmospheric haze) were available, and so cloud-free, dry-season images, primarily between March and May, were used. In addition, for the period from 2004 to 2009 only scan-line-off Landsat 7ETM+ data were available, and composites from several acquisitions were generated to reduce data gaps. With varying feature sets and threshold settings to define mature forest, only mediocre results were achieved, with generally higher than 50% commission and omission error (Colditz et al. 2015a, b, c).

Also, the spatial patterns of our VCT-based change maps do not match well with areas identified in other studies or with other methodologies such as the Hansen forest cover change map (Hansen et al. 2013) or the Iteratively Reweighted Multivariate Alteration Detection (IR-MAD) algorithm (Nielsen et al. 1998). Here, differences may be due to inadequate sets of image observations; however, the differences in change detection methods, even when using the same input data, are generally high, and accuracies in a rigorous assessment are low. Thus, considering the importance of activity data in forest carbon monitoring and GHG assessment, much research remains to be done to reduce uncertainties in land-cover change and other activity data.

4.5 Summary

Change detection based on a comparison of sequential map products is affected by the classification errors in each map and can introduce large uncertainties into the change estimates. Moreover, the persistent problem of inconsistency in stratification and legends of existing map products also limits their use for change detection. While many established remote sensing products and many new ones are readily available, and while computing power has greatly increased in recent years, the algorithms and approaches for change detection are still in need of improvement. Our current ability to detect forest cover change from image time series is constrained by the low accuracies of the resulting products, and these will introduce large uncertainties in the estimates of GHG emissions and removals.

Increasing the spatial resolution of remote sensing products improves the ability to detect changes in tropical regions where small plots of land undergo change (see also Section 6).

The main temporal issue in the tropics is the availability of cloud-free images during the peak of growing season. After resolving the spatial and temporal data issues, analysts need to select an appropriate change detection algorithm that best suits their needs. Further improvements to change detection algorithms are greatly needed to reduce uncertainties in GHG estimates.

5. Using Activity Data in GHG Estimation

D. Greenberg, W.A. Kurz, M. Fellows, S. Morken, A. Dugan

CEC-supported work also focused on enhancing the capacity of the CBM-CFS3 to conduct spatially explicit simulations, in particular its capacity to use emerging and anticipated spatially explicit activity datasets to reduce uncertainties in calculations of landscape-level GHG emissions and removals. Such data sets are derived from time series of land-cover products obtained from remote sensing (see Section 4). The work involved developing, testing, and evaluating new software known within the team as "Recliner," and then using it to conduct demonstrative spatially explicit simulations of forest carbon dynamics within landscapes in North America. In this section we briefly describe the Recliner system and its use in conducting an example of a spatially explicit simulation of carbon dynamics within a forested landscape in the US.

5.1 Integrating activity data into emissions and removals estimation (land-use change matrices and Recliner)

Recliner directly uses rasters or shapefiles of forest type, forest age, any classifiers intended for stratification, and disturbance events to create CBM-CFS3 projects (i.e., the data bases with all input data files). These projects are then used for analyses in which the carbon dynamics for every individual stand (i.e., groups of pixels with similar attributes) is simulated. In contrast, the existing CBM-CFS3 tools use spatially referenced summaries of forest characteristics (i.e., a table indicating the number of hectares of different forest types, stratified by stand age, spatial unit, and desired classifiers) and disturbance events (i.e., a table indicating the number of hectares, stratified by year, forest type, stand age and desired classifiers, affected by different types of disturbance) to create CBM-CFS3 projects. In spatially referenced analyses the carbon dynamics of individual stands are also simulated but the exact locations of stands are not known and stands can represent aggregates of polygons. Figure 5.1 outlines Recliner inputs and workflow in flowchart form. The Recliner data processing system can use activity data in a wide range of map formats that can include a single disturbance type or multiple disturbance types, defined for one or multiple years.

Figure 5.1 Illustration of Recliner inputs and workflow

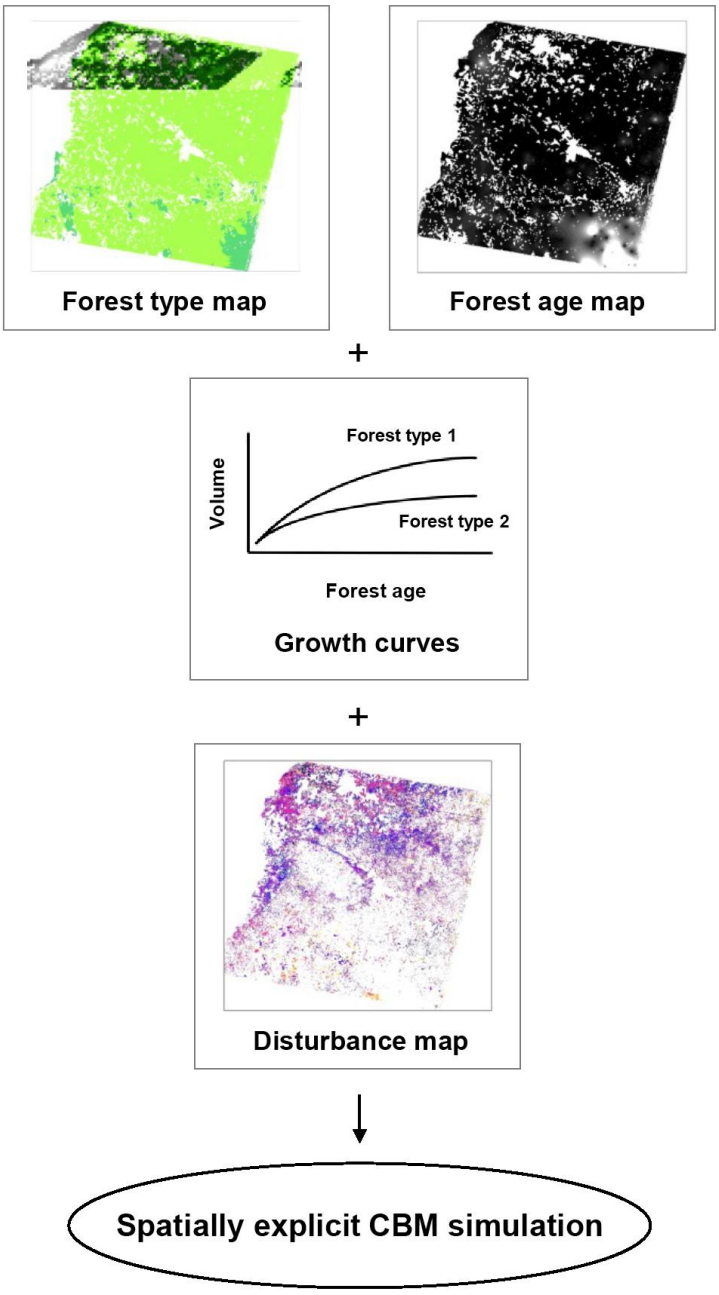

Recliner is capable of processing large raster datasets efficiently by making use of a "hash function." A hash function increases the speed with which a computer accesses large datasets by mapping them to smaller datasets on which the main processing will be conducted (Konheim 2010); Recliner's hash function identifies individual stands—pixels within the input rasters—that have common forest type, starting age, pattern of disturbances, and other characteristics, and then consolidates them into a table of records to be processed by the CBM-CFS3.

To demonstrate Recliner's operation we present the approach and results of a spatially explicit simulation of carbon dynamics within the USFS Nez Perce–Clearwater National Forest (NP). The NP contains ~1.6 million forested hectares in the northwestern US (see Figure 3.3 in Section 3); it has considerable spatial variation in species composition (Figure 5.2a), stand age (Figure 5.2b), and climate (Figure 5.2c), owing to terrain that spans more than 2000 m in elevation, and has as well spatiotemporal variation in the frequency and magnitude of natural and anthropogenic disturbances (Figures 5.3).

Figure 5.2 Tree species composition and stand age, in 2004, and average annual temperature, in the Nez Perce–Clearwater National Forest

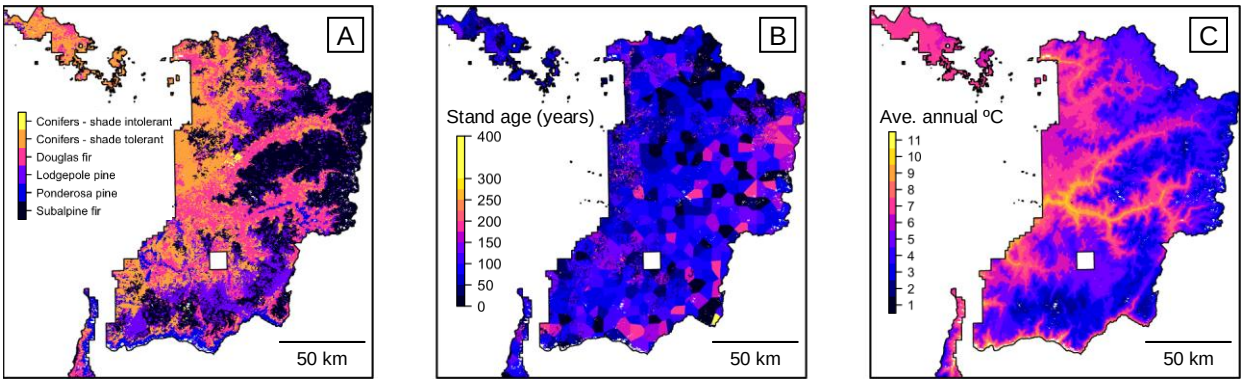

Note: A) Tree species composition, as estimated by USFS R1 Dominance Type, in 2004. B) Stand age in 2004. C) Average annual temperature. US Stand age ranged to 812 years, but the scale in (B) stops at 400, as older stands—which constitute <0.01% of the landscape—cannot be discerned on the map.

Figure 5.3 Forest disturbances within the Nez Perce–Clearwater National Forest, 2004–2011

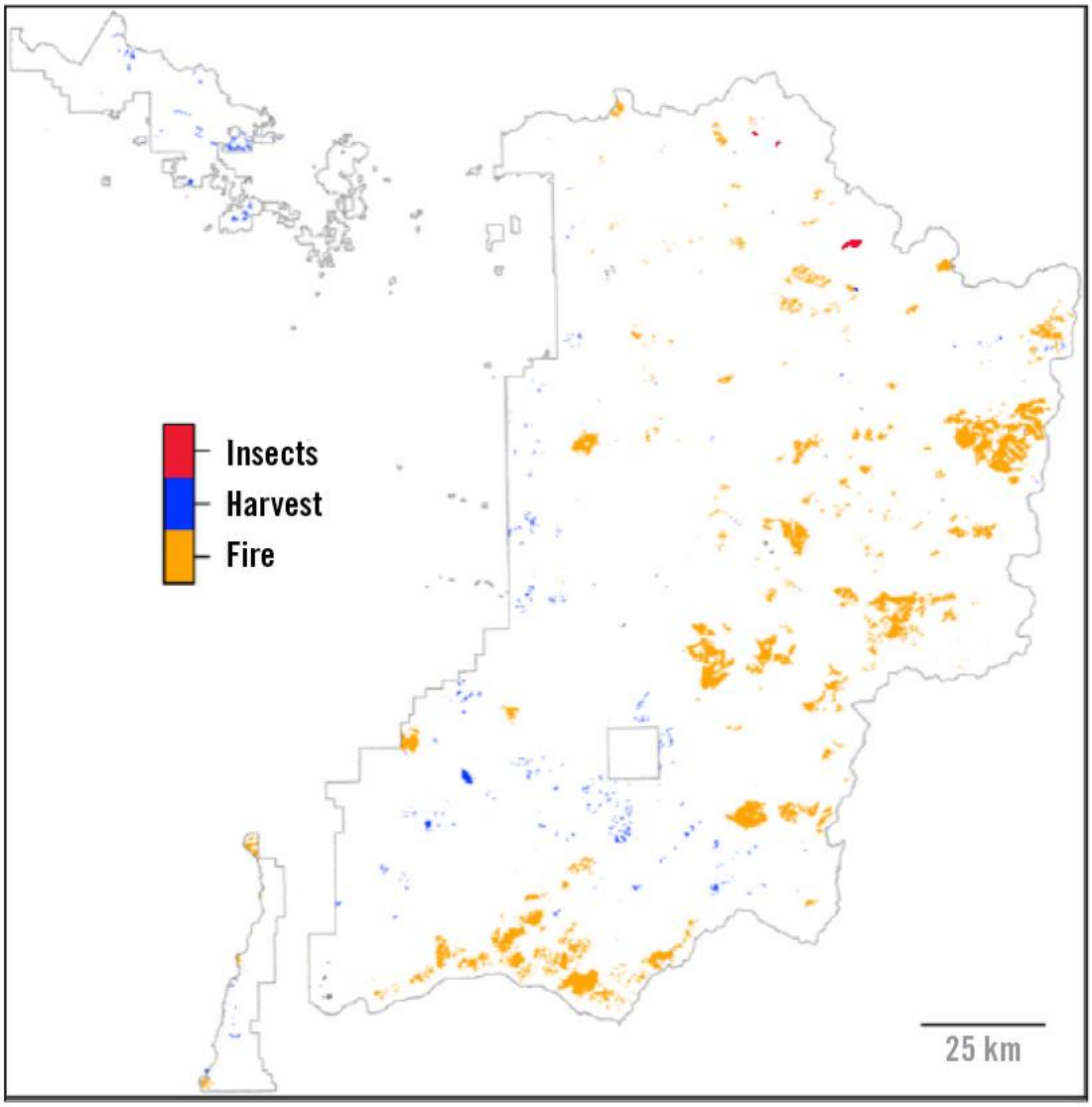

The raster datasets depicted in Figure 5.2, a–c, which we used in the simulation, were created using a variety of data sources and methods. The tree species composition raster was clipped from the USFS map of dominance type for USFS Region 1, which was a reclassification based on algorithms described by Barber et al. (2011) of the Ruefenacht et al. (2008) map of forest type. We created the stand age raster using Voronoi tessellation (Okabe et al. 2000) of estimated stand ages in 2004 at inventory plots in the USFS Forest Inventory and Analysis program (<www.fia.fs.fed.us>), replacing estimates in areas of the tessellation with ones from USFS Common Stand Examinations (<www.fs.fed.us/nrm/fsveg/>) where these were available. The average annual temperature raster (used to inform modeling of temperature-dependent dead organic matter decay (Kurz et al. 2009)) was clipped from the PRISM Climate Group's raster of mean annual temperature across the US (<www.prism.oregonstate.edu/normals/>), which was generated using the PRISM interpolation method (Daly et al. 2008).

The disturbance rasters we used were created by researchers from the Wildland Resources Department at Utah State University, with the Vegetation Change Tracker algorithm (Huang et al. 2010) being run on the Landsat Time Series Stack (Huang et al. 2009) to estimate where and when disturbances occurred. The causes of these disturbances were assessed via post-processing manual classification, using the Landsat stack, Google Earth images, data from Monitoring Trends in Burn Severity (<www.mtbs.gov/>), US Forest Service Activity Tracking System (<www.fs.fed.us/nrm/index.shtml>), and Aerial Detection Survey (<www.fs.fed.us/>) programs (most details in Healey et al. 2014; others unpublished). The magnitudes of disturbance events were estimated using modeled changes in stand volume or percent canopy cover (most details in Healey et al. 2014; others unpublished), and were classified into four categories of change: 0–25%, 25–50%, 50–75%, and 75–100%. We reclassified these, respectively, to 12.5%, 37.5%, 62.5%, and 87.5%, for use with CBM-CFS3, given that the disturbance matrices associated with CBM-CFS3 disturbance types can specify only single values, rather than ranges of values, for disturbance-related carbon transfers among pools. All rasters were originally created at 30-m resolution and subsequently resampled to 90-m resolution.

Yield tables for the six USFS dominance types within the NP (Figure 5.4) were estimated by predicting volumes at the mid-points of 5-year age intervals from von Bertalanffy functions (von Bertalanffy 1934) that we fitted to estimated volumes, which had been modeled using the USFS Forest Vegetation Simulator (<www.fs.fed.us/fmsc/fvs/>), of FIA plots at ages estimated during censuses at irregular intervals.

Figure 5.4 Growth curves used in CBM-CFS3 simulation of the Nez Perce–Clearwater National Forest

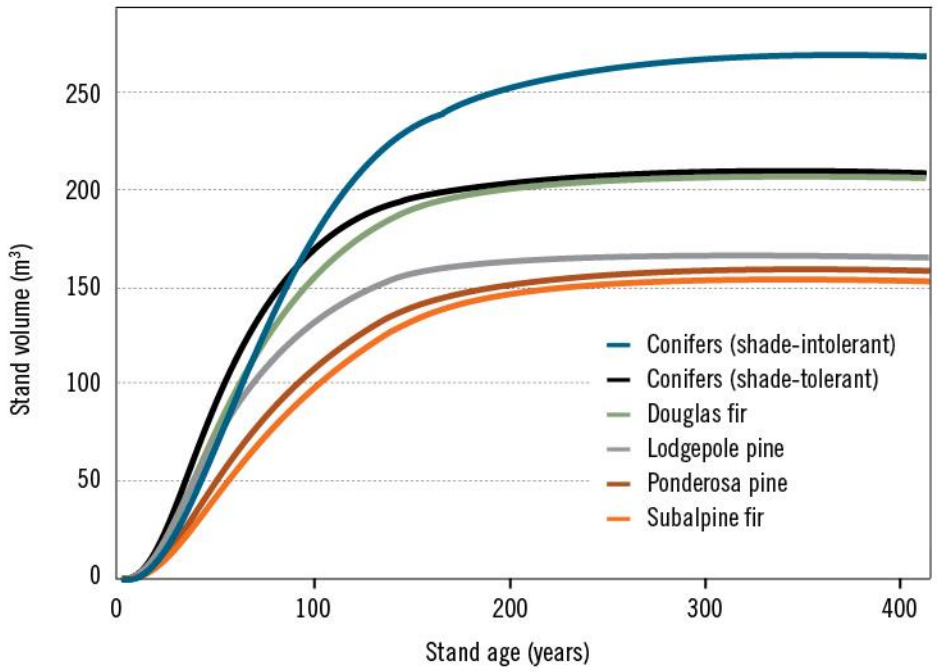

Note: CBM-CFS3 = Carbon Budget Model of the Canadian Forest Sector (Version 3).

Examples of results of the simulation appear in Figures 5.5 and 5.6. These are intended primarily as proof of concept, and our main interest is whether they are consistent with the data that were used in the simulation—in particular, that the carbon dynamics estimated by the CBM-CFS3 make sense in the context of the patterns of disturbance that were simulated. They do, as indicated by the inversely proportional correspondence between change over time in the ratio of NBP to NEP (Figure 5.6a) and by the amount of the landscape disturbed (Figure 5.6b); NBP was roughly 50% of NEP during the first year of the simulation (2004), indicating carbon losses that correspond to a moderate amount of fire and lesser amounts of harvest and insect attack; NBP then increased and was on par with NEP during 2005 and 2006, as the area affected by all three types of disturbance decreased. NBP decreased drastically—to roughly 10% of NEP, in 2007—with a pulse of burning in which the area burned increased by roughly 900%, and there were minor increases in harvest and insect attack. The next year saw the incidence of all three types of disturbance return to pre-2007 levels and NBP become roughly on par with NEP again; it remained so for the final three years of the simulation, with minor annual variation corresponding to minor variation in disturbance rates. The results suggest overall that carbon dynamics within the NP are driven strongly by fire.

The results demonstrate the utility and approach of Recliner to combine pixels with identical attributes. Such pre-processing of model inputs greatly reduces the number of unique pixels that need to be simulated. The additional time required for pre-processing of the input data is more than compensated for by the reduction in simulation time for the landscape. The results are then redistributed to all pixels in the landscape. However, as landscape complexity and the number of data layers increase (e.g., with climate data) and the number of pixels that can be combined decreases, the approach outlined here will become limiting. At present, this remains a pragmatic approach that enables use of the available tools to conduct spatially explicit simulations. An approach that will scale better to larger and more complex landscapes is under development.

Figure 5.5 Change in carbon stocks, by IPCC pool, over time, in the Nez Perce–Clearwater National Forest

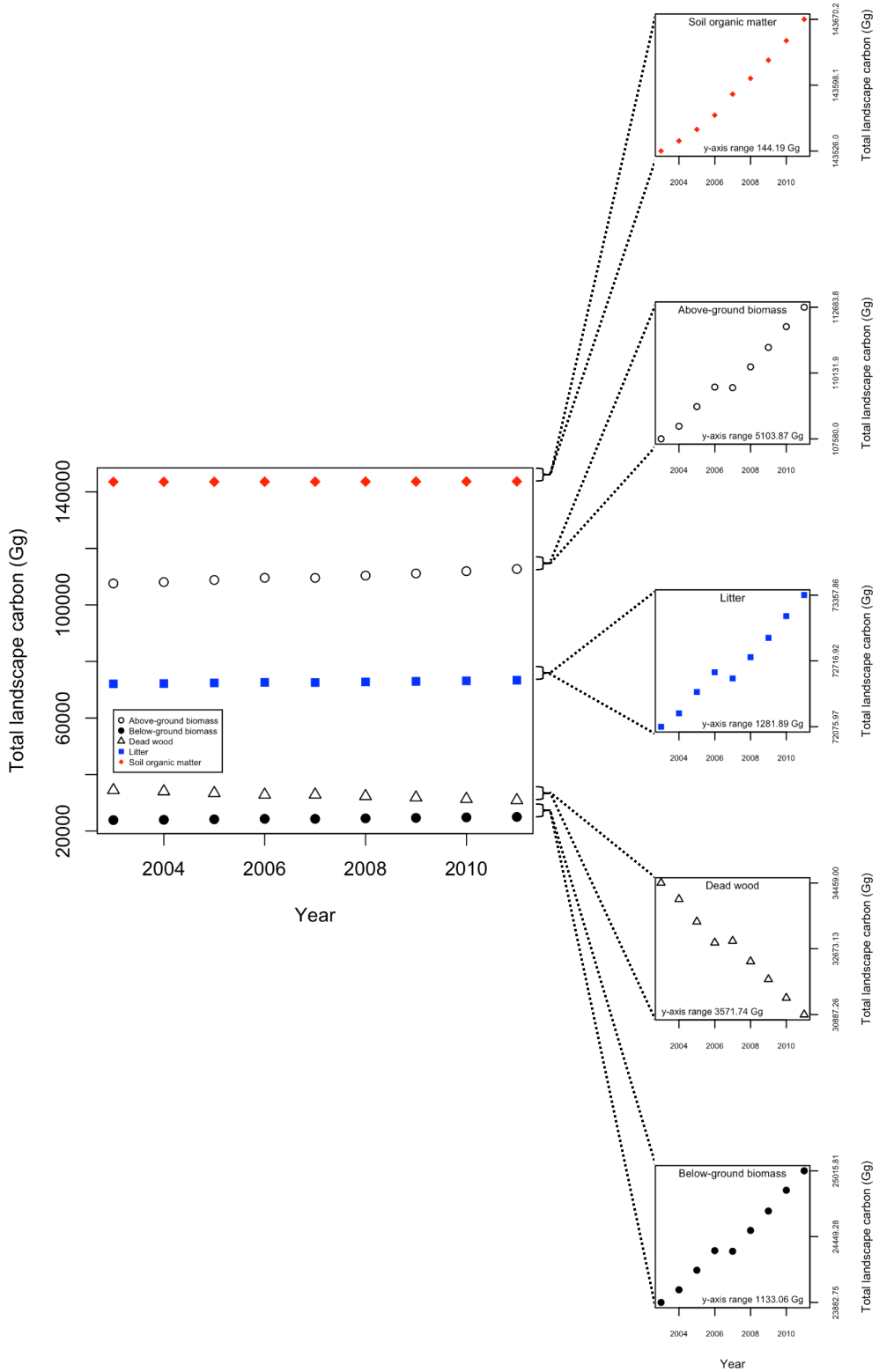

Note: The left side of the figure illustrates relative magnitudes of the patterns in stocks within the five IPCC carbon pools, while the right side illustrates their finer-scale variation over time.

Figure 5.6 Change in net primary production, net ecosystem production, and net biome production, over time, in the Nez Perce–Clearwater National Forest

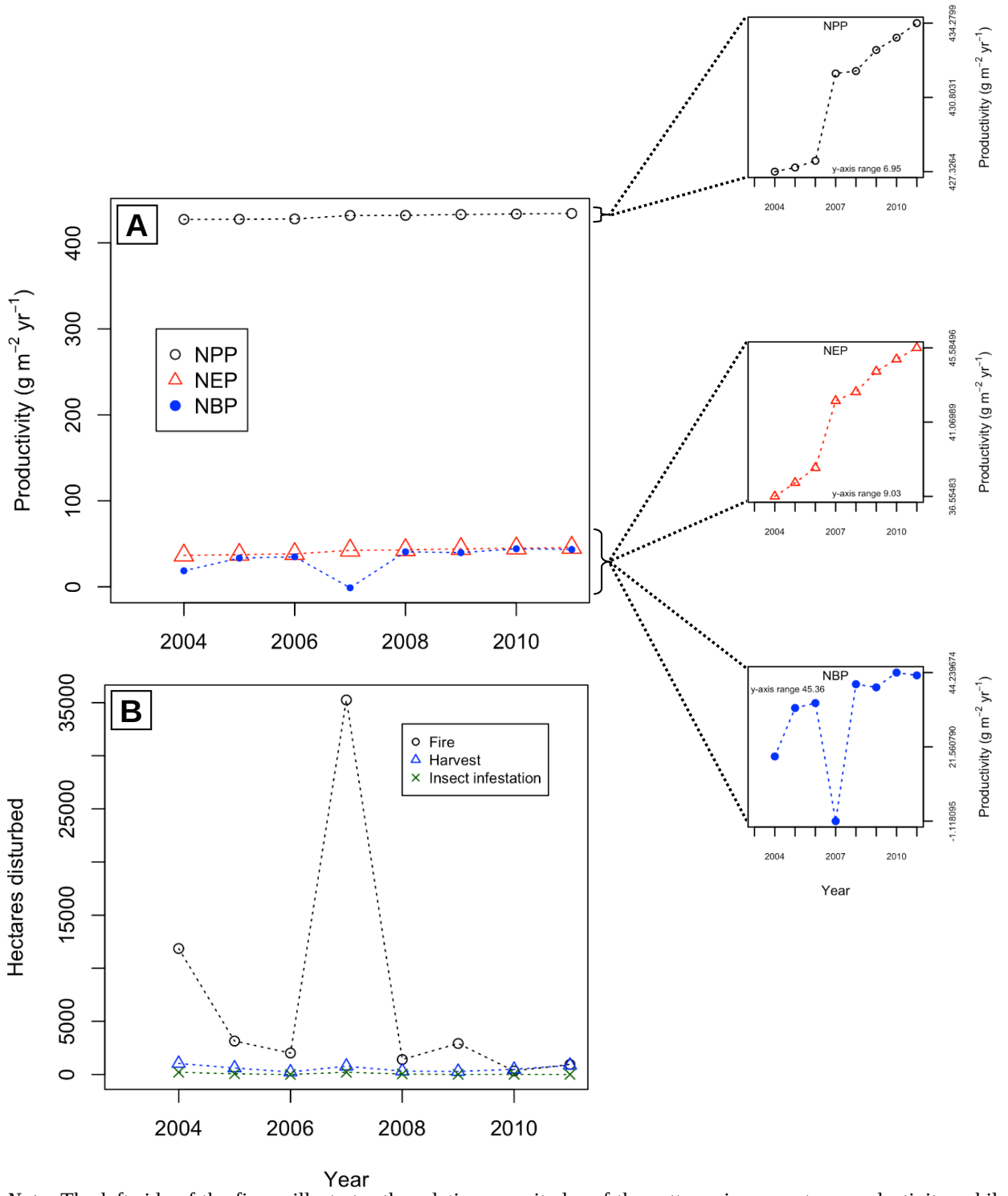

Note: The left side of the figure illustrates the relative magnitudes of the patterns in ecosystem productivity, while the right side illustrates their finer-scale variation over time. See Table 2.3 for a definition of the terms NPP, NEP, and NBP.

5.2 The impact of spatially explicit and spatially referenced approaches on estimates of GHG emissions and removals

One of the main advantages of conducting a spatially explicit simulation with forest inventory and activity data is that the distribution of disturbance events among stands according to the stands' characteristics is fully specified in the simulation. This reduces uncertainty in calculations of the carbon fluxes that result from each disturbance event, which in turn reduces uncertainty in the calculation of total landscape GHG balance over the analysis period. This is compliant with the IPCC recommendation that nations attempt to reduce uncertainties when reporting forest GHG balances to the UNFCCC.

We investigated the reductions in uncertainty that accompany complete specification of the distribution of disturbances among stands according to their characteristics, in CBM-CFS3 calculations of landscape-level forest carbon balances. We ran a series of sets of spatially referenced simulations of carbon dynamics over 2004–2011, within the NP, with the spatially referenced input data being summaries of the rasters used in the spatially explicit simulation (see Section 5.1, above, for details of the site and datasets). We progressively increased the specificity with which disturbances were allocated among individual stands. The results of each set of spatially referenced simulations were then compared to the results of the others and to the results of the spatially explicit simulation, to examine their relative precisions and accuracies.

In a spatially referenced simulation the individual stands affected by disturbances are not individually identified. Instead, the CBM-CFS3 uses rule-based algorithms to allocate the disturbance events among stands that are represented by records created at the outset from a non-georeferenced forest inventory. A user-provided input table specifies how many hectares of the landscape were occupied by stands according to their different sets of characteristics (forest type, forest age, and other classifiers), at the start of the simulation period. The stands are then disturbed during the simulation according to an input table that specifies how many hectares of forest with different characteristics to target by each disturbance type during each year of the simulation (Table 5.1). When a disturbance and its associated carbon fluxes and transfers are simulated, all stand records with the specified characteristics are sorted either randomly or by user-specified rules, and the sorted stands are disturbed sequentially until the target defined by area, volume or proportion of eligible stands is reached.

Table 5.1 Examples of spatially referenced targeting of stands for disturbance

Targeting stands randomly with respect to leading species and age

Leading species	Age (yrs)	Disturbance	Ha to disturb	# of stands to disturb
any	any	clear-cut	500	50
any	any	wildfire	600	60

Targeting stands by leading species but randomly with respect to age

Leading species	Age (yrs)	Disturbance	Ha to disturb	# of stands to disturb
Lodgepole pine	any	clear-cut	200	20
Grand fir	any	"	300	30
Lodgepole pine	any	wildfire	300	30
Grand fir	any	"	300	30

Targeting stands by both leading species and age

Leading species	Age (yrs)	Disturbance	Ha to disturb	# of stands to disturb
Lodgepole pine	40–50	clear-cut	100	10
"	60–70	"	100	10
Grand fir	40–50	"	150	15
"	60–70	"	150	15
Lodgepole pine	40–50	wildfire	200	20
"	60–70	"	100	10
Grand fir	40–50	"	180	18
"	60–70	"	120	12

Note: Spatially referenced targeting of stands for disturbance (assuming 10-hectare [ha] stands) is done according to rules that specify the characteristics by which stands should be targeted. Stands can be targeted by any combination of characteristics. The table illustrates more-specific targeting of stands for disturbance, with the total number of stands being disturbed kept constant (50 by clearcut, 60 by wildfire) but these being progressively more stratified according to their characteristics.

To conduct our investigation we created tables of spatially referenced data from the rasters and conducted four sets of spatially referenced simulations, with the sets increasing in how precisely stands were targeted for disturbance by their characteristics. We calculated cumulative NBP in 400 runs for each of the four sets. We considered the spatially explicit simulation described above in Section 5.1 to provide estimates "closest to truth." The precision of the spatially referenced runs increased—within-set variation in NBP decreased—as stands were targeted more precisely for disturbance by their characteristics (Figure 5.7). Surprisingly however, accuracy decreased rather than increased when compared to the spatially explicit simulation, as the within-set average NBP came to differ more from the spatially explicit NBP estimate (Figure 5.7).

Figure 5.7 Cumulative NBP from four sets of spatially referenced simulations

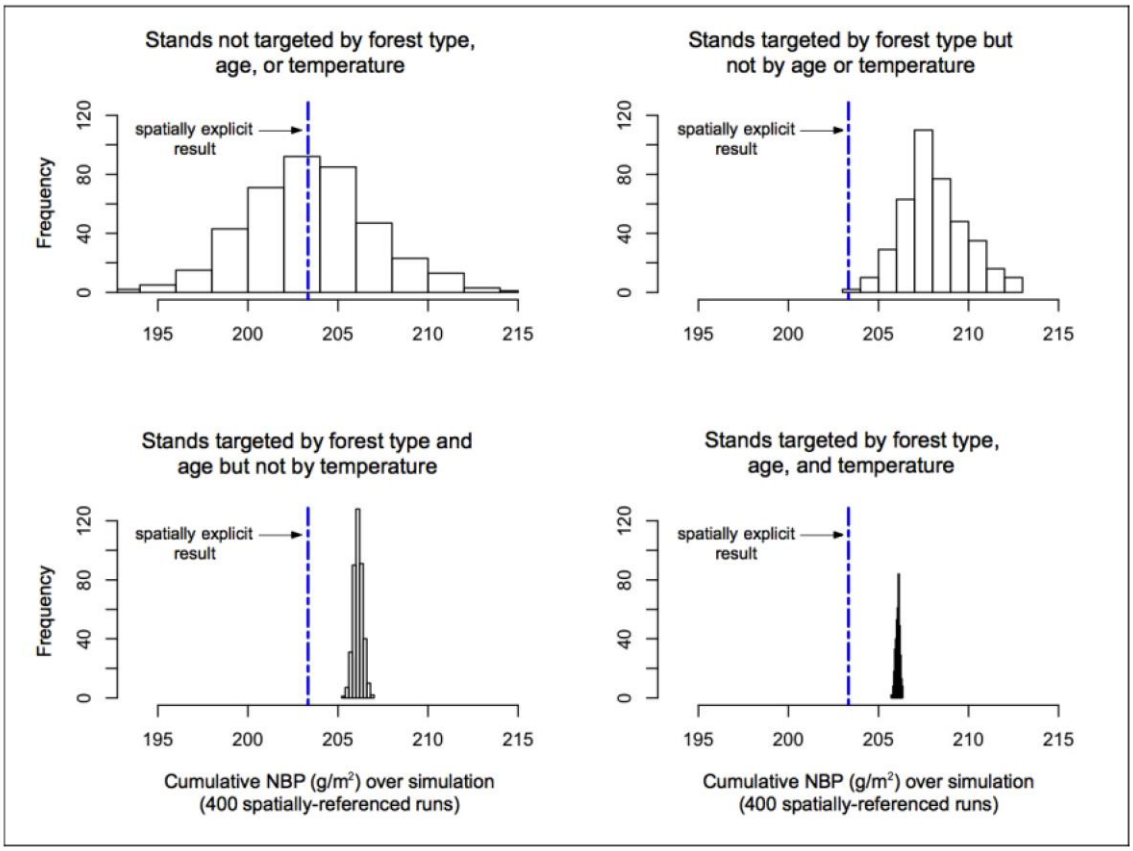

Note: The specificity with which stands were targeted for disturbance was progressively increased. Results are compared to cumulative NBP from a spatially explicit simulation of the same landscape. NBP = net biome production; g/m^2 = grams per square meter.

We suspected that accuracy decreased because targeting stands more specifically by their characteristics makes fewer stands eligible for each disturbance event, increasing the chance that individual stands will receive repeat disturbances during the simulation. Previously disturbed stands have reduced carbon stocks, in which case a second disturbance will cause less carbon loss and thereby increased NBP relative to "true" NBP as estimated by the spatially explicit result. We investigated this by repeating the fourth set of spatially explicit simulations—in which stands were targeted for disturbance with greatest specificity—but this time prohibiting repeat disturbances. This increased the simulation accuracy, bringing average within-set NBP close to the spatially explicit NBP estimate (Figure 5.8).

Figure 5.8 Cumulative NBP from four sets of spatially explicit simulations, with repeat disturbances prohibited

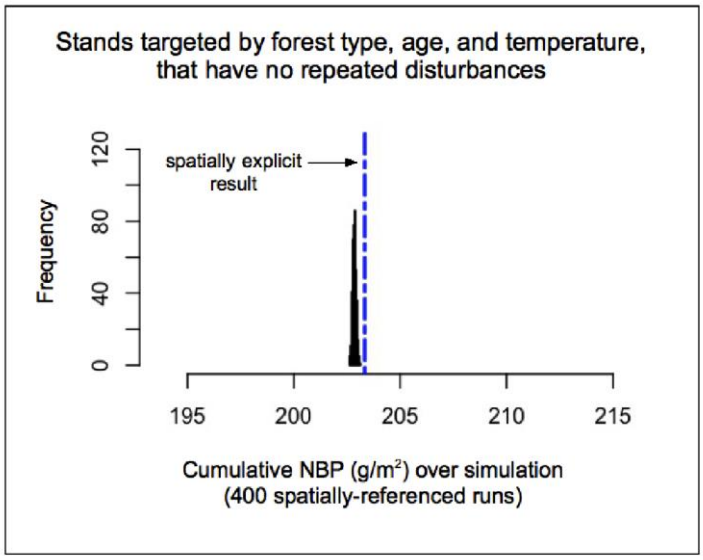

Note: NBP = net biome production; g/m^2 = grams per square meter.

Prohibiting repeat disturbances, however, resulted in smaller estimates of cumulative NBP than in the spatially explicit run. This is because 90 ha of repeat disturbances did in fact occur in the landscape, as recorded in the original disturbance data.

In summary, we investigated uncertainties introduced into Tier 3 carbon budget simulation by data that imprecisely identify which stands were affected by disturbances within the landscape being modeled. The results suggest that precise data on how disturbances were distributed among stands with respect to their characteristics can reduce uncertainties in calculations of landscape carbon balance.

6. Impacts of Activity Data on Estimates of GHG Fluxes

V.S. Mascorro, W.A. Kurz, N. Coops, M. Fellows, M. Olguin

Remote sensing is one of the primary sources of observations of land-cover changes for carbon studies and other ecological applications due to its ability to periodically monitor the Earth's surface, including areas that otherwise are difficult to access (Coops et al. 2006; Wulder et al. 2010). With the ready availability of remotely sensed data, an increasing number of regional and global-scale studies and products has been developed specifically for forest carbon monitoring and REDD+ at different spatial and temporal scales (Achard et al. 2014; Asner et al. 2010; Baccini et al. 2012; Saatchi et al. 2011).

This section emphasizes activity data derived from remote sensing observations from Landsat and Moderate Resolution Imaging Spectroradiometer (MODIS) satellites, two of the most commonly used satellite datasets for land-cover change studies worldwide. Four remote sensing products—two land-cover change maps and two thematic maps—with different spatial and temporal resolutions were compiled to provide inputs of activity data to the CBM-CFS3 and to compare their impacts on estimates of forest carbon dynamics (see Table 6.1).

Two spatially explicit layers were derived from each of the four remote sensing products, one with areas of change and no-change, and the second attributing the change to its underlying disturbance cause. Data were pre-processed with the Recliner tool (see Section 5.1). Annual carbon fluxes were estimated with the CBM-CFS3 from 2002 to 2010 over a 180 x 180 kilometer (km) pilot study area of tropical forests in the Yucatan Peninsula, an area of special interest selected as an "early action" region for REDD+ in Mexico (see blue area in Figure 3.3, Section 3).

Table 6.1 Remote sensing products used as activity data inputs for carbon modeling in the Yucatan Peninsula, from 2002 to 2010

Map alias	Source	Type	Satellite	Spatial resolution	Temporality
VCT	NASA	Vegetation Change Tracker map	LANDSAT	30m	2003, 2004, 2005, 2007, 2008 & 2010
Hansen	University of Maryland	Forest cover loss map	LANDSAT	30m	2002, 2003… 2010
INEGI	INEGI	Classification map	LANDSAT-SPOT	30m (25ha MMU)	2002-2005, 2005-2007, 2007-2011
MODIS	NALCMS/ CONABIO	Classification map	MODIS	250m	2005, 2006… 2010

* MMU: Minimum mapping unit

Source: Mascorro 2014.

In this study, the activity data used for the carbon budget model simulations were derived following the third approach defined by the IPCC (spatially explicit monitoring changes in area or changes between categories, IPCC 2003). Prior to deriving activity data for a forest monitoring system, countries need to establish their definition of forests, deforestation and degradation. For the purpose of this study, the definitions of forest, deforestation, and degradation are those used by the institutions that developed the remote sensing and mapping products. The ability to detect land-cover changes is limited by the spatial resolution of the remote sensing products. (See also Section 6.3)

6.1 How to characterize land-cover changes by disturbance type

Consistent observations of natural and human-induced disturbances that alter the forest structure over time and space are crucial for quantifying changes in the distribution of carbon that is stored in the vegetation and soils, and the corresponding GHG emissions. Each disturbance type affects the landscape in a unique way that can be described by a disturbance matrix (see Section 3.6) that quantifies how much plant biomass was killed; transferred to litter, coarse woody debris, or soil organic carbon; emitted to the atmosphere; or transferred to the forest product sector (Kull et al. 2011; Kurz et al. 1992). Therefore, the accurate estimation of carbon uptake, storage and releases following disturbance requires detailed observations of the areas affected by each disturbance type (Kurz 2010a; Kurz et al. 2009; Spalding 2009).

Knowledge of forest recovery and succession dynamics following disturbance is essential for making reliable predictions about future carbon emissions and removals to assess alternative mitigation scenarios (Kurz 2010a). It is important that countries identify the specific drivers of change in post-disturbance dynamics—forest mortality, decomposition and regrowth—to quantify their individual contributions to the forest carbon dynamics. Following disturbance, the CBM-CFS3 can simulate either regrowth of the same stand type or transitions to other stand types. Based on the stage of stand development and the ecological characteristics of the site, litter fall and decomposition rates are applied, including yield data, to represent natural mortality and forest regrowth.

In this section a comprehensive approach is introduced—the Multi-Scale, Multi-Source Disturbance (MS-D) assessment approach to attributing land-cover change observations by agent of disturbance (Mascorro et al. 2014). This approach integrates remotely sensed data, forest inventory, and ancillary datasets to attribute the land-cover change observations to the most likely disturbance type (natural or anthropogenic), following three main steps:

1. Derive annual spatially explicit layers, by disturbance type.
2. Derive land-cover change observations.
3. Attribute the land-cover changes to their underlying disturbance driver.

A number of major forest disturbance types from national historical records—namely fires, hurricanes, and forest management areas—were characterized in a spatially explicit way on an annual basis in the Yucatan Peninsula from 2005 to 2010. This period was selected based on data availability. Using forest inventory data, forest losses for the study period were estimated from the first forest inventory sampling cycle (2004–2009) and the re-measurement cycle (2009–2013), computing the difference in mean basal

area per hectare for each plot between the two periods. Basal area losses can be explained by tree mortality as the consequence of natural disturbances (e.g., fires, hurricanes) or as a result of tree removals due to harvesting activities (Healey et al. 2006).

Annual spatially explicit layers of forest disturbance types were overlapped with the plots that registered a basal area loss. A regression tree analysis was then used to assess the contribution of each disturbance type—in this case fires, forest management areas, and hurricane categories—as variables that explain the observed reductions in basal area. The technique automatically separates the response variable (reduction in basal area) into a series of choices that identifies the relevance of each constraining variable (De'ath and Fabricius 2000; De'ath 2002; Melendez et al. 2006). At each node, the disturbance types are automatically selected to provide the best partitioning of the data that minimizes the sum of squares of the basal area loss.

6.2 Activity data derived from remote sensing products

Four remote sensing products where obtained from Landsat (VCT, Hansen, INEGI) and MODIS satellites to obtain land-cover changes. These were overlaid with the spatially explicit maps of forest disturbance types. The land-cover change observations were attributed to the most likely disturbance driver according to the relevance authority resulting from the regression tree analysis (Mascorro et al. 2014). A road map was used to characterize the permanent conversion of forestlands to non-forest lands caused by settlement (INEGI 2013). In addition to the roads layer, embedded in the classification maps, land-cover classes that changed to urban areas were attributed as settlement (see Figures 6.1 and 6.2).

Figure 6.1 Land-cover change maps derived from different remote-sensing products

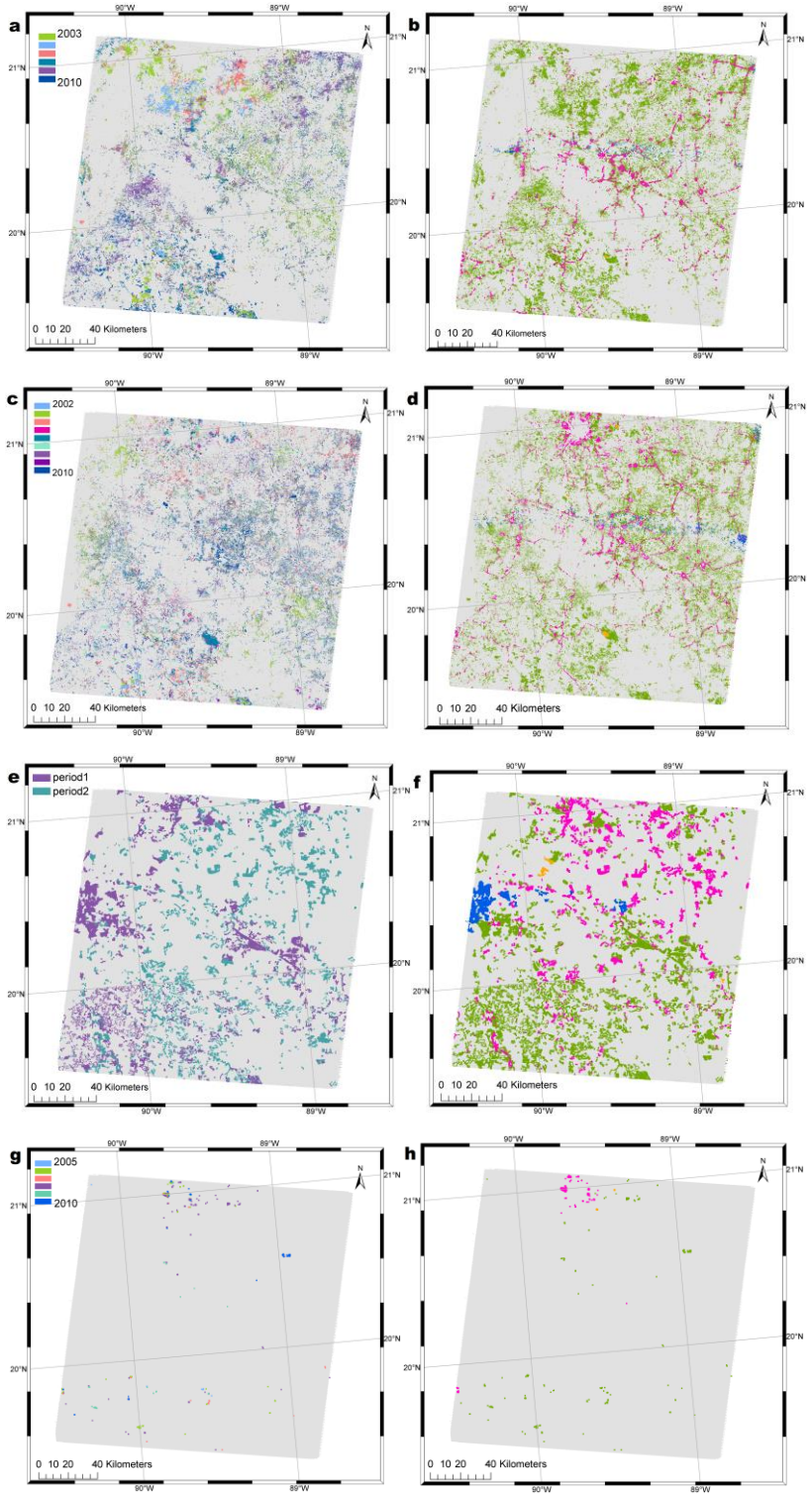

Note: VCT map: (a) and (b); Hansen map: (c) and (d). INEGI maps: (e) and (f); and the MODIS maps: (g) and (h). Left-side maps show annual non-attributed disturbances, right-side show attributed disturbances: green = harvest; pink = settlement; blue = hurricane, orange = fire**.**

Source: Mascorro et al. 2016

Figure 6.2 Annual area (hectares) changed, by disturbance type, derived from different remote sensing land-cover-change products

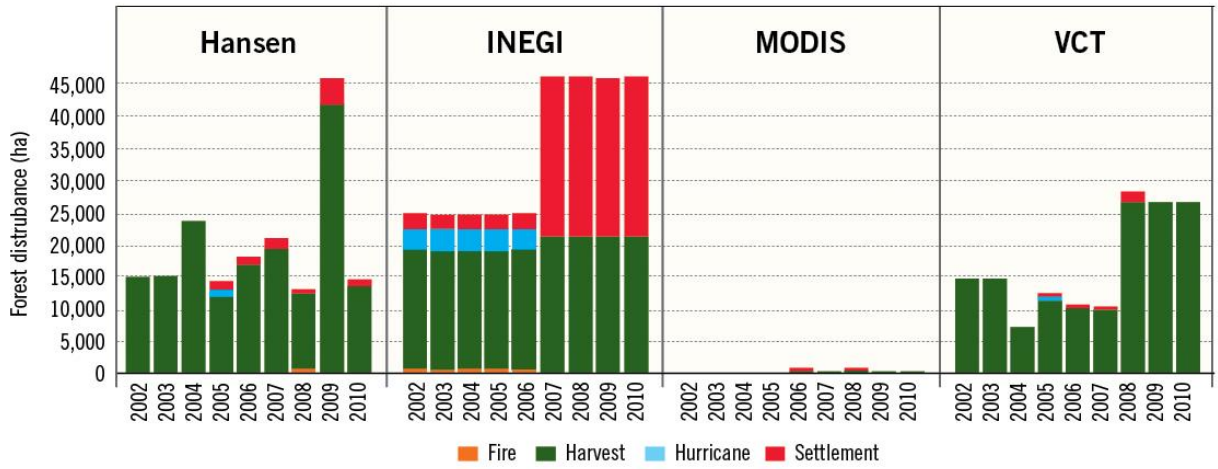

The resulting spatially explicit layers were then used as activity data input for CBM-CFS3 to estimate their effect on the annual carbon emissions and removals from 2002 to 2010 (see Figure 6.3). This approach allows us to combine the best available information from remote sensing products, forest inventories and ancillary datasets developed by various researchers and institutions. Mapping disturbances and attributing observed land-cover changes to the appropriate disturbance type, using the MS-D approach, provides a cost-effective solution to obtaining activity data for carbon modeling and other ecological applications (Mascorro et al. 2014). Its flexibility permits integration of spatially referenced and/or spatially explicit data on an annual or multi-year basis, to characterize forest disturbances by type and attribute changes in land-cover to their underlying causes. Moreover, it provides methods to replicate the study in other "REDD early action" areas of Mexico and other countries.

Figure 6.3 Annual carbon fluxes in the Yucatan Peninsula, 2002–2010, estimated with different sources of activity data

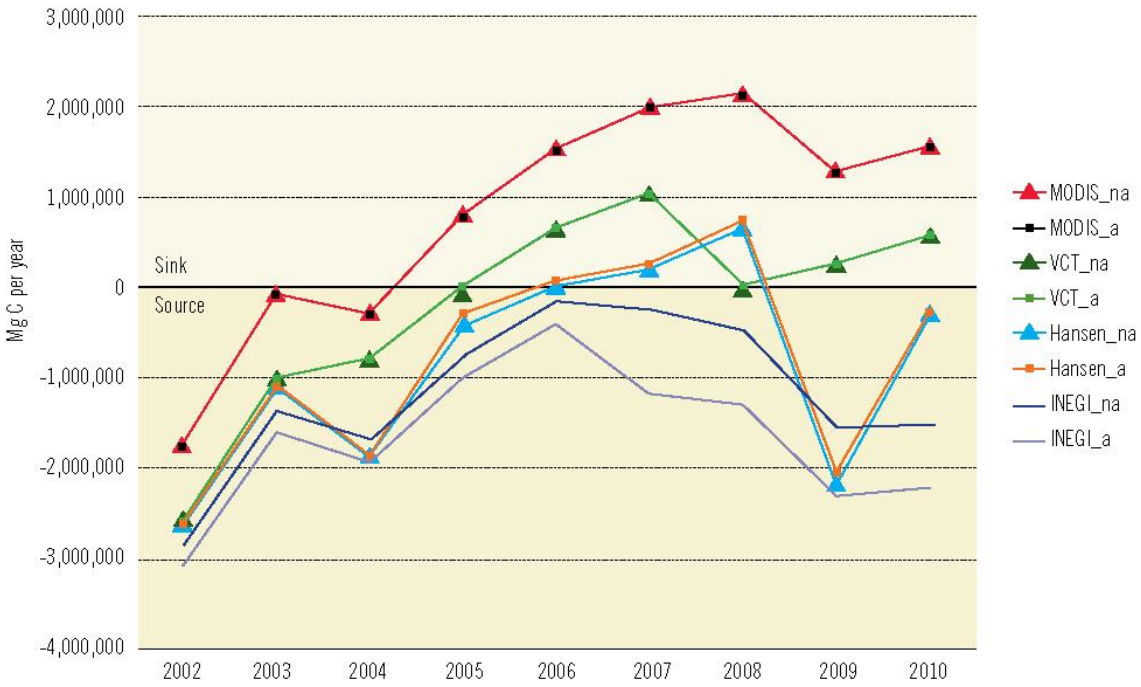

Note: MgC = megagrams of carbon; a = attributed; na = non-attributed
Source: Mascorro 2014

Combining data sources provides a cost-effective approach to reducing uncertainties and increases their potential use for forest monitoring and REDD+, often filling the spatial and temporal gaps between them. Strategies to develop a national monitoring reporting and verification system should include a combination of data sources, not only from remote sensing products, but also from ground-based measurements, intensive monitoring sites, and ancillary datasets.

Results from this study provided insights into which of the following considerations (increased spatial resolution, annual observations, or attributing changes to corresponding disturbance types) are the most critical for deriving activity data for carbon budget modeling.

6.3 Spatial resolution

The differences in results from carbon simulations generated with MODIS and Landsat-derived disturbance observations suggest that increased spatial resolution should be the first priority when deriving activity data for carbon modeling in heterogenous landscapes. Carbon simulations derived from Landsat-based products at higher spatial resolution identified substantially more land-cover changes. In the VCT and the Hansen simulations, the carbon emissions and removals reflect the interannual variations in activity data. In contrast, the coarse resolution of MODIS-derived products detected much fewer land cover changes and generated unrealistic estimates of the carbon balance. The observed land cover

changes were few, despite having MODIS observations on an annual basis from 2005 to 2010. While MODIS satellite imagery can help identify large disturbances, results from this study showed that this coarse spatial-scale satellite imagery has limited ability to provide activity data for carbon modeling in areas with frequent small-scale disturbances. Typically, satellite imagery from this sensor has focused on studies over large areas.

6.4 Annual observations

Reliable estimates of carbon dynamics require detailed observations of drivers of change, on an annual basis (Kurz 2010a). Carbon fluxes predicted with the Hansen product showed a decrease in total ecosystem carbon content in 2009. However, due to the lack of data and of cloud-free image availability, no disturbance events were detected in 2009 with VCT, and so, corresponding decreases in the carbon stocks from the disturbance events were not reflected in the CBM-CFS3 estimates, despite the fact that the disturbance events observed in 2010 were distributed equally between 2009 and 2010.This result showed that even missing a single year in the land-cover observations can lead to substantial errors—especially in ecosystems with rapid-regrowth forests, such as those of the Yucatan Peninsula. The latter trend was observed in both the attributed and the non-attributed observations; which made having annual observations a higher priority than the attribution.

6.5 Attribution of land-cover changes to disturbance type

Identifying the disturbance driver of land-cover change is essential for accurately quantifying its particular impact on forest carbon dynamics. Each disturbance type affects the forest structure and successional dynamics in a unique way, changing the amount of carbon that is stored in vegetation and soils and released into the atmosphere. While 86% of the MODIS land-cover change pixels were attributed to specific disturbance types, due to the product's coarse spatial resolution the difference between attributed and non-attributed observations was not perceptible in the simulation runs.

When increasing the spatial resolution using Landsat observations, only a small percentage of the land-cover change detected was attributed by disturbance type, ascribing most of it as harvesting. However, in the INEGI product's classification approach, the larger areas of change detected over the second-period observations showed that attributing changes by disturbance type is a worthwhile investment. In the second period, the non-attributed estimates dropped 84% more than the attributed ones, yielding higher emissions (3.2 million MgC more). These differences between with and without attribution would be even more pronounced if they were reported as CO_2-equivalent emissions (as required in REDD+ projects), because fires cause additional non-CO_2 GHG emissions (in the form of CH_4 and N_2O), with much higher global warming potentials than CO_2 (Mascorro et al. 2016).

Results summarized here show that average annual differences in the carbon balance estimates obtained from the biggest sink of MODIS and the biggest source of INEGI-derived products reached 2.46 Tg C yr^{-1}. When extrapolating this difference from the area covered by a single Landsat scene to all of Mexico it becomes apparent that investing into high-resolution, annual estimates of land-cover changes with attribution to disturbance types will substantially reduce uncertainties in GHG emission estimates.

7. Estimating Past and Projected Future GHG Emissions

M. Olguín, W.A. Kurz, C. Wayson, M. Fellows, V. Maldonado, D. López-Merlín, O. Carrillo, G. Ángeles

The CBM-CFS3 was selected to conduct state-level analyses in Mexico, because it is a modeling framework that can integrate forest inventory information, growth and yield curves, and activity data about natural and/or anthropogenic disturbances events. In Mexico such information is available or under development at the national scale (e.g., National Forest and Soils Inventory, Conafor 2010; land cover time series from 1990 to 2010, Gebhardt et al. 2014). Also, initial tests of the model at regional scales have shown that this approach is suitable for monitoring recent impacts and projecting future impacts of land-use and land-cover changes on GHG emissions and removals, both at stand and landscape levels (Olguín et al. 2011).

Details on the modeling approach and inputs necessary for the parameterization of the CBM-CFS3 have been widely documented in the literature (Kull et al. 2011; Kurz et al. 2009; Stinson et al. 2011). In addition, the approach follows the 2006 IPCC Guidelines for preparing GHG inventories based on a Tier 3 approach. The analyses presented in this section use the CBM-CFS3 model, with the appropriate modification of parameters and input data to represent forest carbon dynamics in strategic landscapes of the Yucatan Peninsula (Olguín et al. 2015), including a historic scenario from 1995 to 2010, and several future scenarios of REDD+ activities from 2011 to 2030. These efforts contribute to the knowledge and tools to support the regional-scale monitoring of GHG fluxes and the analysis of future GHG emissions and removals resulting from possible REDD+ scenarios.

7.1 Model components and data sources

Spatial framework for model implementation

The initial steps in simulating forest carbon dynamics using the CBM-CFS3 are to stratify the territory into spatial units (SPUs), and to reference all inventory and activity data to these SPUs. This facilitates the integration of inputs with different spatial resolutions within a single assessment framework (Kurz et al. 2009), following the spatially referenced approach (Reporting Method 1) of the IPCC 2006 Guidelines (IPCC 2006). For Mexico we created SPUs by intersecting the boundaries of the 32 federal states and the ecoregions of North America Level 1 (CEC 1997). This resulted in 94 SPUs for Mexico (Figure 7.1) (Olguín et al. 2015).

Figure 7.1 Distribution of 7 North American ecoregions (Level I) intersected with the 32 Mexican states

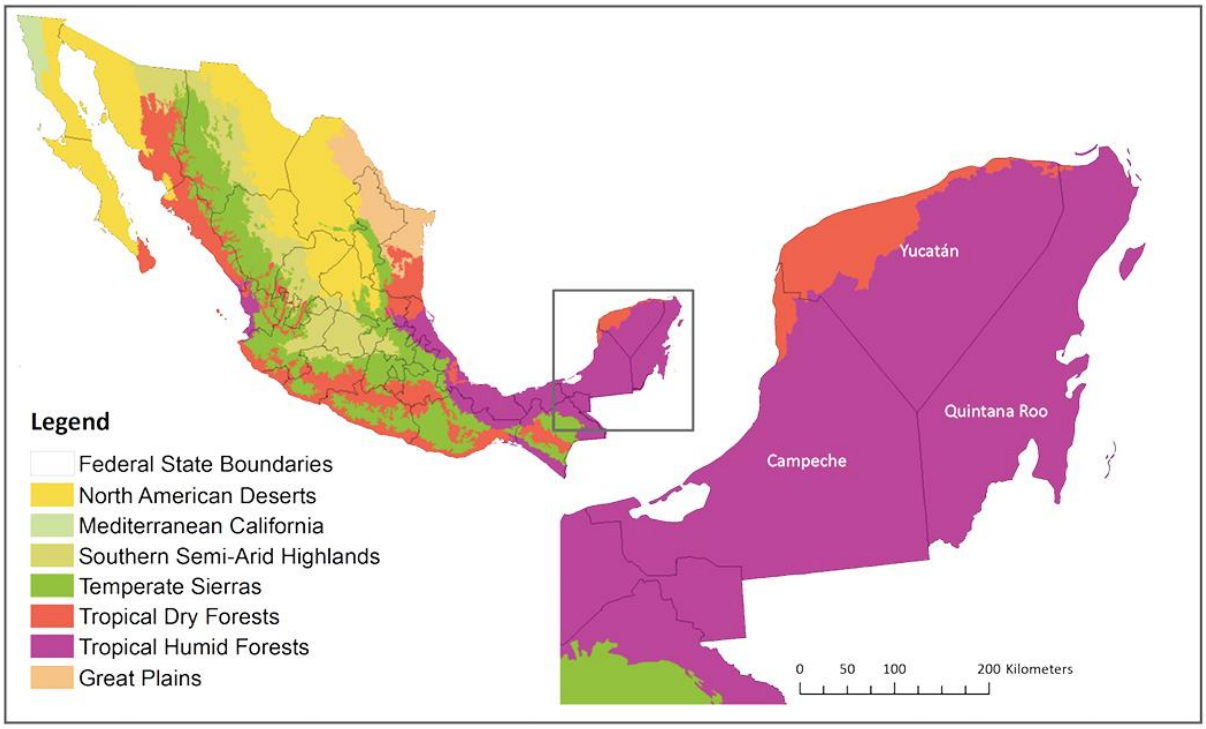

Note: This study is limited to the two ecoregions present in the Yucatan Peninsula.

The total area selected for this study included most of the forested area in the states of Campeche, Quintana Roo and Yucatán (but excluded all mangrove forests). The Yucatan Peninsula is characterized by two ecoregions—tropical humid forests and tropical dry forests—resulting in six spatial units (Figure 7.1). To understand the dynamics of carbon fluxes at a more detailed level within each SPU, we assigned the following classifiers to each stand record: 1) *Ecoregions level IV* (adds detailed information on climate, topography, vegetation types); 2) *Forest cover type* (based on the national forest monitoring system); 3) *Forest condition* (such as forests under a management plan or a protected area; see CEC 2010); and 4) *REDD+* status (i.e., whether or not forests are located within an early action area for REDD+ activities; see Conafor 2012).

Based on the above stratification scheme, we generated the necessary inputs to conduct preliminary runs with the model, using information that is available at the national scale so that these analyses can eventually be expanded from the three states to other forest areas of Mexico (Olguín et al. 2015).

Forest growth and age-class structure

To generate information about forest growth and age-class structure as input to the model, we used aboveground biomass estimates at the plot level, derived from measurement and re-measurement data from the National Forest Inventory and Soils plots (Conafor 2010, 2014a). From these plots we generated seven merchantable volume and biomass growth curves to represent specific growth conditions in the region (Ángeles, in prep.) and generated an initial age-class structure using plot-level biomass content as

a proxy of time since major stand disturbance (Olguín et al. 2015; Wayson et al., in prep.). In the absence of inventory data for 1995, we then made the simplifying assumption that the observed age-class structure of each of these SPUs applies to the initial conditions in 1995, the start year of the model simulations. No inventory rollback was undertaken, in part because the inventory information was collected over a period of years and cannot be attributed to a single year. The impact of this simplifying assumption can be examined further in the future, for example by using the disturbance data from 1995 to 2002 to conduct an inventory rollback to 1995 (see Section 3.2).

Activity data

In accordance with IPCC good practice guidelines (IPCC 2014a), the CBM-CFS3 model was used to account for the emissions and removals that take place during a given period of time that result from the impacts of natural disturbances and human activities (i.e., activity data). Thus, our main focus was on the compilation, harmonization and integration of activity data available from multiple sources (e.g., remote sensing products, forest inventories, official statistics, and expert knowledge) into an internally consistent framework, to assess the effect of disturbances such as deforestation, forest regrowth and fires on the net forest ecosystem carbon balance of the region.

Deforestation and reforestation events. To estimate the area affected annually by land-use/land-cover changes, we used available national-scale land-cover and land-use maps for 1993, 2002, 2007 and 2011, provided by Mexico's National Institute of Statistics and Geography (INEGI) and intersected the study area with these four maps. We reclassified INEGI's map labels according to the 13 land-cover classes proposed by Gebhardt et al. (2014), to be consistent with land-cover data that will soon become available as part of the Mexican MRV system (MAD-MEX) (Gebhardt et al. 2014). This information was then joined with the maps of ecoregion level IV, protected areas, managed forest areas and the REDD+ early action areas. Based on this new map we generated annualized land-cover transition matrices for each period of change—1993–2002, 2002–2007 and 2007–2011—for each of the six spatial units (Table 7.1). Finally, we created an input file of the area annually disturbed by partitioning the change over the observation period into annual changes for each land-cover/land-use (LC/LU) change category, for every transition matrix and spatial unit.

Table 7.1 Example of a land-cover/land-use (LC/LU) change matrix for the Tropical Humid Forest ecoregion within the states of the Yucatan Peninsula (three spatial units), using INEGI LC/LU, for years 2002 (series III) and 2007 (series IV)

2002 land type	Area (ha) change from 2002 - 2007						
	Oak forest	Mixed forest	Humid forest	Dry forest	Non-forest	Others	Total
Oak forest	7.852		172		561		8,586
Mixed forest		2,953	607		338		3,898
Humid forest		1,061	6,268,561	16,022	107,772	8.739	6,402,155
Dry forest		111	63,409	3,300,862	148,221	626	3,513,230
Non-forest	585	4,746	131,878	91,554	1,915,202	4,198	2,148,163
Others			2,668	194	2,922	432,921	438,705
Total	8.437	8,871	6,467,295	3,408,633	2,175,015	446,484	**12,514,736**

Note: Blue: transitions from non-forest land-use class to forest Red: transitions from forest land-use class to non-forest. Gray: forest cover classes that remained unchanged. All other land-use/land cover changes reported in this table were not considered in the simulations (e.g., classification errors). Cells without numbers: represent no changes to or from that land-use class. ha = hectares.

Fire events. We compiled and analyzed available state-level, official statistics on area burned, by stratum (trees/regeneration, scrubs, herbs/grasslands), from Conafor from 1995 to 2013 (Conafor 2014b). Because this information does not provide any indication regarding forest type burned by year, or geographic location of the fire event, we created rules and assumptions based on the information we had, by state, of the predominant forest type in each ecoregion at level IV. For example, most of the area burned in the region belongs to the scrub-stratum type, thus we assumed that most of the events are of the type of surface fires (Jardel et al. 2010) and that the area burned occurs in forest stands that are less than 20 years old (this is also more or less the length of the shifting cultivation cycle).

7.2 Historic net GHG emissions and removals from land-use changes and fires

Considering the input period covered by the available data resulting from forest-cover losses and gains (i.e., deforestation and reforestation, and fire events), the CBM-CFS3 model was run to develop a historic simulation scenario of GHG emissions/removals from 1995 to 2010.

From the data and assumptions used to create the runs of the historic scenario, we noted that, although the forest area decreased because the annual area of gross deforestation rates was greater than the area of gross reforestation rates in the Yucatan Peninsula (YP), GHG removals from 1995 to 2010 were on average greater than the GHG emissions (Figure 7.2). This "net sink" is because GHG uptake from growing forests in forest land remaining forest land was greater than GHG emissions from deforestation and fires. The rate of this sink varies with the net deforestation rates and with the area annually burned.

Figure 7.2 Annualized area of the Yucatan Peninsula affected, by forest land-use change and by annual fire events, 1995–2010, and estimated net CO_2e emissions

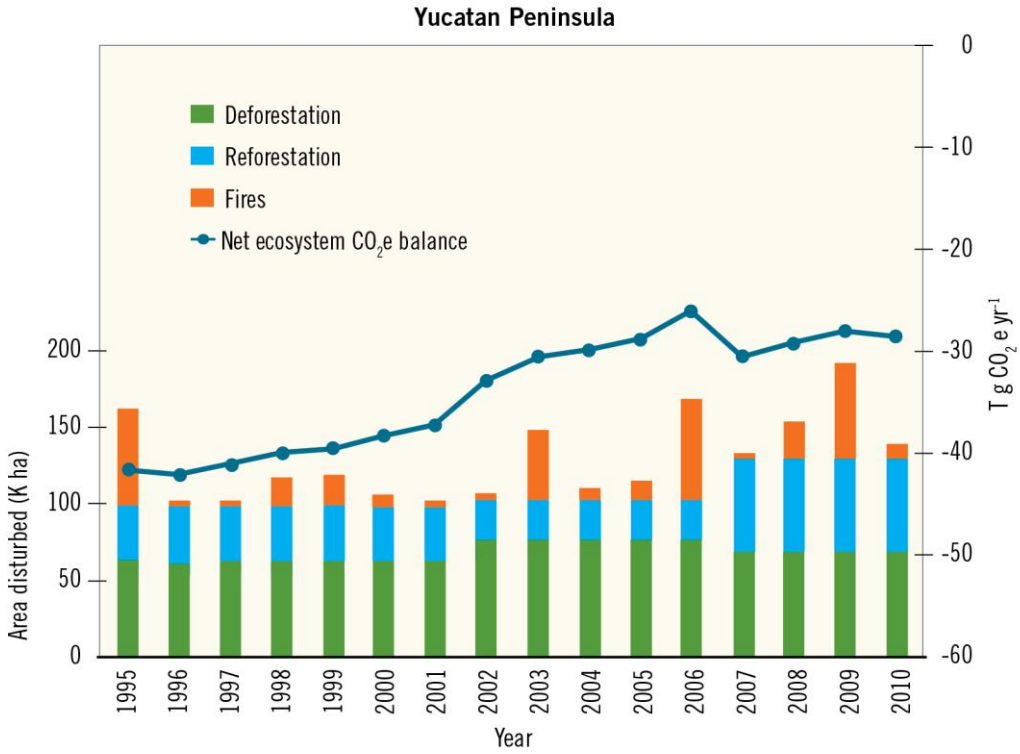

Note: CO_2e = carbon dioxide–equivalent; K ha = thousand hectares; Tg = teragrams. Negative flux denotes removal from the atmosphere, i.e., a sink.

Following IPCC guidelines (see Section 2.7 on UNFCCC land-use categories and transitions), we used the model to estimate the annual contribution of each land-class category to the total net GHG balance for the two main ecoregions of the YP: Tropical Humid Forest (THF) and Tropical Dry Forest (TDF). IPCC guidelines specify that, in the case of land-use change, the emissions and removals are always reported in the new land category (see Section 2.7). Therefore, emissions from deforestation are reported in the category Forest Land converted to Other [non-forest] land (FLOL) (the new non-forest land category is not further specified here, but in this case it is the combination of croplands, grasslands and other lands), while emissions in intact forests are reported in Forest Land remaining Forest Land (FLFL).

Figure 7.3 shows that the two ecoregions differ greatly in terms of their net CO_2e balance: the cumulative value from 1995 to 2010 for the THF ecoregion is 40 times greater than for the TDF. The forest area in the THF ecoregion is much larger than in the TDF ecoregion (THF covers 90% of the YP), and forests in the THF have higher growth rates. The predicted annual GHG balance reflects the activity data. In terms of the estimates of GHG fluxes for the six spatial units, the average values from 2001 to 2010 show that the biggest sink was observed in the category Forest Land remaining Forest Land (FLFL), with -52 Tg CO_2e $year^{-1}$; the largest source was in areas affected by deforestation, the category Forest Land converted to Other [non-forest] Land uses (FLOL), with 27 Tg CO_2e $year^{-1}$; while the inverse process OLFL contributed a small sink of -8 Tg CO_2e $year^{-1}$.

Our preliminary analysis of the age-class structure indicated that the forests of the YP are dominated by younger age classes (Olguín et al. 2015), with a high growth rate (higher capacity to remove CO_2 from the atmosphere). Their contribution to the overall GHG balance is sufficient to generate a sink, even as the net forest cover loss increases and the forest area decreases. These analyses do not yet include more-complex and finer-scale disturbances that contribute to forest degradation, and we anticipate that including disturbances such as selective timber harvesting and firewood collection will reduce the net GHG balance of the YP to near-zero.

Figure 7.3 Sum of GHG emissions/removals from all land class categories in the Tropical Humid Forest and Tropical Dry Forest ecoregions, in the Yucatan Peninsula

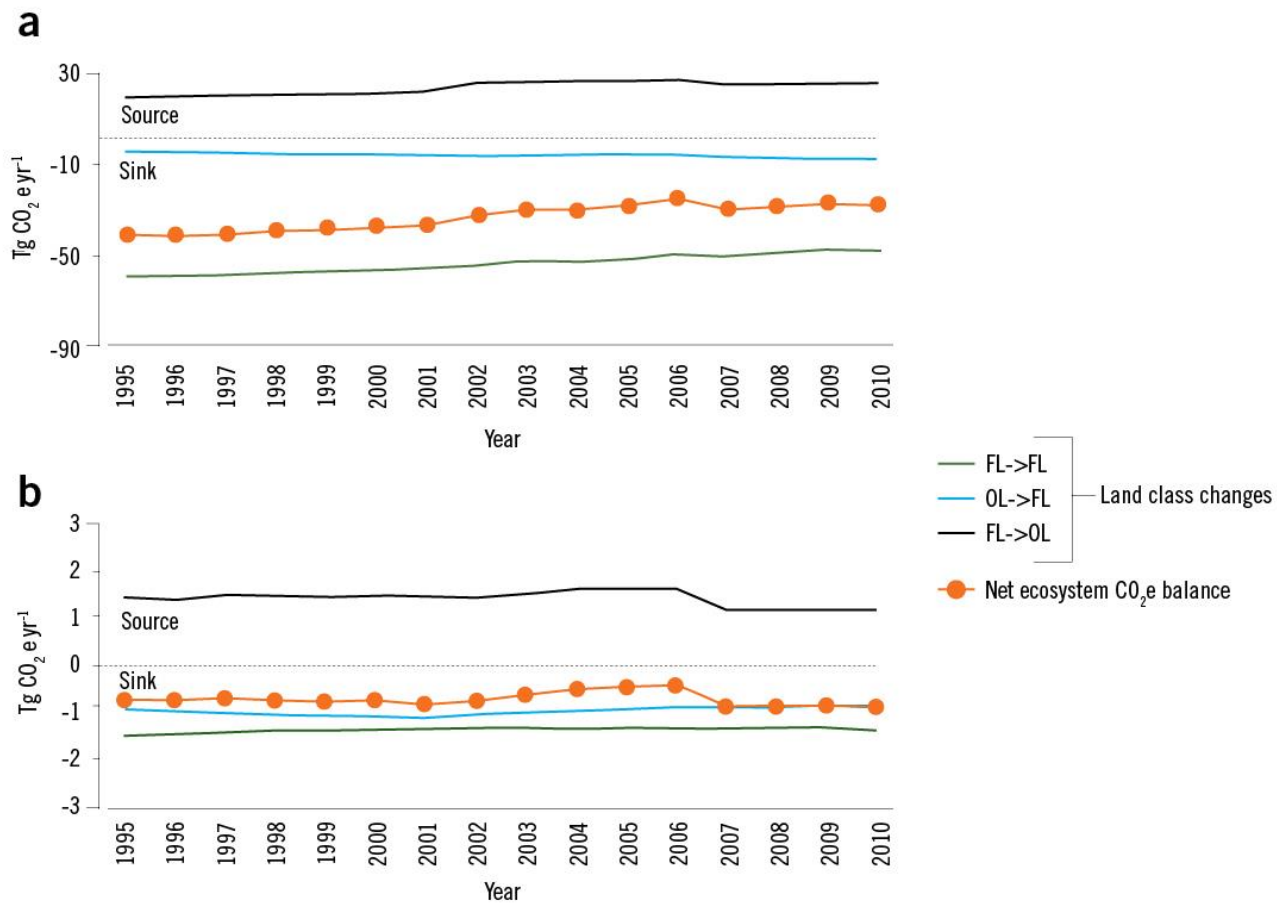

Note: a = Tropical Humid Forest ecoregion; b = Tropical Dry Forest ecoregion; GHG = greenhouse gas; Tg = teragrams; CO_2e = carbon dioxide–equivalent; FL = Forest Land; OL = Other [non-forest] land. Note the difference in Y-scale in graphs a) and b) and that these values are reported consistent with UNFCCC conventions, wherein a sink is a removal from the atmosphere and therefore a negative value.

7.3 Projected future net GHG emission scenarios

Baseline scenario

Figure 7.4 shows estimates of annual GHG emissions/removals (from 1995 to 2010), and the projection of past conditions into the future (from 2011 to 2020). To develop this baseline scenario, we explored two different possible approaches, assuming: a) the average of annual rates of activity data (i.e., land-use changes and fires) from the last 10-year period remain constant from 2011 to 2020, and b) the average of the net GHG balance of the last 10-year period remains constant from 2011 to 2020. We then estimated the annual balance of GHG emissions and removals for the two scenarios.

As in the historic scenario, the growth of remaining and of newly established forests contributed to the removal of atmospheric carbon during the simulation period even when the total forest area decreased. Thus, regardless of the selected baseline, the landscape remains a net sink from 2011 to 2020. This potential sink will decrease, if additional information on non-stand-replacing disturbance events is added to the scenario or as the temporal and spatial resolution of information about stand-replacing disturbances increases (Olguín et al. 2015; Mascorro et al.2016).

Our results clearly illustrate the limitations of the "10-year GHG emissions average approach" as baseline. This simplistic approach supposes that future CO_2e emissions will be the same (on average), without considering possible changes in the dynamics between forest growth conditions and activity data. However, as our example demonstrates (Figure 7.4), projections of the average rate of past activity data to 2020 result in a 30% lower CO_2e removal than using the "10-year GHG emissions average approach." This is the result of the cumulative impact of the net reduction in forest area, the increase in average forest age that results in higher biomass but a lower average growth rate of the remaining forest area, and the increased emissions resulting from deforestation of areas with higher biomass carbon density. The cumulative difference between the two baselines is 86 Tg CO_2e.

Figure 7.4 Annualized area of the Yucatan Peninsula affected, by forest land-use change and by annual fire events, 1995–2010, and estimated net CO_2e emissions

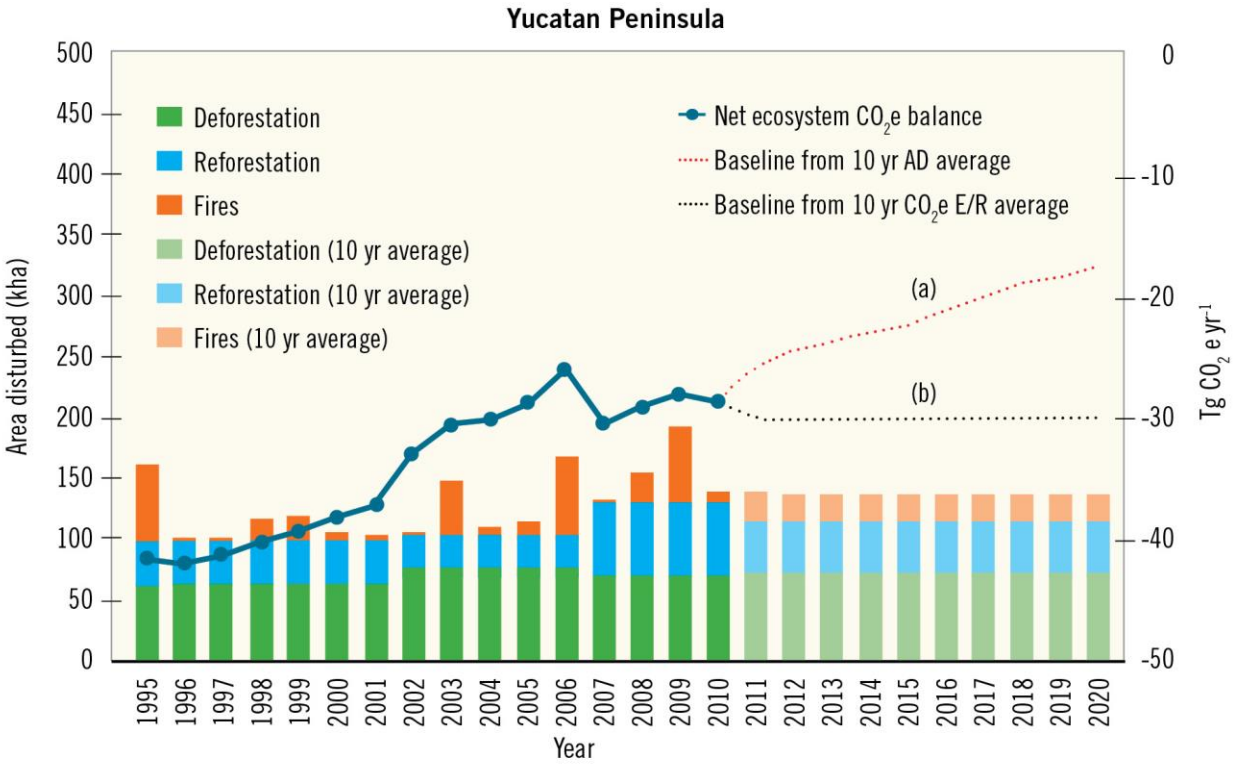

Note: CO_2e = carbon dioxide–equivalent; kha = thousand hectares; Tg = teragrams. Negative flux denotes removal from the atmosphere, i.e., a sink.
Historic information: (a) 10-year activity data (AD) average, and (b) 10-year average of greenhouse gas (GHG) emissions versus removals (E/R).
Source: Adapted from Olguín et al. 2015.

Mitigation scenario

The government of Mexico aims to achieve a 30% and 50% reduction in GHG emissions by 2020 and 2030, respectively, relative to the projected net increase in GHG emissions, using the base year of 2000 for all sectors (Conafor 2013). As an example of a mitigation scenario, we explored the effect of gradually reducing the rate of deforestation by 2.5% annually (of the original value, i.e., 25% reduction over 10 years and 50% reduction over 20 years) for the period 2011 to 2030. We then compared the results of the mitigation scenario against the two possible baselines.

Based on our current estimates of land-use changes for the Yucatan Peninsula, the annual gross deforestation rate was about 0.6% from 2001 to 2010. Thus we used the CBM-CFS3 to estimate the net GHG emissions if the gross deforestation rate is reduced linearly by 25% by 2020 or 50% by 2030. Decreasing the deforestation rate by 25% by 2020 could lower net GHG emissions by 6% relative to the baseline calculated with constant activity data (Figure 7.5). Halving the deforestation rate by 2030 would yield a 41% reduction in net GHG emissions relative to the baseline with constant activity data (Figure 7.5). In contrast, if the mitigation benefits of the reduction in deforestation rates were expressed relative

to the baseline with constant emissions, based on the historic average, mitigation benefits would be negative. Relative to the baseline, emissions are predicted to have increased 24% by 2020 and 33% by 2030. In other words, despite the successful reduction in deforestation rates, the accounted emissions would be higher (or the sink lower) than the selected baseline. This emphasizes the importance of selecting a "forward-looking" baseline as the basis for the evaluation of mitigation and REDD+ strategies (Böttcher et al. 2008; Kurz 2010b). Using a static historic value (as in the first baseline) introduces the risk that the landscape carbon dynamics that result from age-class legacy or changes in forest area are not adequately considered.

Figure 7.5 Example of cumulative reduction in GHG emissions by decreasing annual deforestation rates by 2.5% (of the original rate) per year relative to the two baseline scenarios: from 2011 to 2020 and from 2011 to 2030

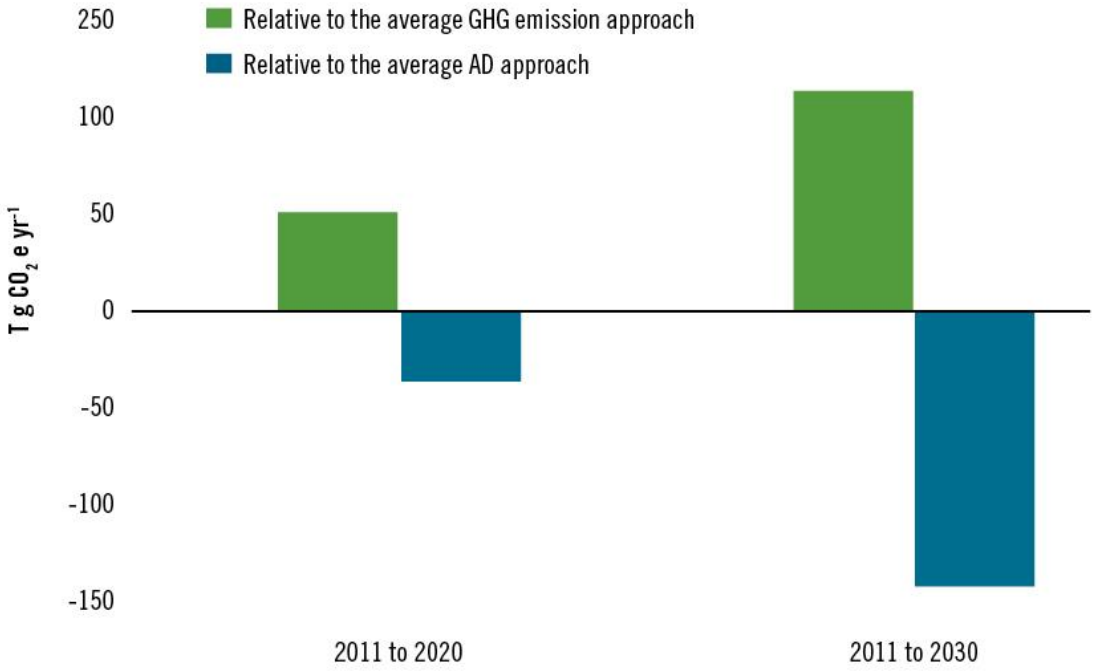

Note: GHG = greenhouse gas; AD = activity data; Tg CO_2e yr^{-1} = teragrams carbon dioxide–equivalent per year. Relative to a baseline derived using the average GHG emission approach, accounted emissions would increase despite the reduction of deforestation rates.

7.4 Lessons learned and future work

This chapter has presented examples of the use of modeling tools to identify, integrate and analyze information from inventories, ground plots, activity data, and other sources into internally consistent estimates of past and projected future GHG emissions and removals. Through close collaboration with key partners in Mexico, the US and Canada, these efforts contribute to improving the design and assessment of activities in the forest sector that can contribute to meeting national and regional GHG emission reduction targets. For example, we presented methods to develop projections about future emissions resulting from reductions in deforestation rates. These modeling results can be used to compare and rank alternative mitigation scenarios. This information can enhance collaboration between the scientific and policy-maker communities in Mexico to improve the understanding of the effects that policy decisions can have on future GHG emissions.

There are ongoing efforts to refine the simulation of carbon dynamics for the range of ecosystem types and conditions in selected Mexican states. Improvement to activity data is being sought through use of higher-resolution remote sensing products combined with information derived from National Forest Inventory data that includes attribution of changes. Updated growth curves and better information on the initial age-class structures are also expected to improve emissions estimates. Efforts to increase the level of complexity of the simulations by including forest management practices, forest degradation, and fires, using spatially referenced and spatially explicit approaches are also in process. Work is being conducted to assess the impacts of different assumptions and data sources on GHG estimates, through sensitivity analyses and the evaluation of model results using independent data (e.g., new state-level forest inventories, intensive carbon monitoring sites; Olguín et al. 2015) that can ultimately help identify, quantify and prioritize efforts to reduce uncertainty in estimates on forest carbon dynamics (see Section 2.8).

8. Using Process-based Models to Support GHG Estimates and Simulate Effects of Disturbance and Climate on Forests

Z. Dai and R.A. Birdsey

Assessing carbon sequestration in forest ecosystems is fundamental to supplying information for GHG estimation in support of reducing emissions from deforestation and degradation (REDD+). Modeling carbon dynamics in forests using process-based models contributes to the methodology and protocol for assessing North American forest carbon dynamics, and provides unique capability to simulate the complex effects of disturbances, climate variability and change, and their interactions.

8.1 Model parameters and validation

Data needed to initialize ecosystem process models for assessing carbon stocks in forest ecosystems differ among models. Biomass observations from study targets are mainly necessary for empirical models to predict growth curves. However, process-based models need various data on factors that influence plant growth—mainly including vegetation species, soil, climate, and factors that affect forests, such as disturbances and other activity data as described in previous sections (Table 8.1). Results from evaluation of several process-based models (Dai and Birdsey 2015) showed that Forest-DNDC can perform well and have high modeling efficiency. It was selected for estimating carbon stocks, sequestration, and various disturbance and climate scenarios, including thinning, hurricane, fire, and a combined scenario of warming with disturbances at the landscape level. The main model parameters needed by the DNDC process model are shown in Table 8.2. Similarly to in empirical models, a good representation of the age of the forests and an accurate representation of time since disturbance are critical input parameters.

Table 8.1 Data needed for modeling forest carbon dynamics, using the DNDC model

Parameters	Data Needed: Forest-DNDC
Location and topography	Simulation units, latitude for each simulation unit
Climate data	Maximum and minimum temperature, Precipitation (daily)
Atmospheric parameters	Carbon dioxide concentration, nitrogen deposition, solar radiation (optional)
Soil	Depth, texture, layers, hydraulic conductivity; soil porosity, field capacity and wilting point, nitrogen, and carbon content in different soil layers and organic matter components (litter and mineral soil)
Vegetation	Initial age and biomass in different storeys (overstorey, understorey and ground), based on species/cover type; and phenology
Hydrology	Water table; needed only for wetlands
Scale	Spatially explicit
Disturbance	Wild and prescribed fires, thinning, planting, harvest, insects, hurricane ; includes timing and intensity of disturbances
Time-step	Daily/ hourly

Table 8.2 Key vegetation and soil parameters for Forest DNDC model

Parameter	Parameter
Initial leaf N (%)	Leaf start growing degree days (GDD)
AmaxA (μmol g-1s-1)	Wood start GDD
AmaxB	Leaf end GDD
Optimum photosynthetic temperature (°C)	Wood end GDD
Minimum photosynthetic temperature (°C)	Leaf N re: translocation
AmaxFrac	Senescence start day
Growth respiration fraction	Leaf C/N
Dark respiration fraction	Wood C/N
Wood maintenance respiration fraction	Leaf retention years
Root maintenance respiration fraction	C reserve fraction
Light half saturation constant	C fraction of dry matter
Respiration Q10	Specific leaf weight (g m^{-2})
Canopy light attenuation	Minimum wood/leaf
Water use efficiency	Leaf geometry
Intercept of vapor pressure deficit	Maximum N storage (kg N ha^{-1})
Slope of vapor pressure deficit	Maximum wood growth rate
Maximum leaf growth rate (% yr-1)	Coefficient of stem density (0–1)#
Overstorey species	Overstorey age
Understorey species	Understorey age
Ground growth (sedge and moss)	Daily minimum temperature (°C)
Daily maximum temperature (°C)	Daily precipitation (mm)

Spatial soil, climate, vegetation and hydraulic parameters

Soil organic carbon (%)	Hydraulic conductivities (cm hr^{-1})
pH	Wilting point (0–1)
Clay (%)	Capacity (0–1)
Soil depth (cm, ≤150cm)	Porosity (0–1)
Overstorey species	Overstorey age
Understorey species	Understorey age
Ground growth (sedge and moss)	Daily minimum temperature (°C)
Daily maximum temperature (°C)	Daily precipitation (mm)

[#] Usually, the coefficient of stem density is the ratio of forest to the bare (non-forest) areas in each simulating unit, and from 0 to 1.

Note: AmaxA = photosynthetic constant (intercept of leaf nitrogen concentration); AmaxB = photosynthetic coefficient (slope of leaf nitrogen concentration); AmaxFrac = daily average maximun photosynthesis; μ mol $g^{-1}s^{-1}$ = micromolecules per gram per second; Q10 = temperature coefficient; C = carbon; N = nitrogen; g m^{-2} = grams per square meter; kg N ha^{-1} = kilograms nitrogen per hectare; mm = millimeters; cm hr^{-1} = centimeters per hour.

In the Yucatan Peninsula (YP), DNDC was validated using the observed biomass from 276 circular plots (Dupuy et al. 2012) in the Kaxil Kiuic forest. Figure 8.1 shows that the biomass simulated by DNDC was significantly correlated with the observed values (R^2=0.83, P<0.001); the slope of the regression model between observed and simulated values was close to 1.0 (b=1.03); and the intercept (a=1.33) was only about 2.84% of the observed average. These metrics show that the DNDC can be used to assess carbon stocks in the Kaxil Kiuic forest with a performance of E≥0.79 and R^2≥0.83.

Figure 8.1 Total aboveground biomass carbon observed vs. total simulated using Forest-DNDC for the 276 plots in the tropical dry forest at Kiuic in the Yucatan Peninsula

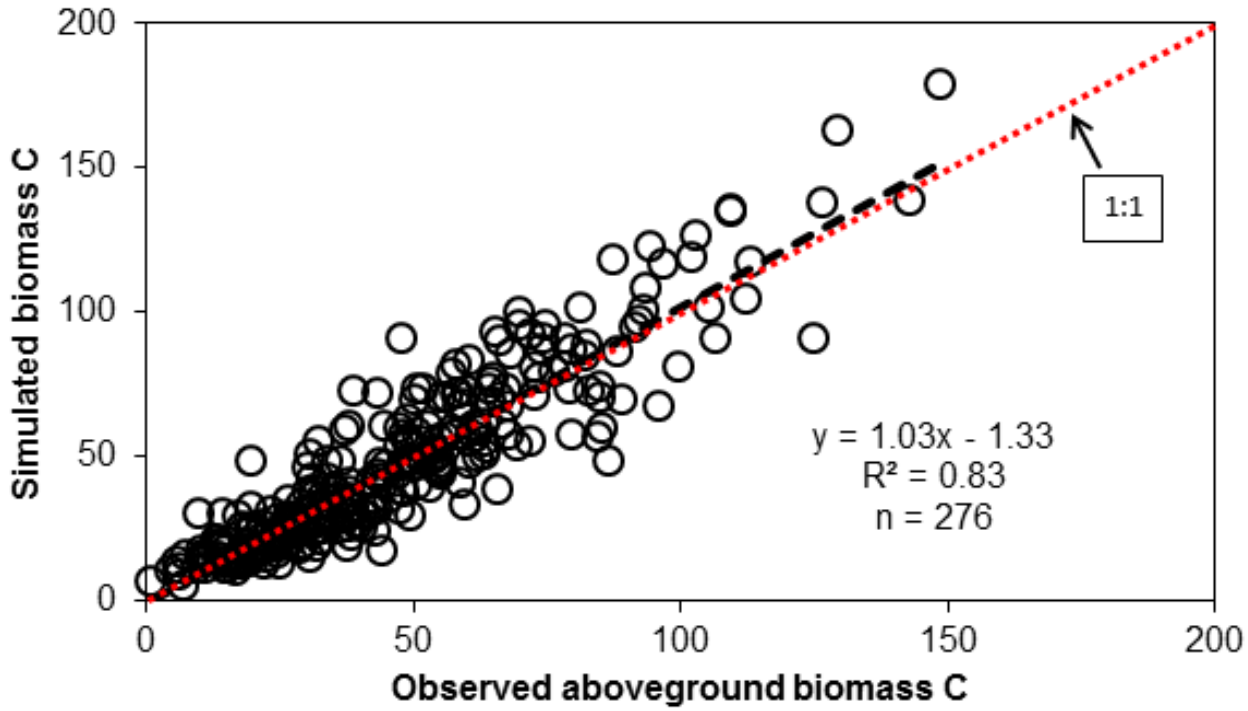

Note: C = carbon; Mg ha^{-1} = megagrams per hectare; y = 1.03x – 1.33; R^2 = 0.83; n = 276;

The simulated aboveground biomass using DNDC was compared to an empirical growth curve (Figure 8.2) (Ángeles, in prep.), which was produced using datasets from the National Forest and Soils Inventory of Mexico observed for this type of forests. The comparison shows that the simulated results are consistent with those values calculated using the empirical growth curve for this type of forest.

Figure 8.2 Comparison of growth curves, derived using different methods

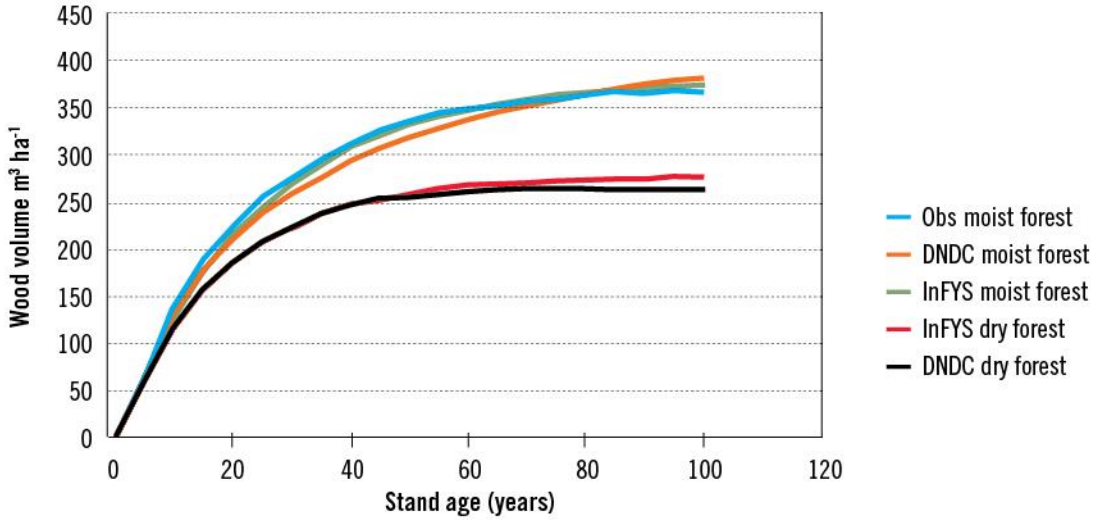

Note: The observed volume (Obs) is from the independent field measurements of intensive-site sample plots in the Kaxil Kiuic area; the DNDC estimates are from the model (Forest-DNDC) results for the same sample plots; the INFyS estimates are calculated from the National Forest and Soils Inventory of Mexico for the moist and dry forest types (for comparison). Independent field measurements for the dry forests were not available.
m^3 ha^{-1} = cubic meters per hectare.

DNDC was also calibrated and validated for the Nez Pearce–Clearwater National Forest (NP) in Idaho, US. Comparison with observations from 381 sample plots (results not shown) indicated that DNDC performed well, with a proper slope (0.94) and a small intercept (5.87 Mg C ha^{-1}, about 7.4% of observation average) of the regression model between observation and simulation. The simulated mean (80.34 Mg C ha^{-1}) was only about 1.9% higher than the observed mean (78.83 Mg C ha^{-1}). A quantitative evaluation concluded that DNDC performs well when estimating carbon sequestration in the NP forest with high performance efficiency (Dai and Birdsey 2015). DNDC was parameterized for the Prince George (PG) study site in British Columbia, Canada, but was not validated because of a lack of independent observed data.

8.2 Forest carbon dynamics at the study sites

Carbon stocks in the forests of the area surrounding Kaxil Kiuic (the area of the Landsat scene used in earlier Sections of this report) under conditions of disturbances were simulated using DNDC and spatially explicit disturbance data. From 1984 to 2010, following disturbance, biomass increased linearly with an increase in stand age, at a rate of about 2.3 Mg C ha^{-1} yr^{-1} (Figure 8.3). The dynamics of several key variables are depicted in Figure 8.3, which also shows interannual variations associated with disturbances. Spatial variability was significant across the study area (Dai and Birdsey 2015). NPP varied spatially from 0.1 to 9.2 Mg C $ha^{-1}yr^{-1}$ in 2010, due to differences in forest type, stand age and climate. High NPP occurs in both moist and young forest areas, and lower NPP in drier and older forests. Similarly to NPP, NEP and Rh varied considerably. NEP ranged between -3.1 and 6.9 Mg C ha^{-1} yr^{-1} in 2010. Rh ranged from 0.9 to 4.5 Mg C ha^{-1} yr^{-1} in the same year.

Figure 8.3 Temporal changes in NPP, NEP, NBP (Mg C ha^{-1} yr^{-1}) and aboveground biomass (Mg C ha^{-1}), in the Yucatan Peninsula

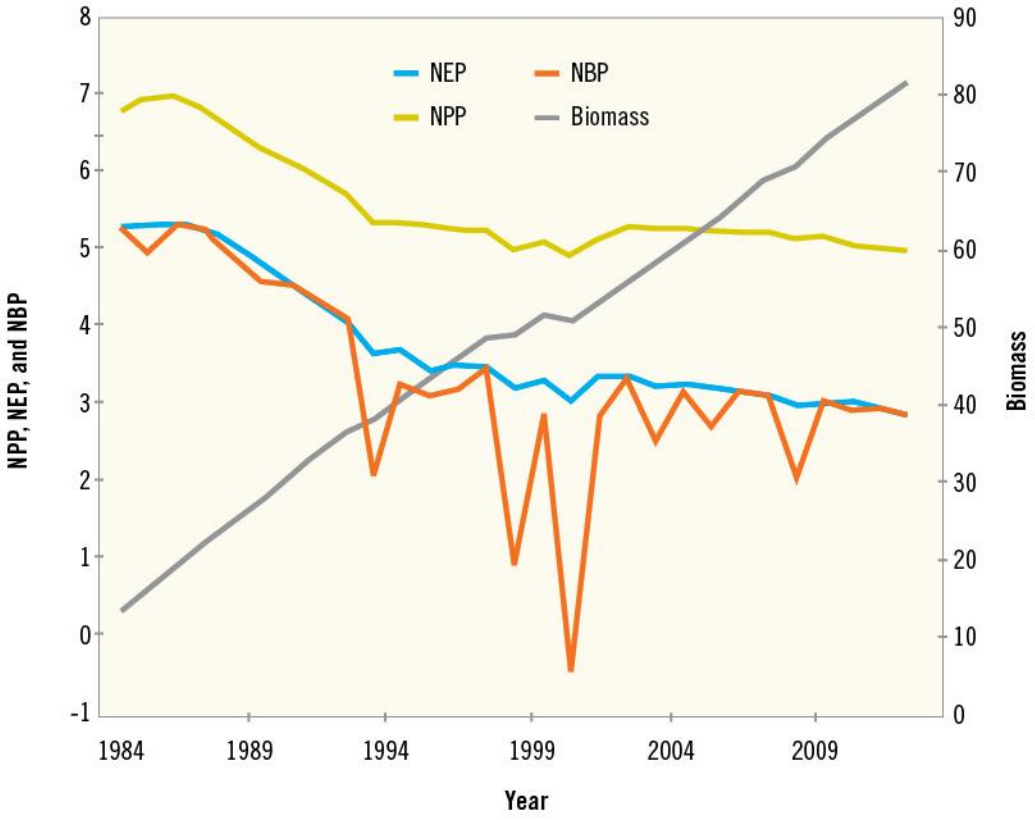

Note: NEP = net ecosystem production; NBP = net biome production; NPP = net primary production; Mg C ha^{-1} yr^{-1} = megagrams carbon per hectare per year.

Similarly to in the Yucatan Peninsula, disturbances had a significant impact on carbon storage in the NP forest (Figure 8.4). Harvests during the period from 1991 to 2011 reduced live biomass by about 1 Tg C, including both above- and belowground losses. Other disturbances caused a larger loss of live trees than did harvest over the same period—about 4.1 Tg C of live aboveground biomass lost to fires and insects, of which most of the live biomass lost was added to the deadwood pools. These disturbances also left a large amount of dead roots in the soils of the forest, which produced a subsequent increase in heterotrophic respiration (Rh) due to decomposition. Fires caused significant loss of litter carbon, over 10 Mg C ha^{-1}, at the locations where canopy fires occurred. The spatial difference in carbon sequestration in this forest varied considerably. The net primary production (NPP) and net ecosystem production (NEP) ranged spatially from 0.4 to 6.5 Mg C $^{-1}$ yr^{-1}, and -0.5 to 5.7 Mg C ha^{-1} yr^{-1}, respectively, in 2010, due to differences in stand age caused by disturbances, harvest/thinning, insects, and fires. Similarly, Rh (Figure 8.4c) from this forest differed spatially, ranging from 0.4 to 2.6 Mg ha^{-1} yr^{-1} in 2010, due mainly to the differences in heterotrophic respiration related to root mass and litter on the forest floor, and also to organic matter in mineral soils.

Figure 8.4 NPP, NEP and Rh in the Nez Perce–Clearwater National Forest, in 2010.

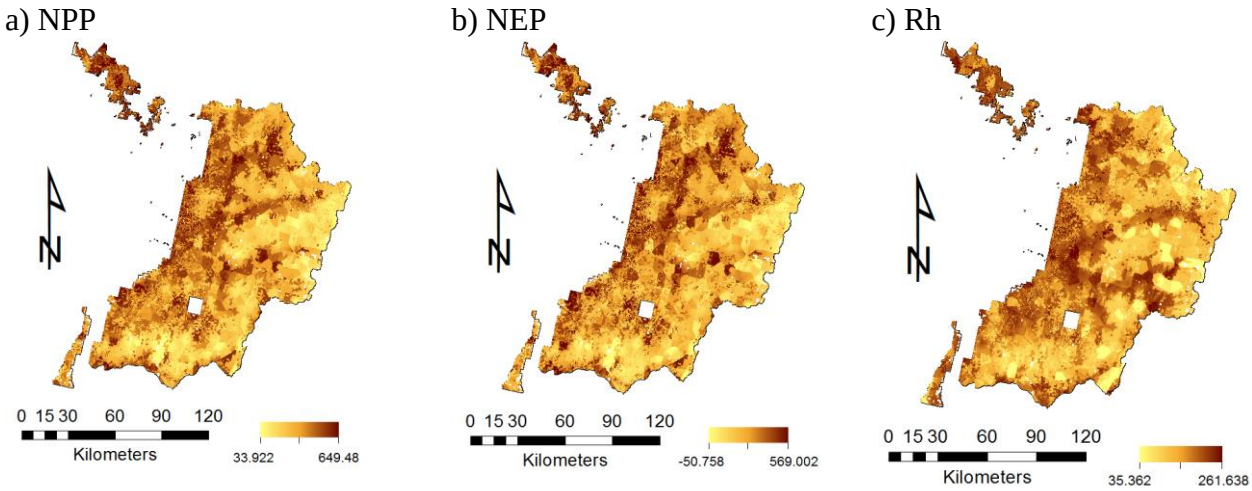

Note: NPP = net primary production. Spatial NPP (g C ha^{-1}) in the forest of Nez Perce Clearwater National Forest in 2010; NEP = net ecosystem production. Spatial NEP (g C m^{-2}) in the Nez Perce Clearwater National Forest in 2010;Rh = heterotrophic respiration; g C ha^{-1} yr^{-1} = grams carbon per hectare per year. Spatial Rh (g C m^{-2}) in the Nez Perce Clearwater National Forest in 2010.

The temporal dynamics of carbon stocks in the PG forest show that disturbances have a substantial influence on carbon storage in the forest (Figure 8.5), which was reduced in 1994 and 1997 by about 1242.1 and 304.7 Gg carbon through harvest, respectively, and by about 14.7 and 5.6 Gg carbon through loss to land-use conversion from forest to non-forest, respectively. These disturbances led to a large decrease in NBP so that the NBP negative in 1994, and to an increase in forest floor by about 300 kg C ha^{-1} on average in that year due to the production of residues (leaves and fine branches) left by harvest. An average of about 940 kg dead roots remained in soils after the harvest in 1994. The residues, especially those on the forest floor, produced a subsequent increase in CO_2 flux for a short time period after the disturbance, due to decomposition.

Spatially, aboveground biomass ranged from 7.5 to 243.6 Mg C ha^{-1} in 2010, with a mean of 94.2 Mg C ha^{-1}. Similarly to in the YP and the NP, this spatial difference in carbon density is mainly associated with stand age and secondarily with climate. NPP, NEP, and Rh ranged from -58.4 to 550.9, -120 to 478.5, and 17.7 to 172.1 g C m^{-2} yr^{-1}, respectively, in the years from 1988 to 2012; the means were 172.6, 91.4 and 71.4 g C ha^{-1} yr^{-1}, respectively (based on the formula [NEP = NPP – Rh – DOC – other losses]—which includes C losses to dissolved organic carbon [DOC] and other pathways that are not included in other models described in this report). These differences were mainly related to disturbances producing spatial divergences in stand age.

Figure 8.5 Temporal changes in landscape aboveground biomass, net ecosystem production, and net biome production in Prince George Forest of BC, Canada

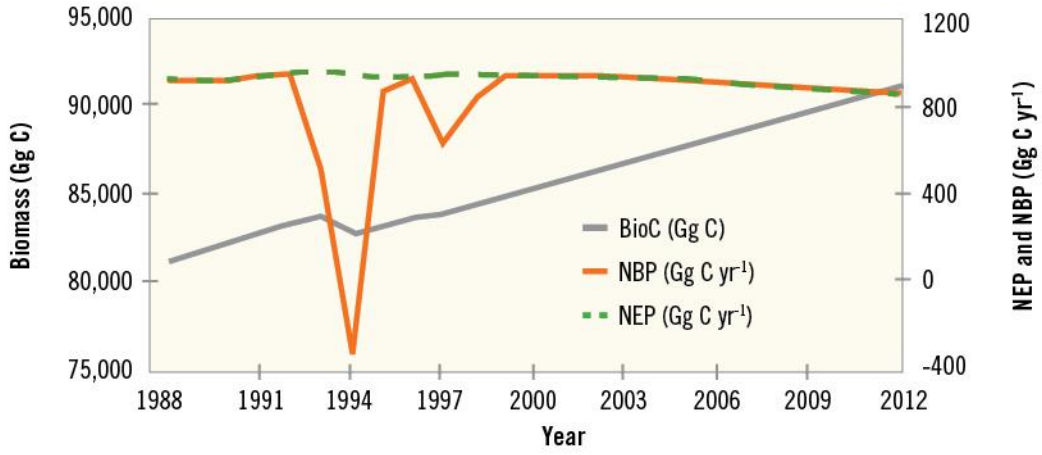

Note: Gg C yr^{-1} = gigagrams carbon per year; BioC = aboveground biomass; NEP = net ecosystem production; NBP = net biome production.

8.3 Assessing impacts of climate variability and disturbances on carbon sequestration, using scenarios and a process model

Climate data for a 33-year period (1981–2013) were used to assess the impact of climate variability on carbon sequestration in the YP. Figure 8.6a shows that temperature rise can significantly decrease carbon storage in dry forests in the YP ($P<0.05$). However, carbon storage in moist forests in this area can significantly increase with higher temperature (Figure 8.6b; $P<0.01$).

There is also a difference in the impact of precipitation fluctuation on the carbon storage in stands, between dry and moist forests in this area. The aboveground biomass of dry forests increases at a low rate of about 11 kg ha^{-1} yr^{-1} with an increase in precipitation of 100 mm (Figure 8.6c; $P<0.05$). However, biomass in moist forests in this area increases at a higher rate (86 kg ha^{-1} yr^{-1}) with an increase in precipitation of 100 mm (Figure 8.6d; $P<<0.001$). The carbon stocks in the dry forest increase only slightly with an increase in precipitation, due mainly to a specific hydrogeological environment, thin soil covering on limestone bed rock (Perry et al. 2003), and an imbalance between precipitation and evapotranspiration in this area (Dai et al. 2014).

Figure 8.6 Impact of temperature and precipitation on annual mean biomass change (kg C ha^{-1} yr^{-1}) in dry forest and moist forest

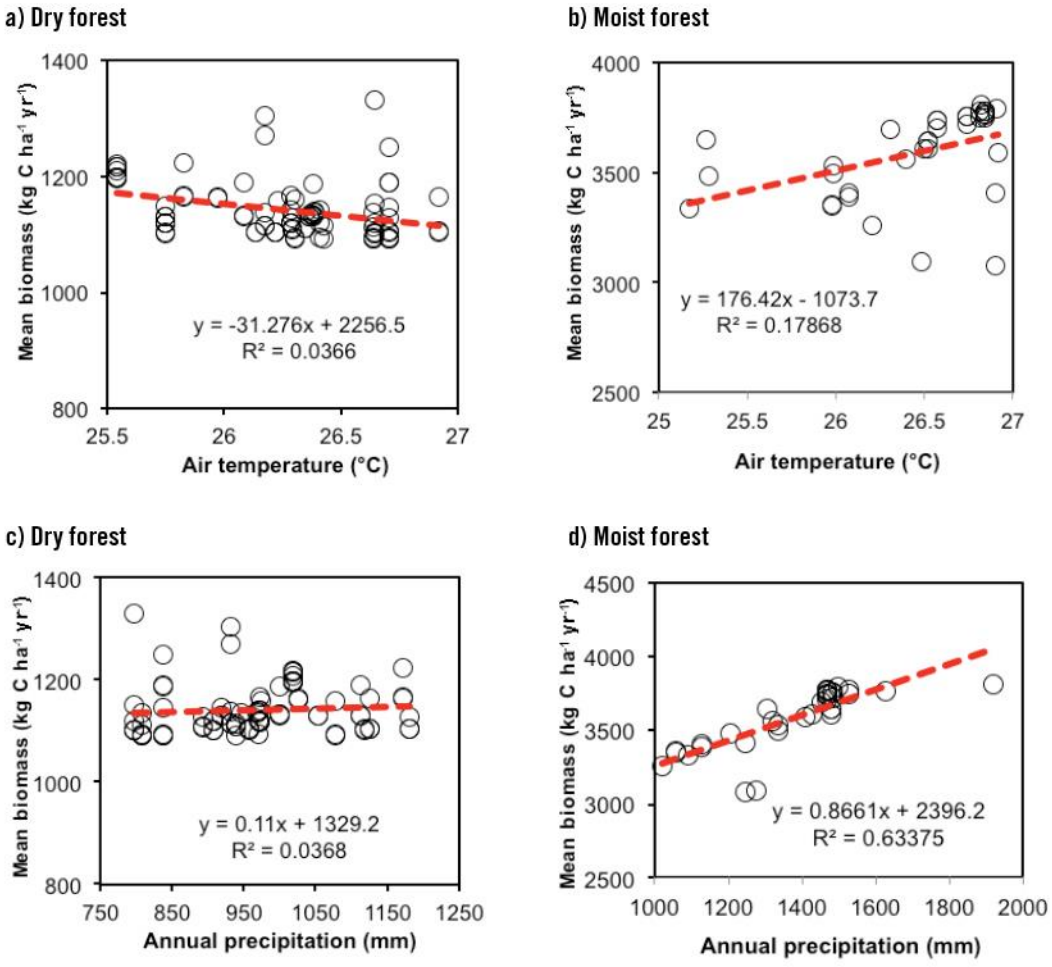

Note: kg C ha^{-1} yr^{-1} = kilograms carbon per hectare per year

Analysis of climate variability on carbon stocks in the NP shows that climate variability can substantially affect carbon stocks in the NP forest (data not shown). Aboveground biomass in NP increases with an increase in temperature, at an average rate of about 248 kg C ha^{-1} per °C increase. Biomass can substantially decrease with an increase in precipitation, at a rate of about 98.5 kg C ha^{-1} per 100 mm, the opposite impact of precipitation increases in the Yucatan, where biomass is predicted to increase with higher precipitation. However, there are some divergences in the impact of precipitation on carbon stocks in this forest, among the vegetation types. The biomass in the forestlands dominated by Ponderosa pine, subalpine fir and subalpine spruce does not decrease substantially with an increase in precipitation (R=0.107, *n*=204, *P*>0.1 for subalpine fir and spruce; R=0.145, *n*=51, *P*>0.2 for ponderosa pine).

The DNDC model was also used to assess the potential effects of disturbances and climate change on carbon stocks, using four scenarios compared with a baseline that includes ground fire (S-F); thinning (S-TH); hurricane (S-HR); and multiple effects (S-ME)—the last of which assumed a temperature rise of

2°C accompanied by an increase in precipitation of 10% per °C, combined with all the aforementioned factors (Table 8.3). Stand age, vegetation structure and soil conditions for simulating the effect of climate change on carbon dynamics under all scenarios were the same as those for the baseline scenario (S-BL). We ran the model to assess the effect of climate change on carbon sequestration in the Kaxil Kiuic forest for a 75-year period, using the scenarios compared with the baseline. We assumed that: (1) trees regenerated from the first year of this 75-year period, and (2) no other disturbances apart from climate change occurred in this forest during the simulation period.

Table 8.3 Scenarios for simulating the response of carbon sequestration in the Kaxil Kiuic forest to selected disturbances and climate change

Disturbance Type	SimulationCode	Scenario Description
Fire	S-F	A low-intensity ground fire was assumed to occur in the 30th year after forest regeneration; the mean forest floor loss to the fire was estimated using a fuel consumption coefficient derived from the study for the fuel consumption on Upper Coastal Plain, in South Carolina, US, conducted by Goodrick et al. (2010).
Thinning	S-TH	A forest management practice was assumed to cut 20% of the overstorey and 90% of the understorey in the 40th year; the overstorey cut by thinning was considered as a forest harvest; and 70% of the understory cut was merchantable; tree crown and non-harvestable woody materials were left in the field during thinning.
Hurricane	S-HR	A hurricane categorized as a class IV storm was assumed to pass through the whole forest, with a wind speed of 250 km hr^{-1}, in the 50th year; salvage logging was 70% of the trees destroyed due to the wind damage; and we assumed that the forest after this hurricane was from natural regeneration, with wood residues.
Multiple effects	S-ME	We assumed that carbon sequestration would be affected by multiple factors, including thinning (S-TH), burning (S-F), hurricane (S-HR), and an increase in air temperature accompanying an increase in precipitation (S-TP), or S-ME = S-F + S-TH + S-HR + S-TP.
Baseline	S-BL	The 75-year climate dataset used in the model validation (see Model Setup and Validation) was used as baseline.

Note: All climate change scenarios were designed based on current climate conditions for a 43-year period, 1970–2012.

Thinning practice

The simulated result under thinning (S-TH) (Figure 8.7) indicates that an intensive thinning, in which 20% of overstorey and 90% of understorey were cut at age 40 years, substantially reduced carbon storage in the semi-dry forest. Aboveground biomass decreased by 28 Mg C ha^{-1} (from 82 to 54 Mg C ha^{-1}), of which about 21.5 Mg C ha^{-1} were harvested as forest product and 6.5 Mg C ha^{-1} were left on the forest floor, mainly from the understorey because 30% of that forest layer was assumed to be non-harvestable (Table 8.3). After the thinning the remaining biomass increased significantly.

Figure 8.7 Impacts of a low-intensity ground fire, thinning, hurricane, and multiple disturbances plus warming, on biomass carbon stocks in the semi-dry forest in the Yucatan Peninsula relative to the base scenario

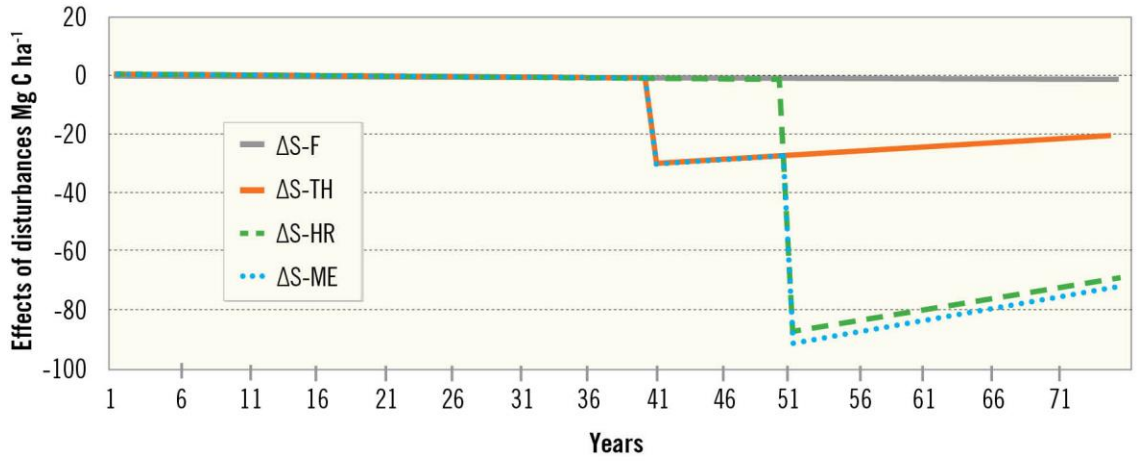

Note: Mg C ha^{-1} = megagrams carbon per hectare; Δ = difference in carbon stock between base scenario and scenario; S-F = fire scenario; S-TH = thinning scenario; S-HR = hurricane scenario; S-ME = scenario of multiple disturbances (effects) plus warming. Note that the ground fire in year 30 of the S-F scenario had only a negligible effect on ecosystem carbon stocks.

After reducing stand biomass through thinning, the mean biomass increment of the remaining stand following the S-TH management was, relative to the simulation with no thinning, 360 kg C ha^{-1} yr^{-1} higher in the first 10-year period and 285 kg C ha^{-1} yr^{-1} higher over 30 years. This indicates that forest thinning can increase carbon removal rates from the atmosphere in this semi-dry forest.

Storms

The simulation results of the hurricane (S-HR) demonstrated substantial influence on carbon sequestration in this tropical forest (Figure 8.7). A large loss of live biomass storage occurs during a disastrous storm but most of this biomass is added to the dead organic matter pools, with no net loss in ecosystem carbon until dead trees are salvage-logged or start to decompose. Figure 8.7 showed that S-HR decreased carbon storage in the forest by 86%, due to destruction of the forest, and S-HR added about 31.9 Mg C ha^{-1} to the forest floor (Figure 8.8) because we assumed a high rate of salvage logging (70%).

Carbon sequestration in forests can recover quickly after hurricanes. The results from the S-HR simulation showed that, similarly to with thinning, carbon sequestration rates in the forest increased relative to the baseline (S-BL) by over 915 kg C ha^{-1} yr^{-1} within several years after S-HR.

Fires

A low-intensity ground fire (S-F) can cause a small decrease in aboveground biomass. The simulated result under S-F (Figure 8.7) showed a decrease in biomass in year 30 of about 0.8 Mg C ha^{-1} in total during the burning. However, aboveground biomass can significantly (R^2=0.999, n=42, P<0.001) increase at a low rate, but the burning can bring a large carbon loss to atmosphere (see below).

Changes in soil carbon pool under disturbances

Fires can cause a large carbon loss to air—about 3.0 Mg C ha^{-1}, based on this simulation (S-F)—due to burning of shrubs/small trees and forest floor. The result for the simulation under a ground fire scenario (S-F) showed a decrease in soil carbon pool (Figure 8.8), due primarily to a decrease in forest floor burnt by the fire. However, a forest floor can recover within several years following the fire event.

Figure 8.8 Potential effects of disturbances and climate change on soil carbon pool relative to the base scenario in the Kaxil Kiuic forest of the Yucatan Peninsula

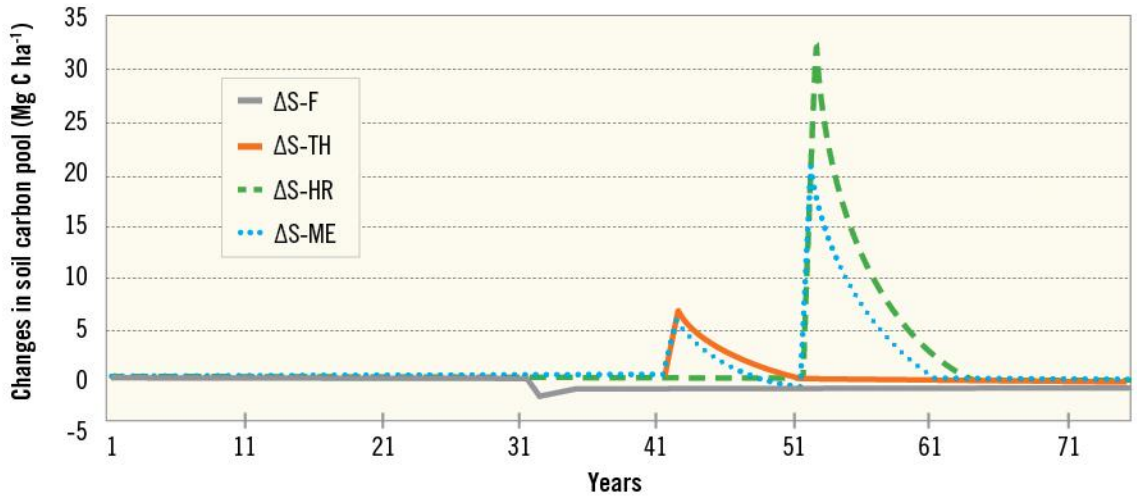

Note: Changes in soil carbon pool = the net increments under different scenarios relative to base scenario; Mg C ha^{-1} = megagrams carbon per hectare; Δ = difference in carbon stock between base scenario and scenario; S-F = fire scenario; S-TH = thinning scenario; S-HR = hurricane scenario; S-ME = scenario of multiple disturbances (effects) plus warming.

Simulated results demonstrated that S-HR substantially disturbed the soil carbon pool because a strong storm adds debris to the forest floor and dead roots to mineral soils. The impact of debris and dead roots on the soil carbon pool decreases over 10 years due to a fast decomposition of organic matter under tropical climate (Figure 8.8). Changes in Rh (Figure 8.9) also indicate that the influence of a strong storm on the soil carbon pool diminishes within several years after the event (Dai et al. 2013).

The impact of thinning on the soil carbon pool depends strongly on thinning intensity and harvest rate. A large amount of biomass and root residues can be added to the forest floor and mineral soil (Figure 8.8)

after thinning. Similarly to with a disastrous storm, the debris and dead roots from a thinning practice can decompose fast in the tropical climate, producing a high Rh for a short period after thinning (Figure 8.9).

There are differences in changes in Rh (Figure 8.9) under the various disturbances (S-F, S-TH and S-HR). The impact of a ground fire (S-F) on Rh (Figure 8.9) is small, due to a low fuel loading of less than 400 g C m^{-2} on average before the fire (S- F), which reflects fast decomposition in tropical climate. Moreover, coarse woody debris and standing deadwood are typically not consumed in a ground fire unless there is high fuel loading.

Figure 8.9 Potential effects of disturbances on heterotrophic respiration (Rh) relative to the base scenario in the Kaxil Kiuic forest of the Yucatan Peninsula

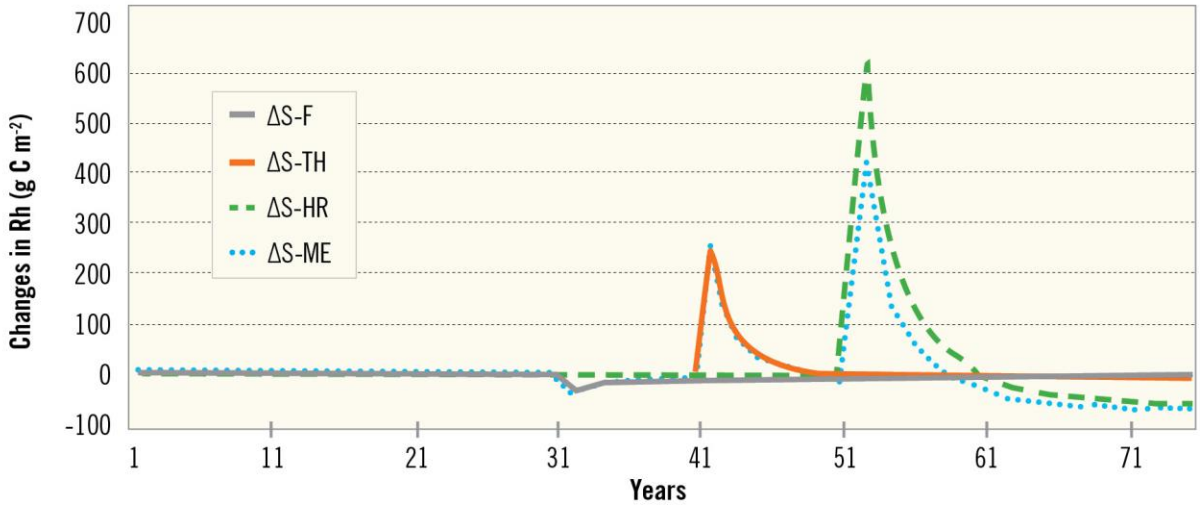

Note: Changes in Rh = the differences between each of the disturbance scenarios and the base scenario. Rh = Changes in soil CO_2 flux due to decomposition (heterotrophic respiration)
g C m^{-2} = grams carbon per square meter; Δ = difference in carbon stock between the base scenario and a given disturbance scenario; S-F = fire scenario; S-TH = thinning scenario; S-HR = hurricane scenario; S-ME = scenario of multiple disturbances (effects) plus warming.

Thinning (S-TH) and strong storms (S-HR) can generate large amounts of debris and dead roots, leading to a temporary increase in forest floor and dead roots, which is followed by increased heterotrophic respiration (Figure 8.9).

9. Comparing Results from Different Modeling Approaches and Data

R.A. Birdsey, Z. Dai, D. Greenberg and W.A. Kurz

In this chapter we review common approaches, using empirical and process models, to estimating carbon stocks and stock changes and show some examples of model calibration, validation, and comparisons of results from different models and data. Such comparisons improve understanding of the ecosystem responses to perturbations, and can lead to greater certainty about how the system will respond in the future to anthropogenic or natural factors.

Availability of data representing the population of interest is a prerequisite for estimating carbon stocks and stock changes. As described earlier, the three countries have interest in estimates at national, regional, state, project, and other scales. Yet data are seldom available that are fully representative across this broad range of scales and for the different forest types and activities (including natural disturbances) that are common or of particular interest. However, all three countries have substantial forestry data assets that can support estimating carbon stocks and stock changes at multiple spatial and temporal scales, all of which involve modeling to varying degrees because it is not possible to directly measure ecosystem carbon stocks or stock changes. The available data typically include variables such as tree diameters and heights, wood density, and leaf area that may be related to carbon stocks. Measured variables must then be related to the variables of interest, using a modeling method.

9.1 Model calibration

Model calibration involves the initial testing of a model and if necessary, adjusting model parameters, based on empirical observations, to reflect the specific conditions to which the model will be applied. Because model results are inherently uncertain, it is important to properly calibrate and validate models prior to widespread applications of model results.

In practice, empirical models are well suited to representing changes in the different carbon pools due to impacts from management activities, fires, pests, and land-use change; to quantifying the uncertainty of directly measured carbon pools; and to validating the independent estimates from process models (Kurz et al. 2009; Shaw et al. 2014; Stinson et al. 2011). However, using empirical models to extrapolate in time and space should be done cautiously and with acknowledgement of possible sources of error or bias such as failure to account for rising CO_2 concentrations or for changes in growing-season length (Kurz et al. 2013). Empirical models should be validated if applied to a different population from that represented by the data used to parameterize the model. Process models are, in theory, more useful for simulating forest ecosystem response to changes in climate or the concentration of atmospheric CO_2, and may be used to make estimates or projections outside the spatial and temporal boundaries of the data used for parameterization. In practice, numerous comparisons of process model predictions have demonstrated lack of agreement on the magnitude, and at times even the direction of ecosystem responses to environmental changes (Huntzinger et al. 2012; Wang et al. 2011). Therefore, ongoing research and monitoring of past tree growth and of mortality rate responses to changes in atmospheric CO_2 concentration and climate are required (Hember et al. 2012). It is important to calibrate process models to

reflect the environmental and vegetation conditions of the target populations, and to validate them with independent data sets before attempting to use them outside the range of parameterization data.

In this carbon modeling project we allocated a considerable amount of time to examining data sets and applying empirical and process models of various kinds as described in this document and, in more detail, in the individual consultant reports and related peer-reviewed publications (Birdsey et al. 2013; Dai et al. 2014; Greenberg 2015). However, we did not have sufficient time or resources to fully identify the underlying reasons for different results. Here we provide some examples of model calibration, validation, and comparisons between models, using the Nez Perce–Clearwater National Forest (NP) in the US as an example. We chose to highlight this pilot study area because all of the required data and modeling elements are available, including good independent data for validation. In the summary of this section we will refer to some of the challenges of implementing this phase of the work at the other pilot study sites, because there are some useful lessons to be learned and applied in phase 2 of this project.

DNDC was calibrated before application to the NP by comparing selected input variables to data collected at sample sites in the NP. The main tunable parameters are presented in Table 9.1. Other parameters, including soil, climate and vegetation type, should not be revised, unless those data are not obtained from observations or reliable estimations. The result of the model calibration, using 203 sample plots with a stand age range of 4–215 years in 2012, and all main tree species in the NP, shows that the simulated aboveground biomass from DNDC is in good agreement with the observations (Dai and Birdsey 2015).

Table 9.1 Tunable parameters for estimating carbon stocks, using DNDC

Parameter	Annotation	Example
AmaxA	Photosynthetic constant (μmol CO_{2g}-1 s-1)	15.2 to 15.0, representing values for spruce in Russia and NP
AmaxB	Photosynthetic coefficient (no unit)	22.5 to 25.0, representing values for spruce in Russia and NP
start GDD	Accumulated degree days at start of plant growth	
end GDD	Accumulated degree days at the end of plant growth	

Note: μmol CO_2 g^{-1} s^{-1} = micromole carbon dioxide per gram per second; NP = Nez Perce–Clearwater National Forest.

For NP, validation of the calibrated DNDC model against observations from 381 sample plots (from the national forest inventory) is shown in Figure 9.1, indicating that DNDC performed well and had a proper slope (0.94) and a small intercept (5.87 Mg C ha^{-1}, about 7.4% of observation average) of the regression model between observation and simulation. The simulated mean (80.34 Mg C ha^{-1}) was only about 1.9% higher than the observed mean (78.83 Mg C ha^{-1}). In addition, analysis of four quantitative evaluation variables (E = 0.83, R^2 = 0.94, PBIAS = -0.02 and RRS = 0.41) concluded that DNDC performs excellently in estimating carbon sequestration in the forest of NP with high performance efficiency. Based on the model performance rating, DNDC performance for assessing carbon stocks in stands over the forest of NP was within the range of "very good" ($E \geq 0.75$; $RRS \leq 0.7$; $-25 \leq PBIAS \leq 25$) (Dai and Birdsey 2015).

Figure 9.1 Model validation: Observed aboveground biomass vs simulated using biomass Forest-DNDC for the forest in Nez Perce–Clearwater National Forest, in Idaho, US

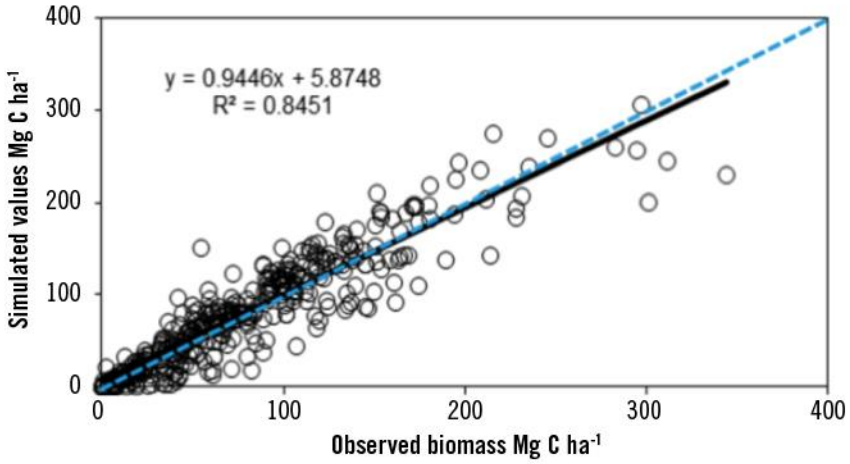

Note: Black line = regressed; blue dashed line = one to one; Mg C ha^{-1}= megagrams carbon per hectare,

9.2 Model comparison

The models and data used for comparing results are briefly described in Table 9.2. Note that we include results from one model that was not part of the CEC project but was applied to the NP forest as part of another project. Figures 9.2 through 9.4 illustrate the results for selected variables. Estimates of the carbon density in aboveground biomass (Figure 9.2) are nearly identical for three of the models (InTEC, CCT, and CBM-CFS3) and also nearly identical for the Forest Inventory and Analysis (FIA) data (2003 only) and DNDC. One of the main reasons for these two groupings' differing by 10% or so is that different sets of biomass equations were used. FIA now uses the "component ratio method" (CRM) (Chojnacky 2012), and this approach to estimating biomass is reflected in the Carbon Calculation Tool (CCT) results, which are derived from FIA data. The FIA estimates reported for 2003 used an earlier set of biomass equations (Jenkins et al. 2003) that generally produced significantly higher results compared with the CRM method (Chojnacky 2012). Another factor influencing biomass estimates is the classification of vegetation into types, which is not consistent among models; and also, both the FIA and CCT biomass estimates are not compiled by vegetation type but rather by individual species, from data collected at sample plots. Estimates of biomass for individual trees are then summed up to the population total and divided by the area to get average biomass density. Therefore, the approach to assigning weights to each sample plot based on sampling probability was inconsistent among approaches. Estimates of total biomass (right side of Figure 9.2) do not exactly follow the relative pattern of average biomass density for the different approaches, indicating that the area estimates are not the same among the different approaches. FIA and CCT use the same areas, but in CCT the area changes over time whereas the area used by Intec is constant and derived slightly differently since Intec is a spatially explicit model. Also, the area estimates for different forest classifications are not the same, contributing to inconsistency of landscape-scale aboveground biomass estimates. This is just one example of the complexity that makes direct comparison of model estimates so challenging.

Table 9.2 Description of data and models used in the model comparison for Nez Perce–Clearwater National Forest

Data or Model	Brief description
Forest Inventory and Analysis (FIA) data	Data collected by the US national forest inventory, using a standard sampling grid and methodology. The average measurement date for this study is 2003.
Carbon Calculation Tool (CCT)	Tool used to statistically combine, interpolate and extrapolate the national forest inventory data for a state or region of the US, to support annual GHG inventory reporting from 1990 to the present (Smith et al. 2007).
Carbon Budget Model (CBM-CFS3)	Empirical model of tree growth, with process respresentation of dead organic matter and soil carbon dynamics (Kurz et al. 2009). For the NP simulations, it was used in a spatially-explicit simulation using default parameter values without any additional calibration.
Integrated Terrestrial Ecosystem Carbon Model (Intec)	Hybrid empirical and process model driven by remote -sensing data, disturbances, and productivity estimates, that has been calibrated to FIA data, and validated for application in the conterminous US (Zhang et al. 2012) and at the scale of individual National Forests.
Forest DeNitrification-DeComposition Model (DNDC)	Spatially-explicit process model simulating effects of forest growth, carbon and nitrogen dynamics, and emissions of trace gases on the balance of water, light, and nutrients in forest ecosystems (Li et al. 2000). The model was calibrated and validated with independent data, where available.

Figure 9.2 Average and total aboveground biomass, estimated with different methods, for the Nez Perce–Clearwater National Forest

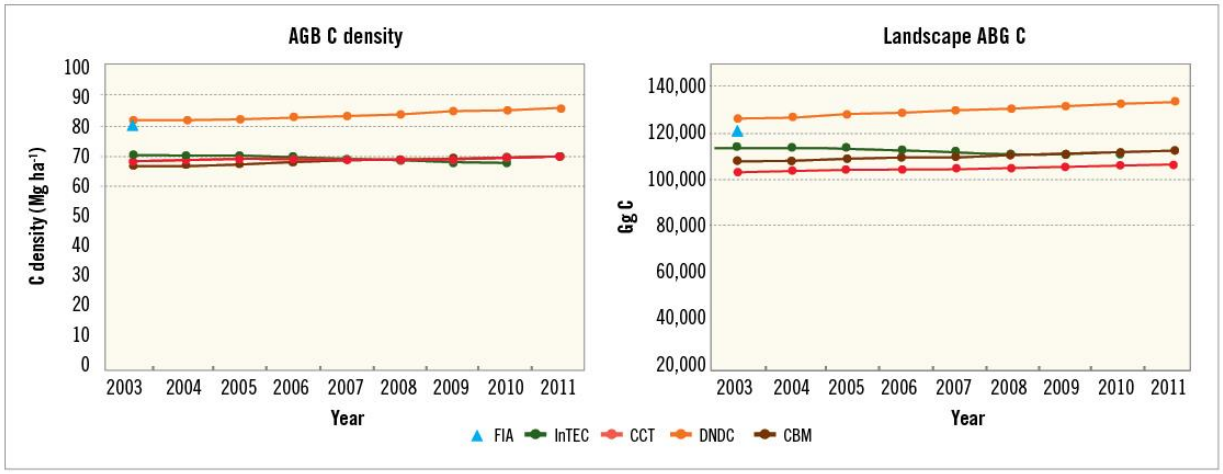

Note: AGB = aboveground biomass; C = carbon; Mg ha^{-1} = megagrams per hectare; Gg = gigagrams; FIA = Forest Inventory and Analysis data; InTEC = Integrated Terrestrial Ecosystem Carbon model; CCT = Carbon Calculation Tool; DNDC = DeNitrification-DeComposition Model; CBM-CFS3 = Carbon Budget Model of the Canadian Forest Sector. See Table 9.2 for description of methods used.

Figure 9.3 Average deadwood carbon density and litter carbon density, estimated with different methods, for the Nez Perce–Clearwater National Forest

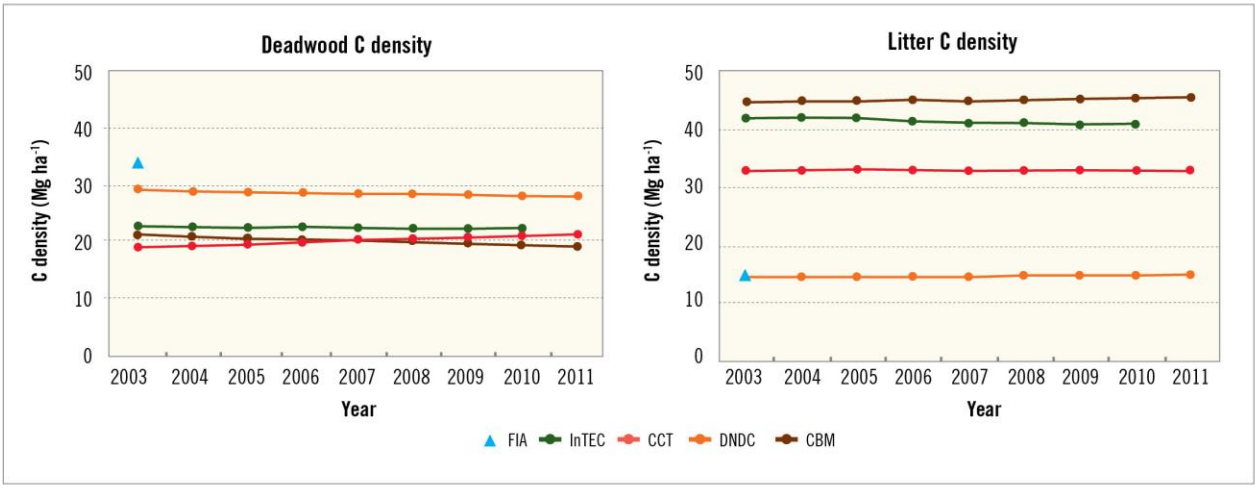

Note: C = carbon; Mg ha^{-1} = megagrams per hectare; FIA = Forest Inventory and Analysis data; InTEC = Integrated Terrestrial Ecosystem Carbon model; CCT = Carbon Calculation Tool; DNDC = DeNitrification-DeComposition Model; CBM-CFS3 = Carbon Budget Model of the Canadian Forest Sector. See Table 9.2 for description of methods used.

Figure 9.4 Average net primary production (NPP), average net ecosystem production (NEP), net biome production (NBP), and net carbon emissions due to disturbances, estimated with different methods, for the Nez Perce–Clearwater National Forest

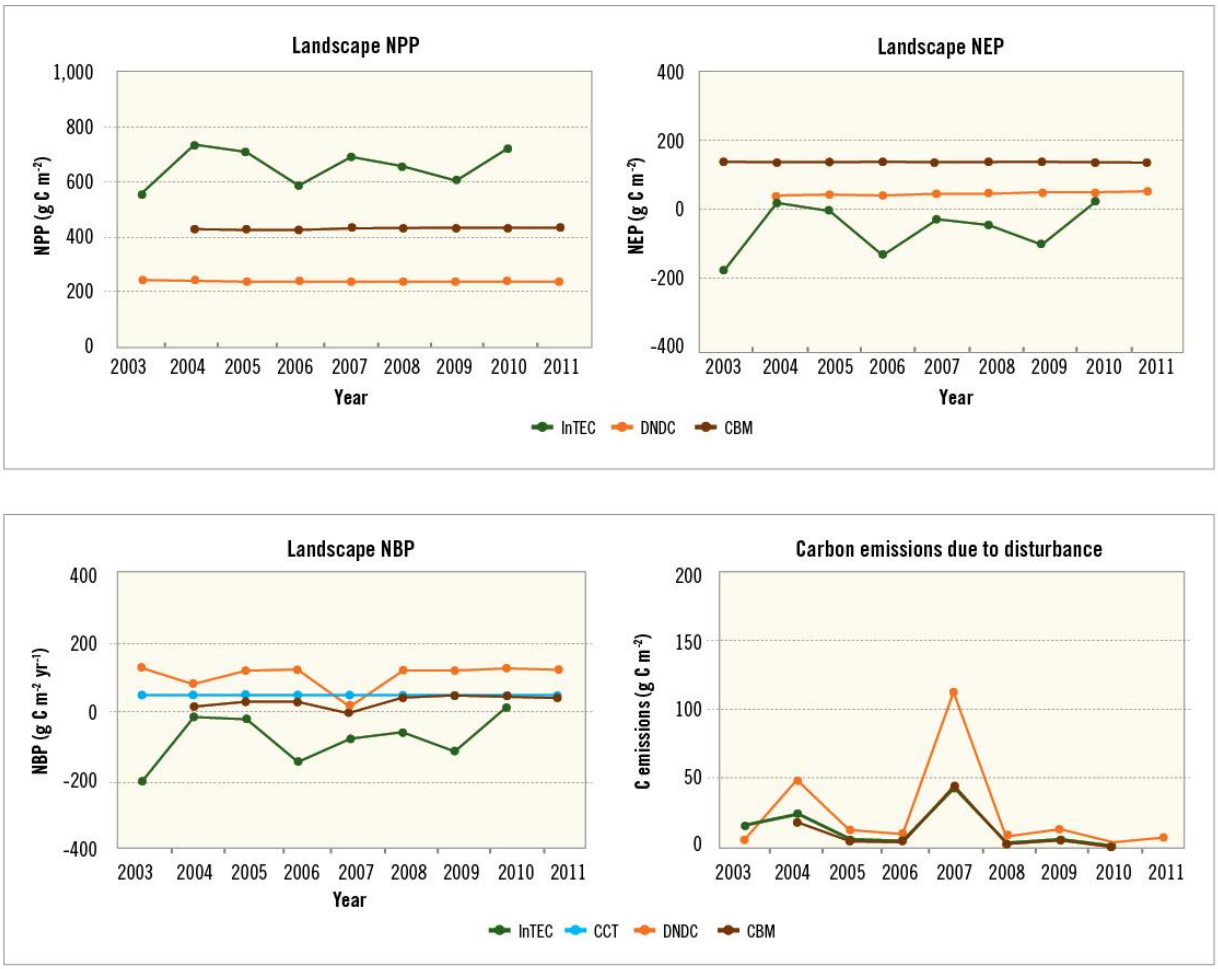

Note: g C m^{-2} = grams carbon per square meter; y^{-1} = per year; DNDC = DeNitrification-DeComposition Model; CBM-CFS3 = Carbon Budget Model of the Canadian Forest Sector. See Table 9.2 for description of methods used.

Deadwood is another important carbon pool strongly affected by natural disturbances. The differences among methods are more pronounced in terms of percentages than the differences for aboveground biomass, although the groupings are similar (Figure 9.3). Deadwood estimates are affected by the selection of biomass equations and the estimation approach used, just like livewood, and also the modeling approaches are quite different. Even the FIA "data" are actually based in part on an empirical model rather than being a direct calculation based on field measurements. Field measurements are routinely made only for standing-dead trees and not for downed-deadwood, which is measured on only a subset of inventory plots. These downed-deadwood data are used to formulate a simple model for deadwood density based on livewood density (Woodall et al. 2008). DNDC generates deadwood estimates based on disturbance data because empirical data from inventories are not used as an input, and

thus the buildup of deadwood is affected by the period of known and simulated disturbances. Estimates of the carbon density of litter are even more divergent and show an opposite pattern among approaches, compared to that for deadwood (Figure 9.3). It is possible that opposing differences in these pools also reflect different definitions of the components that are included in each pool. For example, DNDC and CBM-CFS3 have the highest and lowest estimates of deadwood carbon densities, respectively. But they have the lowest and highest estimates of litter pools. The difference among the four models in the combined litter and deadwood pools are considerably smaller than the differences in the individual pools.

Estimates of NPP, NEP and NBP are significantly different among CBM-CFS3, DNDC, and InTEC, and the causes of differences are hard to identify (Figure 9.4). One model, InTEC, estimates the highest rates of NPP, and yet predicts a carbon source (NEP<0, NBP <0). InTEC estimates the highest rates of heterotrophic respiration (the difference between NEP and NPP) and estimates direct losses from disturbances that are similar to those estimated by CBM-CFS3. The annual average NBP estimates are highest for DNDC (108.3 g m^{-2} yr^{-1}), lowest (and negative) for InTEC (-72.7 g m^{-2} yr^{-1}), with CCT (51.4 g m^{-2} yr^{-1}) and CBM-CFS3 (31.7 g m^{-2} yr^{-1}) estimating intermediate rates of NBP. The two process-based models differ in sign of Net Biome Production estimate and are at opposite ends of the range of estimated values.

A very significant factor underlying these differences among approaches is related to age classifications, which may consider both a young forest and a degraded forest (e.g., from a high-severity disturbance) as the same age, whereas these two would have very different estimates of decay from deadwood and other carbon pools. Stand age differences also affect the estimates of disturbance impacts that are obtained by the different approaches. Data-based approaches rely on observed values for deadwood and litter pools, applied by developing empirical models to represent how these pools are related to stand age and forest type. Process models are more likely to generate these pools based on history of disturbances, and therefore are limited by knowledge of past disturbances and land use.

Further research based on updated forest inventories, intensive site measurements and repeated ground plot measurements will be required to identify, quantify, and reduce uncertainties as far as is practicable. Models can be improved through the application of rigorous comparisons of model predictions against ground plot measurements (Shaw et al. 2014), permanent sample plot measurements (Hember et al. 2012), and through data-model assimilation (Hararuk and Luo 2014; Hararuk et al. 2014).

9.3 Lessons learned from model comparisons

In summary, the comparison of estimates from empirical and process models, not only in NP but in the other pilot study sites, has resulted in some lessons that can help guide similar efforts.

- Model calibration is an important consideration when applying a model to a different region or forest type from that used to develop the original application.
- When possible, it is strongly recommended that model results be compared with independent data sets for validating results. This is particularly important when a model is applied to a different population from that used for developing the model application.
- A high level of skill may be required to use empirical and process models. Both classes of model usually require significant efforts for acquiring and managing the input data, which may not be

readily available, representative of the region or forest type of interest, or properly prepared for the model. As a general rule, empirical models are easier to understand and require fewer input data, whereas process models usually involve detailed representation of mechanisms and their response to environmental drivers, which should be well understood by the analyst.

- Model comparisons are always difficult to perform. Different models have different data requirements, may or may not be spatially explicit, may include representation of different environmental drivers, and may use different definitions of variables and pools. Sorting out these differences is labor intensive and may not always be possible unless well planned from the start.

Some of the important lessons learned about harmonizing data inputs to the different models from this project are as follows:

- Area estimates must be harmonized among models. Inconsistencies may involve discrepancies among forest area estimates, forest type classifications, and age estimates. Area differences may be related to whether the area data are spatially explicit or spatially referenced and to how the data were derived. Differences in area can be overcome partly by comparing carbon stock density and flux density values, i.e., estimates expressed on a per unit area basis.
- Age assignment and disturbance history are critical variables for carbon modeling and should be reconciled among models. This is especially true in tropical regions, where forest degradation and lack of obvious age of trees may make age assignments difficult to employ.
- Area classification, such as forest type, needs to be harmonized with variables pertaining to the forest type classification, such as average carbon stocks or productivity estimates, and with age or disturbance classifications.
- Activity data, including the impacts of disturbances on carbon pools and emission, also need to be harmonized because forest management, natural disturbances and land-use change are the dominant drivers of carbon dynamics in North American forest ecosystems.

10. Next Steps: Forests and Forest-sector Contributions to Mitigating Climate Change Impacts

W.A. Kurz, R.A. Birdsey, E. Serrano and K. Richardson

The forest sector is expected to play an important role in domestic GHG mitigation portfolios in Canada, Mexico and the US, and the potential to do so is large in the medium to long term (McKinley et al. 2011; Smyth et al. 2014). As shown in this report, the primary drivers of forest carbon stock changes, emissions and removals differ among the three countries, but for each country, opportunities exist to reduce emissions and increase removals of GHG through changes in forest management, reduction of emissions from deforestation and degradation, and the expanded use of products derived from forests.

The IPCC has emphasized the need to take a system's perspective when designing climate change mitigation strategies in the forest sector: assessing the climate benefits of proposed mitigation activities requires the evaluation of the net GHG emissions resulting from changes in carbon stocks in forest ecosystems and harvested wood product carbon pools, as well as the avoidance of emissions that result from the use of forest products to substitute for other emissions-intensive materials such as concrete, steel, plastics, and fossil fuels (Lemprière et al. 2013; Nabuurs et al. 2007).

This study has demonstrated the use of carbon budget models to quantify the GHG emissions and removals associated with forest management and land-use decisions. These models can estimate and report the rates of lateral carbon transfer from forests to other sectors of society. The combined average annual harvest in North America is about 625 million m^3 wood under bark (FAO 2015, Table 24), for the period 1990 to 2011, with 2011 values about 75% of the average). This annual harvest represents a carbon transfer in wood that is equivalent to more than 600 Tg CO_2 yr^{-1}. How this carbon is used will affect North America's GHG balance.

New forest carbon reporting and accounting rules (IPCC 2006, 2014a) that came into effect in 2015 replace the assumption that any material removed from the forest is instantly oxidized and released to the atmosphere with a requirement to account for the fate of carbon removed from the forest. Countries are now expected to report carbon storage in harvested wood products (HWPs) that are produced from all wood harvested in the country, and to track storage and emissions of carbon regardless of where in the world the wood products are used. This reporting methodology, which is based on the IPCC "Production Approach," increases the need to understand the fate of carbon in HWP domestically and in export markets (IPCC 2006, 2014a). Moreover, by quantifying the carbon storage, half-life, and release from HWP, opportunities can be identified to prolong carbon retention in HWP. For example, the IPCC default half-life for carbon in pulp and paper products is two years, while that in sawn-wood commodities is 35 years. Thus, shifting wood use from short-lived to longer-lived products can contribute to climate change mitigation (Lemprière et al. 2013; Smyth et al. 2014; Werner et al. 2010). Cascading wood use strategies that maximize carbon retention at every stage in the life cycle can contribute to climate change mitigation (Höglmeier et al. 2015).

Using wood instead of other materials or fossil fuels can also benefit GHG balances. However, so-called substitution benefits that arise through the displacement of emissions-intensive materials with wood products are typically observed and reported outside the forest sector. For example, if wood use reduces demand for concrete or steel, the associated emission reductions are reported elsewhere, both in other sectors and, at times, in other countries. For example, the export of wood pellets from North America to Europe is associated with carbon stock reductions in forests in North America, reported emissions in North America from the burning of pellets in Europe, and reductions in fossil fuel emissions in Europe.

Developing policies that address climate change mitigation objectives in the forest sector therefore requires new tools and the supporting data to quantify carbon storage in HWP, as well as the substitution benefits that may result from wood product use in North America or in export markets. The next phase of this CEC-funded project will conduct research aimed at developing, testing and harmonizing models and approaches in the three countries that will inform policy makers about the potential of the North American forest sector to contribute to climate change mitigation. In addition to researching and improving the science-based tools that can inform policy, the project will facilitate trinational communication, information exchange, and capacity building so that the scientific and policy communities can design, assess and potentially implement forest-sector activities that can contribute to meeting national GHG emission reduction targets.

The next phase of this project will use the models of carbon dynamics in forest ecosystems that were studied in phase 1 in combination with models of carbon dynamics in HWP to quantify the GHG impacts of various forest-sector mitigation options to meet national objectives of GHG emission reductions, for selected landscapes in Canada, Mexico and the US. The project will focus only on representative, selected landscapes in all three countries—national-scale analyses of mitigation options will remain the responsibility of respective national agencies, but such national analyses can be informed by the results of this coordinated research project. This work will also facilitate the development of mitigation strategies at the continental scale that take strategic advantage of the most effective options in each country. Coordination under the sponsorship of the CEC will enable the project team to identify and analyze the most efficient GHG mitigation options and improve understanding of regional differences between the available mitigation options and their mitigation potentials. If implemented, they can make significant long-term contributions to reducing GHG emissions in each country.

The next phase of this project will also continue to improve the available models for assessment of carbon stocks and GHG balances in forest ecosystems through ongoing validation and model testing, and by enhancing and harmonizing the linkages between remote sensing-derived information on activities (forest management, land-use change, and natural disturbances) and regional forest carbon balances.

Improving the transparency, accuracy, and completeness of forest-sector GHG emissions and removals estimates will increase the likelihood that mitigation strategies in North America's forest sector are identified, quantified and implemented. Information generated from this research will enable the forest sector to make material contributions to GHG emission reduction targets in North America through reductions in deforestation and degradation, and through sustainable forest management and the use of harvested wood products.

References

Achard, F., R. Beuchle, P. Mayaux, H.J. Stibig, C. Bodart, A. Brink, S. Carboni, et al. 2014. Determination of tropical deforestation rates and related carbon losses from 1990 to 2010. *Global Change Biology* 20(8): 2540–54. doi:10.1111/gcb.12605.

Ángeles, G. n.d. Growth curve generation routine using national scale forest inventory data from Mexico.

Asner, G.P., G.V.N. Powell, J. Mascaro, D.E. Knapp, J.K. Clark, J. Jacobson, T. Kennedy-Bowdoin, et al. 2010. High-resolution forest carbon stocks and emissions in the Amazon. *Proceedings of the National Academy of Sciences of the United States of America* 107(38): 16738–42. doi:10.1073/pnas.1004875107.

Baccini, A., S.J. Goetz, W.S. Walker, N.T. Laporte, M. Sun, D. Sulla-Menashe, J. Hackler, et al. 2012. Estimated carbon dioxide emissions from tropical deforestation improved by carbon-density maps. *Nature Climate Change* 2(3): 182–85. doi:10.1038/nclimate1354.

Barber, J., R. Bush, and D. Berglund. 2011. *The Region 1 Existing Vegetation Classification System and Its Relationship to Region 1 Inventory Data and Map Products*. USDA: US Forest Service. <www.fs.usda.gov/Internet/FSE_DOCUMENTS/stelprdb5366381.pdf>.

Bertalanffy, L. von, 1934. Untersuchungen über die Gesetzlichkeit des Wachstums. I. Allgemeine Grundlagen der Theorie; mathematische und physiologische Gesetzlichkeiten des Wachstums bei Wassertieren. *Arch. Entwicklungsmech.* 131: 613–652.

Birdsey, R.A., G. Ángeles Pérez, W.A. Kurz, A. Lister, M. Olguín, Y. Pan, C. Wayson, B. Wilson, and K. Johnson. 2013. Approaches to monitoring changes in carbon stocks for REDD+. *Carbon Management* 4(5): 519–537. doi: 10.4155/cmt.13.49.

Blanco, P.D., R.R. Colditz, G. López Saldaña, L.A. Hardtke, R.M. Llamas, N.A. Mari, A. Fischer, et al. 2013. A land cover map of Latin America and the Caribbean in the framework of the SERENA project. *Remote Sensing of Environment* 132: 13–31. doi:10.1016/j.rse.2012.12.025.

Bona, K.A., J.W. Fyles, C. Shaw, and W.A. Kurz. 2013. Are mosses required to accurately predict upland black spruce forest soil carbon in National-Scale Forest C Accounting Models? *Ecosystems* 16(6): 1071–86. doi:10.1007/s10021-013-9668-x.

Böttcher, H., W.A. Kurz, and A. Freibauer. 2008. Accounting of Forest Carbon Sinks and Sources under a Future Climate Protocol-Factoring out Past Disturbance and Management Effects on Age-Class Structure. *Environmental Science and Policy* 11(8): 669–86. doi:10.1016/j.envsci.2008.08.005.

Boudewyn, P., X. Song, S. Magnussen, and M.D. Gillis. 2007. *Model-Based, Volume-to-Biomass Conversion for Forested and Vegetated Land in Canada*. Natural Resources Canada, Canadian Forest Service, Pacific Forestry Centre, Victoria, BC. Information Report BC-X-411. 112 p.

Canadell, J.G., and E.D. Schulze. 2014. Global Potential of Biospheric Carbon Management for Climate Mitigation. *Nature Communications* 5(5282): 1–12. doi:10.1038/ncomms6282.

CEC. 1997. *Ecological Regions of North America: Towards a Common Perspective*. Commission for Environmental Cooperation. Montreal, Quebec, Canada: Commission for Environmental Cooperation. <www3.cec.org/islandora/en/item/1701-ecological-regions-north-america-toward-common-perspective-en.pdf>.

CEC. 2010. *Terrestrial Protected Areas of North America*. Montréal, Québec, Canada: Commission for Environmental Cooperation. <www.cec.org/tools-and-resources/map-files/terrestrial-protected-areas-2010>.

Chapin, F.S., G.M. Woodwell, J.T. Randerson, E.B. Rastetter, G.M. Lovett, D.D. Baldocchi, D.A. Clark, et al. 2006. Reconciling carbon-cycle concepts, terminology, and methods. *Ecosystems* 9(7): 1041–50. doi:10.1007/s10021-005-0105-7.

Chojnacky, D.C. 2012. FIA's volume-to-biomass conversion method (crm) generally underestimates biomass in comparison to published equations. In: *Moving from Status to Trends: Forest Inventory and Analysis (FIA) Symposium 2012*. Gen. Tech. Rep. NRS-P-105, edited by Morin, Randall, and G.C. Liknes, 396–402. Baltimore, MD: US Department of Agriculture, US Forest Service, Northern Research Station.

Climate Action Reserve. 2013. Climate Action Reserve. <www.climateactionreserve.org/wp-content/uploads/2014/04/CAR-AnnualReport-FINAL.pdf>.

Colditz, R.R., R.M. Llamas, S. Gebhardt, T. Wehrmann, and J. Equihua. 2015. Comparison of change detection techniques for the Yucatan Peninsula using Landsat image time series. In *IEEE International Geoscience and Remote Sensing Symposium IGARSS*, 1–4. Milan, Italy.

Colditz, R.R., R.M. Llamas, V.S. Mascorro, and R.A. Ressl. 2015. Land cover change analysis of the Yucatan Peninsula using Landsat data from 1985–2010. In *IEEE International Geoscience and Remote Sensing Symposium IGARSS*, 1–4. Milan, Italy.

Colditz, R.R., R.M. Llamas, and R.A. Resssl. 2015. Land cover change analysis in Mexico using 30m Landsat and 250m MODIS data. In *36th International Symposium on Remote Sensing of Environment, ISRSE*, 367–74. Berlin, Germany: The International Archives of the Photogrammetry, Remote Sensing and Spatial Information Sciences.

Conafor. 2010. Inventario nacional y de suelos. Manual y procedimientos para el muestreo de campo: re-muestreo 2010. Zapopan, Jalisco, México: Comisión Nacional Forestal de Mexico.

Conafor. 2012. *Acciones Tempranas REDD+*. <www.conafor.gob.mx/portal/index.php/proceso-nacional-redd/e-acciones-tempranas>.

Conafor. 2013. *Estrategia Nacional Para REDD+*. <www.conafor.gob.mx:8080/documentos/docs/35/4861Estrategia Nacional para REDD_.pdf>.

Conafor. 2014a. *Estimación de las reservas de carbono en la biomasa forestal en México*. Zapopan, Jalisco, México: Comisión Nacional Forestal de México. Internal Report.

Conafor. 2014b. *Información estadísticas anual de incendios forestales en México*. Coordinación General de Conservación y Restauracíon. Geréncia de Protección Contra Incendios Forestales. <www.conafor.gob.mx/portal/index.php/temas-forestales/incendios>.

Coops, N.C., M.A. Wulder, and J.C. White. 2006. Identifying and describing forest disturbance and spatial pattern: Data selection issues and methodological implications. Chapter 2 of M.A. Wulder and S.E. Franklin, *Understanding Forest Disturbance Spatial Pattern: Remote Sensing and GIS Approaches.* Boca Raton, FL: CRC Taylor & Francis Group. 31–62.

Coppin, P., I. Jonckheere, K. Nackaerts, B. Muys, and E. Lambin. 2004. Digital change detection methods in ecosystem monitoring: A review. *International Journal of Remote Sensing* 25(9): 1565–96. doi:10.1080/0143116031000101675.

Dai, Z., and R.A. Birdsey. 2015. Estimating carbon dynamics and potential impacts of climate change and disturbances on carbon sequestration in the North American forests using process models: Model evaluation and case study.

Dai, Z., R.A. Birdsey, K.D. Johnson, J.D. Dupuy, J.L. Hernandez-Stefanoni, and K. Richardson. 2014. Modeling carbon stocks in a secondary tropical dry forest in the Yucatan Peninsula, Mexico. *Water, Air, & Soil Pollution* 225(4): 1925. doi:10.1007/s11270-014-1925-x.

Dai, Z., C.C. Trettin, and D.M. Amatya. 2013. Effects of Climate Variability on Forest Hydrology and Carbon Sequestration on the Santee Experimental Forest in Coastal South Carolina. Asheville, NC: US Department of Agriculture, US Forest Service, Southern Research Station.

Daly, C., M. Halbleib, J.I. Smith, W.P. Gibson, M.K. Doggett, G.H. Taylor, J. Curtis, and P.P. Pasteris. 2008. Physiographically sensitive mapping of climatological temperature and precipitation across the conterminous United States. *International Journal of Climatology* 28(15): 2031–64. doi:10.1002/joc.1688.

De Jong, B., C. Anaya, O. Masera, M. Olguín, F. Paz, J. Etchevers, R.D. Martínez, G. Guerrero, and C. Balbontín. 2010. Greenhouse gas emissions between 1993 and 2002 from land-use change and forestry in Mexico. *Forest Ecology and Management* 260(10): 1689–1701. doi:10.1016/j.foreco.2010.08.011.

De'ath, G. 2002. Multivariate regression tree: A new technique for modeling species–environment relationships. *Ecology* 83(4): 1105–17. doi:10.1890/0012-9658(2002)083[1105:MRTANT]2.0.CO;2.

De'ath, G., and K.E. Fabricius. 2000. Classification and regression trees: A powerful yet simple technique for ecological data analysis. *Ecology*. doi:10.1890/0012-9658(2000)081[3178:CARTAP]2.0.CO;2.

DiGregorio, A. 2005. Land Cover Classification System (LCCS), Version 2: Classification Concepts and User Manual. FAO FAO: Environment and Natural Resources Service Series.

Domke, G.M., C.W. Woodall, B.F. Walters, and J.E. Smith. 2013. From models to measurements: Comparing downed dead wood carbon stock estimates in the US Forest Inventory. *PLoS ONE* 8(3). doi:10.1371/journal.pone.0059949.

Dupuy, J.M., J.L. Hernández-Stefanoni, R.A. Hernández-Juárez, E. Tetetla-Rangel, J.O. López-Martínez, E. Leyequién-Abarca, F.J. Tun-Dzul, and F. May-Pat. 2012. Patterns and correlates of tropical dry forest structure and composition in a highly replicated chronosequence in Yucatan, Mexico. *Biotropica* 44(2): 151–62. doi:10.1111/j.1744-7429.2011.00783.x.

Environment Canada. 2015. *National Inventory Report 1990–2013: Greenhouse Gas Sources and Sinks in Canada*. The Canadian Government's Submission to the UN Framework Convention on Climate Change, 199.

FAO. 2010. *Global Forest Resources Assessment 2010*. FAO Forestry, Rome, Italy.

FAO. 2015. *Global Forest Resources Assessment 2015*. Desk Reference. FAO Forestry, Rome, Italy.

FCPF. 2013. Emission reductions program idea note (ER-PIN). Forest Carbon Partnership Facility (FCPF) Carbon Fund. <www.forestcarbonpartnership.org/mexico>.

Feranec, J., G. Jaffrain, T. Soukup, and G. Hazeu. 2010. Determining changes and flows in european landscapes 1990-2000 using CORINE land cover data. *Applied Geography* 30(1): 19–35. doi:10.1016/j.apgeog.2009.07.003.

Fisher, P.F. 2010. Remote sensing of land cover classes as Type 2 Fuzzy Sets. *Remote Sensing of Environment* 114(2): 309–21. doi:10.1016/j.rse.2009.09.004.

Friedlingstein, P., P. Cox, R. Betts, L. Bopp, W. von Bloh, V. Brovkin, P. Cadule, et al. 2006. Climate–carbon cycle feedback analysis: Results from the C 4 MIP Model intercomparison. *Journal of Climate* 19(14): 3337–53. doi:10.1175/JCLI3800.1.

Fry, J.A., G. Xian, S. Jin, J.A. Dewitz, C.G. Homer, L. Yang, C.A. Barnes, N.D. Herold, and J.D. Wickham. 2011. Completion of the 2006 National Land Cover Database for the conterminous United States. *Photogrammetric Engineering and Remote Sensing* 77: 858–64.

Gebhardt, S., T. Wehrmann, M. Ruiz, P. Maeda, J. Bishop, M. Schramm, R. Kopeinig, et al. 2014. MAD-MEX: Automatic wall-to-wall land cover monitoring for the Mexican REDD-MRV program using all Landsat data. *Remote Sensing* 6(5): 3923–43. doi:10.3390/rs6053923.

GOFC-GOLD (COP 19, version 2). 2014. A Sourcebook of Methods and Procedures for Monitoring and Reporting Anthropogenic Greenhouse Gas Emissions and Removals Caused by Deforestation, Gains and Losses of Carbon Stocks in Forests Remaining Forests, and Forestation. Global Observation of Forest and Land Cover Dynamics. <www.wmo.int/pages/prog/gcos/documents/Mitigation_GOFC-GOLD_REDD_Sourcebook.pdf>.

Goodrick, S.L., D. Shea, and J. Blake. 2010. Estimating fuel consumption for the upper coastal plain of South Carolina. *Southern Journal of Applied Forestry* 34(1): 5–12.

Greenberg, D. 2015. Estimating North American Carbon Budgets: Development and Testing of Computational Tools and Modeling Approaches. Montreal, Quebec, Canada: Commission for Environmental Cooperation.

Griffiths, P., S. van der Linden, T. Kuemmerle, and P. Hostert. 2013. A pixel-based Landsat compositing algorithm for large area land cover mapping. Selected topics in applied earth observations and remote sensing, *IEEE Journal 6*: 2088–2101. doi:10.1109/JSTARS.2012.2228167.

Hansen, M.C., P.V. Potapov, R. Moore, M. Hancher, S.A. Turubanova, A. Tyukavina, D. Thau, et al. 2013. High-resolution global maps of 21st-century forest cover change. *Science* 342(6160): 850–53. New York, N.Y. doi:10.1126/science.1244693.

Hararuk, O., and Y. Luo. 2014. Improvement of global litter turnover rate predictions using a Bayesian MCMC approach. *Ecosphere* 5(12): 163. doi:http://dx.doi.org/10.1890/ES14-00092.1.

Hararuk, O., J. Xia, and Y. Luo. 2014. Evaluation and improvement of a global land model against soil carbon data using a Bayesian Marcov Monte Carlo method. *Journal of Geophysical Research Biogeosciences* 119(3): 403–17. doi:10.1002/2013JG002535.

Healey, S., W. Cohen, Y. Zhiqiang, and O. Krankina. 2005. Comparison of tasseled cap-based Landsat data structures for use in forest disturbance detection. *Remote Sensing of Environment* 97(3): 301–10. doi:10.1016/j.rse.2005.05.009.

Healey, S.P., S.P. Urbanski, P.L. Patterson, and C. Garrard. 2014. A framework for simulating map error in ecosystem models. *Remote Sensing of Environment* 150: 207–17. doi:10.1016/j.rse.2014.04.028.

Healey, S.P., Z. Yang, W.B. Cohen, and D.J. Pierce. 2006. Application of two regression-based methods to estimate the effects of partial harvest on forest structure using Landsat data. *Remote Sensing of Environment* 101(1): 115–26. doi:10.1016/j.rse.2005.12.006.

Heath, L.S., J.E. Smith, K.E. Skog, D.J. Nowak, and C.W. Woodall. 2011. Managed forest carbon estimates for the US Greenhouse Gas Inventory, 1990–2008. *Journal of Forestry* 109(3): 167–73.

Hember, R.A., W.A. Kurz, J.M. Metsaranta, T.A. Black, R.D. Guy, and N.C. Coops. 2012. Accelerating regrowth of temperate-maritime forests due to environmental change. *Global Change Biology* 18(6): 2026–40. doi:10.1111/j.1365-2486.2012.02669.x.

Höglmeier, K., B. Steubing, G. Weber-Blaschke, and K. Richter. 2015. LCA-based optimization of wood utilization under special consideration of a cascading use of wood. *Journal of Environmental Management* 152: 158–70. doi:10.1016/j.jenvman.2015.01.018.

Huang, C., S. Goward, J. Masek, F. Gao, E. Vermote, N. Thomas, K. Schleeweis, et al. 2009. Development of time series stacks of Landsat images for reconstructing forest disturbance history. *International Journal of Digital Earth* 2(3): 195–218. doi:10.1080/17538940902801614.

Huang, C., S.N. Goward, J.G. Masek, N. Thomas, Z. Zhu, and J.E. Vogelmann. 2010. An automated approach for reconstructing recent forest disturbance history using dense Landsat time series stacks. *Remote Sensing of Environment* 114(1) 183–98. doi:10.1016/j.rse.2009.08.017.

Huntzinger, D.N., W.M. Post, Y. Wei, a.M. Michalak, T.O. West, a.R. Jacobson, I.T. Baker, et al. 2012. North American Carbon Program (NACP) regional interim synthesis: Terrestrial biospheric model intercomparison. *Ecological Modelling* 232: 144–57. doi:10.1016/j.ecolmodel.2012.02.004.

INEGI. 2013. Conjunto de datos vectoriales de carreteras y vialidades urbanas edición 1.0. Aguascalientes, Mexico: *Instituto Nacional de Estadística y Geografía*.

IPCC. 2000. Good Practice Guidance and Uncertainty Management in National Greenhouse Gas Inventories. Hayama, Japan: Intergovernmental Panel on Climate Change.

IPCC. 2003. *Good Practice Guidance for Land Use, Land-Use Change and Forestry*. Edited by J. Penman, M. Gytarsky, T. Hiraishi, T. Krug, D. Kruger, R. Pipatti, L. Buendia, et al. Hayama, Japan: Intergovernmental Panel on Climate Change (IPCC), IPCC/IGES.

IPCC. 2006. Generic methodologies applicable to multiple land-use categories. *2006 IPCC Guidelines for National Greenhouse Gas Inventories*, Ed. by S. Eggleston, L Buendia, K. Miwa, T. Ngara and K. Tanabe. Hayama, Japan: Intergovernmental Panel on Climate Change (IPCC). 1–59.

IPCC. 2011. *Use of Models and Facility-Level Data in Greenhouse Gas Inventories* (Report of IPCC Expert Meeting on Use of Models and Measurements in Greenhouse Gas Inventories 9-11 August 2010, Sydney, Australia). Edited by H.S. Eggleston, N. Srivastava, K. Tanabe, J. Baasansuren, and M. Fukuda. Japan: IGES.

IPCC. 2014a. 2013 *Revised Supplementary Methods and Good Practice Guidance Arising from the Kyoto Protocol*. Edited by T.G. Hiraishi, T., Krug, T., Tanabe, K., Srivastava, N., Baasansuren, J., Fukuda, M. and Troxler. Switzerland: Intergovernmental Panel on Climate Change (IPCC).

IPCC. 2014b. 2013 *Supplement to the 2006 IPCC Guidelines for National Greenhouse Gas Inventories: Wetlands*. Edited by T. Hiraishi, T. Krug, K. Tanabe, N. Srivastava, J. Baasansuren, M. Fukuda, and T.G. Troxler. Switzerland: Intergovernmental Panel on Climate Change (IPCC).

Jardel, P.E.J., J.M Frausto-Leyva, D. Pérez-Salicrup, E. Alvarado, J.E. Morfín-Ríos, R. Landa, and P. Llamas-Casillas. 2010. *Prioridades de Investigación en Manejo del Fuego en México*. Fondo Mexicano Para La Conservación de La Naturaleza.

Kasischke, E.S., T. Loboda, L. Giglio, N.H. F. French, E.E. Hoy, B. de Jong, and D. Riano. 2011. Quantifying burned area for North American forests: Implications for direct reduction of carbon stocks. *Journal of Geophysical Research* 116(G4). doi:10.1029/2011JG001707.

Kennedy, R.E., P.A. Townsend, J.E. Gross, W.B. Cohen, P. Bolstad, Y.Q. Wang, and P. Adams. 2009. Remote sensing change detection tools for natural resource managers: Understanding concepts and tradeoffs in the design of landscape monitoring projects. *Remote Sensing of Environment* 113 (7): 1382–96. doi:10.1016/j.rse.2008.07.018.

Konheim, A.G. 2010. Hashing in Computer Science: Fifty Years of Slicing and Dicing. Edited by 1. Wiley-Interscience.

Kull, S.J., W.A. Kurz, G.J. Rampley, G.J. Banfield, R.K. Schivatcheva, and M.J. Apps. 2011. *Operational-Scale Carbon Budget Model of the Canadian Forest Sector (CBM-CFS3).* Version 1.0, User's Guide. Natural Resources Canada. Edmonton, Alberta.

Kurz, W.A., and M.J. Apps. 2006. Developing Canada's National Forest Carbon Monitoring, Accounting and Reporting System to meet the reporting requirements of the Kyoto Protocol. *Mitigation and Adaptation Strategies for Global Change* 11(1): 33–43. doi:10.1007/s11027-006-1006-6.

Kurz, W.A. 2010a. Large inter-annual variations in carbon emissions and removals, Invited background paper. In IPCC 2010, *Revisiting the Use of Managed Land as a Proxy for Estimating National Anthropogenic Emissions and Removals*, edited by H.S. Eggleston, N. Srivastava, K. Tanab, and J. Baasansuren, 41–48. INPE, São José dos Campos, Brazil: IGES.

Kurz, W.A. 2010b. An ecosystem context for global gross forest cover loss estimates. *Proceedings of the National Academy of Sciences of the United States of America* 107(20): 9025–26. doi:10.1073/pnas.1004508107.

Kurz, W.A., and M.J. Apps. 1999. A 70-year retrospective analysis of carbon fluxes in the Canadian forest sector. *Ecological Applications* 9(2): 526–47. doi:10.1890/1051-0761(1999)009[0526:AYRAOC]2.0.CO;2.

Kurz, W.A., M.J. Apps, T.M. Webb, and P.J. McNamee. 1992. The Carbon Budget of the Canadian Forest Sector: Phase I. Information Report NOR-X-326.

Kurz, W.A., C.C. Dymond, G. Stinson, G.J. Rampley, E.T. Neilson, A.L. Carroll, T. Ebata, and L. Safranyik. 2008. Mountain pine beetle and forest carbon feedback to climate change. *Nature* 452(7190): 987–90. doi:10.1038/nature06777.

Kurz, W.A., C.C. Dymond, T.M. White, G. Stinson, C.H. Shaw, G.J. Rampley, C. Smyth, et al. 2009. CBM-CFS3: A model of carbon-dynamics in forestry and land-use change implementing IPCC standards. *Ecological Modelling* 220(4): 480–504. doi:10.1016/j.ecolmodel.2008.10.018.

Kurz, W.A., C.H. Shaw, C. Boisvenue, G. Stinson, J. Metsaranta, D. Leckie, A. Dyk, C. Smyth, and E.T. Neilson. 2013. Carbon in Canada's boreal forest — a synthesis. *Environmental Reviews* 292(January): 260–92. doi:Doi 10.1139/Er-2013-0041.

Landsberg, J.J., and R.H. Waring. 1997. A generalised model of forest productivity using simplified concepts of radiation-use efficiency, carbon balance and partitioning. *Forest Ecology and Management* 95(3): 209–28. doi:10.1016/S0378-1127(97)00026-1.

Le Quéré, C., R. Moriarty, R.M. Andrew, G.P. Peters, P. Ciais, P. Friedlingstein, S.D. Jones, et al. 2015. Global carbon budget 2014. *Earth System Science Data* 7(1). Copernicus GmbH: 47–85. doi:10.5194/essd-7-47-2015.

Lehrter, J.C., and J. Cebrian. 2010. Uncertainty propagation in an ecosystem nutrient budget. *Ecological Applications* 20(2): 508–24. doi:10.1890/08-2222.1.

Lemay, V.M., and W.A. Kurz. 2008. Estimating carbon stocks and stock changes in forests: Linking models and data across scales. In *Managing Forest Ecosystems: The Challenge of Climate Change*. Edited by F. Bravo, V. Lemay, R. Jandl, and K.V. Gadow, 63–81. New York: Springer.

Lemprière, T.C., W.A. Kurz, E.H. Hogg, C. Schmoll, G.J. Rampley, D. Yemshanov, D.W. Mckenney, et al. 2013. Canadian Boreal Forests and Climate Change Mitigation 1. *Environmental Reviews* 21(4): 293–321. doi:10.1139/er-2013-0039.

Li, C., J. Aber, F. Stange, K. Butterbach-Bahl, and H. Papen. 2000. A process-oriented model of N_2O and NO emissions from forest soils: 1. model development. *Journal of Geophysical Research*: *Atmospheres* 105(D4): 4369–84. doi:10.1029/1999JD900949.

Li, Z., W.A. Kurz, M.J. Apps, and S.J. Beukema. 2003. Belowground biomass dynamics in the carbon budget model of the Canadian Forest Sector: Recent improvements and implications for the estimation of NPP and NEP. *Canadian Journal of Forest Research* 33(1): 126–136. doi:10.1139/x02-165.

Liu, S., B. Bond-Lamberty, J.A. Hicke, R. Vargas, S. Zhao, J. Chen, S.L. Edburg, et al. 2011. Simulating the impacts of disturbances on forest carbon cycling in North America: Processes, data, models, and

challenges. *Journal of Geophysical Research: Biogeosciences* 116(G4): 1–22. doi:10.1029/2010JG001585. <http://onlinelibrary.wiley.com/doi/10.1029/2010JG001585/epdf>.

Lorenz, K., and R. Lal. 2010. Effects of disturbance, succession and management on carbon sequestration. In *Carbon Sequestration in Forest Ecosystems*, pp. 103–57. Dordrecht: Springer Netherlands. doi:10.1007/978-90-481-3266-9.

Lu, D., P. Mausel, E. Brondízio, and E. Moran. 2004. Change detection techniques. *International Journal of Remote Sensing* 25(12): 2365–2401. doi:10.1080/0143116031000139863.

Lu, X., D.W. Kicklighter, J.M. Melillo, J.M. Reilly, and L. Xu. 2015. Land carbon sequestration within the conterminous United States: Regional- and state-level analyses. *Journal of Geophysical Research. Biogeosciences* 120(2): 379–98. doi:10.1002/2014JG002818.

Luo, Y., K. Ogle, C. Tucker, S. Fei, C. Gao, S. LaDeau, J.S. Clark, and D.S. Schimel. 2011. Ecological forecasting and data assimilation in a data-rich era. *Ecological Applications* 21(5): 1429–42. doi:10.1890/09-1275.1.

Mascorro, V.S. 2014. Assessing Forest Disturbances for Carbon Modelling: Building the Bridge between Activity Data and Carbon Budget Modelling, M.Sc. Thesis, Faculty of Forestry, University of British Columbia, Vancouver, Canada. 106 pp.

Mascorro, V.S., N.C. Coops, W.A. Kurz, and M. Olguín. 2016. Choice of satellite imagery and attribution of changes to disturbance type strongly affects forest carbon balance estimates. *Carbon Balance and Management* 10(1): 30. doi: 10.1186/s13021-015-0041-6.

Mascorro, V.S., N.C. Coops, W.A. Kurz, and M. Olguín. 2014. Attributing changes in land cover using independent disturbance datasets: A case study of the Yucatan Peninsula, Mexico. *Regional Environmental Change* 16(1): 213-228. doi:10.1007/s10113-014-0739-0.

Masek, J.G., W.B. Cohen, D. Leckie, M.A. Wulder, R. Vargas, B. de Jong, S. Healey, et al. 2011. Recent rates of forest harvest and conversion in North America. *Journal of Geophysical Research* 116: G00K03. doi:10.1029/2010JG001471.

Masek, J.G., C. Huang, R. Wolfe, W. Cohen, F. Hall, J. Kutler, and P. Nelson. 2008. North American forest disturbance mapped from a decadal Landsat record. *Remote Sensing of Environment* 112(6): 2914–2926. doi:10.1016/j.rse.2008.02.010.

Mayaux, P., H. Eva, A. Brink, F. Achard, and A. Belward. 2008. Remote sensing of land-cover and land-use dynamics. In *Earth Observation of Global Change: The Role of Satellite Remote Sensing in Monitoring the Global Environment*, 85–108. doi:10.1007/978-1-4020-6358-9_5.

McKinley, D.C., M.G. Ryan, R.A. Birdsey, C.P. Giardina, M.E. Harmon, L.S. Heath, R.A. Houghton, et al. 2011. A synthesis of current knowledge on forests and carbon storage in the United States. *Ecological Applications* 21(6): 1902–1924. doi:10.1890/10-0697.1.

Melendez, K.V., D.L. Jones, and A.S. Feng. 2006. Classification of communication signals of the little brown bat. *The Journal of the Acoustical Society of America* 120(2): 1095–1102. doi:10.1121/1.2211488.

Nabuurs, G.J., O. Masera, K. Andrasko, P. Benitez-Ponce, R. Boer, M. Dutschke, E. Elsiddig, et al. 2007. Forestry: In Climate Change 2007: Mitigation. Contribution of Working Group III to the Fourth Assessment Report of the Intergovernmental Panel on Climate Change. Edited by B. Metz, O.R. Davidson, P.R. Bosch, R. Dave, and L.A. Meyer. United Kingdom and New York, NY, USA: Cambridge University Press, Cambridge.

Natural Resources Canada. 2014. *The State of Canada's Forests: Annual Report 2014*. Natural Resources Canada.

Nielsen, A.A., K. Conradsen, and J.J. Simpson. 1998. Multivariate Alteration Detection (MAD) and MAF postprocessing in multispectral, bitemporal image data: New approaches to change detection studies. *Remote Sensing of Environment* 64(1): 1–19. doi:10.1016/S0034-4257(97)00162-4.

Ojima, D.S., W.J. Parton, D.S. Schimel, and C.E. Owensby. 1990. Simulated impacts of annual burning on prairie ecosystems. In *Fire in North American Prairies*, edited by S.L. Collins and L. Wallance. University of Oklahoma Press, Norman, OK.

Okabe, A., B. Boots, K. Sugihara, and S.N. Chiu. 2000. *Spatial Tessellations: Concepts and Applications of Voronoi Diagrams*. John Wiley & Sons.

Olguín, M., W.A. Kurz, B. de Jong, F. Paz, G. Ángeles, C. Zermeño, and R Flores. 2011. Hacia el uso del modelo CBM-CFS3 a Escala Nacional en México: Proyecto Piloto Chiapas. In *Memorias del III Simposio Internacional del Carbono en México*. Baja California, Mexico.

Olguín, M., C. Wayson, W.A. Kurz., M. Fellows, V. Maldonado, D. López, G. Ángeles, O. Carrillo, and V.S. Mascorro. 2015. *Adaptation of the CBM-CFS3 Modeling Framework to Mexico: Towards a Tier 3 Reporting in Strategic Landscapes for REDD+*. Mexico City, Mexico: Mexico-Norway Project of the National Forestry Commission of Mexico.

Olofsson, Pontus, Giles M. Foody, Martin Herold, Stephen V. Stehman, Curtis E. Woodcock, and Michael A. Wulder. 2014. Remote sensing of environment good practices for estimating area and assessing accuracy of land change. *Remote Sensing of Environment* 148: 42–57. doi:10.1016/j.rse.2014.02.015.

Oswalt, S.N., W.B. Smith, P.D. Miles, and S.A. Pugh. 2014. Forest Resources of the United States, 2012: A Technical Document Supporting the Forest Service 2015 Update of the RPA Assessment. Gen. Tech. Rep. WO-91. US Department of Agriculture, US Forest Service, Washington Office. Washington, DC

Pan, Y, R.A. Birdsey, J. Fang, R. Houghton, P.E. Kauppi, W.A. Kurz, O.L. Phillips, et al. 2011. A large and persistent carbon sink in the world's forests. *Science* 333(6045): 988–93. doi:10.1126/science.1201609.

Pan, Y, J.M. Chen, R.A. Birdsey, K. McCullough, L. He, and F. Deng. 2011. Age structure and disturbance legacy of North American forests. *Biogeosciences* 8(3): 715–32. doi:10.5194/bg-8-715-2011.

Perez-Garcia, J., B. Lippke, J. Comnick, and C. Manriquez. 2005. An assessment of carbon pools, storage, and wood products market substitution using life-cycle analysis results. *Wood and Fiber Science* 37 (Corrim Special Issue): 140–48.

Perry, E., G. Velazquez-Oliman, and R.A. Socki. 2003. Hydrogeology of the Yucatan Peninsula. In *The Lowland Maya: Three Millennia at the Human-Wildland Interface*. Edited by A. Gómez-Pompa, M.F. Allen, S.L. Fedick, and J. Jiménez-Osornio, 115–34. Binghampton, NY: The Haworth Press Inc.

Pouliot, D., R. Latifovic, N. Zabcic, L. Guindon, and I. Olthof. 2014. Development and assessment of a 250m spatial resolution MODIS annual land cover time series (2000-2011) for the forest region of Canada derived from change-based updating. *Remote Sensing of Environment* 140: 731–43. doi:10.1016/j.rse.2013.10.004.

Raymond, C.L., S. Healey, A. Peduzzi, and P. Patterson. 2015. Representative regional models of post-disturbance forest carbon accumulation: Integrating inventory data and a growth and yield model. *Forest Ecology and Management* 336(1): 21–34. doi:10.1016/j.foreco.2014.09.038.

Roy, D.P., J. Ju, K. Kline, P.L. Scaramuzza, V. Kovalskyy, M. Hansen, T.R. Loveland, E. Vermote, and C. Zhang. 2010. Web-enabled Landsat Data (WELD): Landsat ETM+ composited mosaics of the conterminous United States. *Remote Sensing of Environment* 114(1): 35–49. doi:10.1016/j.rse.2009.08.011.

Ruefenacht, B., M.V. Finco, M.D. Nelson, R. Czaplewski, E.H. Helmer, J.A. Blackard, G.R. Holden, A.J. Lister, D. Salajanu, D. Weyermann, and K. Winterberger. 2008. Conterminous US and Alaska forest type mapping using forest inventory and analysis data. *Photogrammetric Engineering & Remote Sensing* 74(11): 1379–1388.

Russell, M.B., S. Fraver, T. Aakala, J.H. Gove, C.W. Woodall, A.W. D'Amato, and M.J. Ducey. 2015. Quantifying carbon stores and decomposition in dead wood: A review. *Forest Ecology and Management* 350: 107–28. doi:10.1016/j.foreco.2015.04.033.

Saatchi, S.S, N.L. Harris, S. Brown, M. Lefsky, E.T.A. Mitchard, W. Salas, B.R. Zutta, et al. 2011. Benchmark map of forest carbon stocks in tropical regions across three continents. *Proceedings of the National Academy of Sciences of the United States of America* 108 (24): 9899–9904. doi:10.1073/pnas.1019576108.

Schlamadinger, B., and G. Marland. 1996. The role of forest and bioenergy strategies in the global carbon cycle. *Biomass and Bioenergy* 10:275–300. doi:10.1016/0961-9534(95)00113-1.

Schulze, E.D., and M. Heimann. 1998. Carbon and water exchange of terrestrial systems. In *Asian Change in the Context of Global Change*. Edited by J.N. Galloway and J. Melillo, 145–61. Cambridge: Cambridge University Press.

Shaw, C.H., A.B. Hilger, J. Metsaranta, W.A. Kurz, G. Russo, F. Eichel, G. Stinson, C. Smyth, and M. Filiatrault. 2014. Evaluation of simulated estimates of forest ecosystem carbon stocks using ground plot data from Canada's National Forest Inventory. *Ecological Modelling* 272: 323–347. doi:10.1016/j.ecolmodel.2013.10.005.

Skog, K.E. 2008. Sequestration of carbon in harvested wood products for the United States. *Forest Products Journal* 58(6): 56–72.

Smith, J.E., L.S. Heath, and M.C. Nichols. 2007. *US Forest Carbon Calculation Tool: Forest-Land Carbon Stocks and Net Annual Stock Change*. Newtown Square, PA, US: US Department of Agriculture, US Forest Service, Northern Research Station.

Smyth, C.E., G. Stinson, E. Neilson, T.C. Lemprière, M. Hafer, G.J. Rampley, and W.A. Kurz. 2014. Quantifying the biophysical climate change mitigation potential of Canada's forest sector. *Biogeosciences* 11(13): 3515–29. doi:10.5194/bg-11-3515-2014.

Spalding, D., E. Kendirli, and C.D. Oliver. 2011. The role of forests in global carbon budgeting. In *Managing Forest Carbon in a Changing Climate*. Edited by M.S. Ashton, M.L. Tyrrell, D. Spalding, and B. Gentry, 165–179. Springer.

Stange, F., K. Butterbach-Bahl, H. Papen, S. Zechmeister-Boltenstern, C.S. Li, and J. Aber. 2000. A process-oriented model of N_2O and NO Emissions from Forest Soils 2. Sensitivity analysis and validation. *Journal of Geophysical Research-Atmospheres* 105(D4): 4385–98. doi:10.1029/1999JD900948.

Stinson, G., W.A. Kurz, C.E. Smyth, E.T. Neilson, C.C. Dymond, J.M. Metsaranta, C. Boisvenue, et al. 2011. An inventory-based analysis of Canada's managed forest carbon dynamics, 1990 to 2008. *Global Change Biology* 17(6): 2227–2244. doi:10.1111/j.1365-2486.2010.02369.x.

Thornton, P.E., S.W. Running, and E.R. Hunt. 2005. Biome-BGC: Terrestrial Ecosystem Process Model, Version 4.1.1. Available online [http://www.daac.ornl.gov] from Oak Ridge National Laboratory Distributed Active Archive Center, Oak Ridge, Tennessee, US. doi:10.3334/ORNLDAAC/805.

Turner, M. 1989. Landscape ecology: The effect of pattern on process. *Annual Review of Ecology and Systematics* 20(1): 171–97. doi:10.1146/annurev.ecolsys.20.1.171.

US EPA. 2010. *Inventory of US Greenhouse Gas Emissions and Sinks: 1990-2009*. Washington, DC, US Environmental Protection Agency.

US EPA. 2014. *Inventory of US Greenhouse Gas Emissions and Sinks: 1990-2012*. Washington, DC, US Environmental Protection Agency.

US Forest Service. 2010. *Major Forest Insect and Disease Conditions in the United States: 2009 Update*. Washington, DC: US Dept. of Agriculture, US Forest Service.

Verbesselt, Jan, Rob Hyndman, Glenn Newnham, and Darius Culvenor. 2010. Detecting trend and seasonal changes in satellite image time series. *Remote Sensing of Environment* 114(1): 106–15. doi:10.1016/j.rse.2009.08.014.

Wang, Z., R. F. Grant, M. A. Arain, B. N. Chen, N. Coops, R. Hember, W. A. Kurz, et al. 2011. Evaluating weather effects on interannual variation in net ecosystem productivity of a coastal temperate forest landscape: A model intercomparison. *Ecological Modelling* 222(17): 3236–3249. doi:10.1016/j.ecolmodel.2011.06.005.

Wayson, C.A., K.D. Johnson, J.A. Cole, M.I. Olguín, O.I. Carrillo, and R.A Birdsey. 2014. Estimating uncertainty of allometric biomass equations with incomplete fit error information using a pseudo-data approach: Methods. *Annals of Forest Science* 72(6): 825-834. doi:10.1007/s13595-014-0436-7.

Werner, F., R. Taverna, P. Hofer, E. Thürig, and E. Kaufmann. 2010. National and global greenhouse gas dynamics of different forest management and wood use scenarios: A Model-based assessment. *Environmental Science and Policy* 13(1): 72–85. doi:10.1016/j.envsci.2009.10.004.

Wieder, W.R., C.C. Cleveland, W. K. Smith, and K. Todd-Brown. 2015. Future productivity and carbon storage limited by terrestrial nutrient availability. *Nature Geoscience* 8: 441–444. doi:10.1038/ngeo2413.

Woodall, C.W., L.S. Heath, and J.E. Smith. 2008. National inventories of down and dead woody material forest carbon stocks in the United States: Challenges and opportunities. *Forest Ecology and Management* 256(3): 221–28. doi:10.1016/j.foreco.2008.04.003.

Wulder, M.A., J.C. White, R.A. Fournier, J.E. Luther, and S. Magnussen. 2008. Spatially explicit large area biomass estimation: Three approaches using forest inventory and remotely sensed imagery in a GIS. *Sensors* 8(1): 529–560. doi:10.3390/s8010529.

Wulder, M.A., J.C. White, M.D. Gillis, N. Walsworth, M.C. Hansen, and P. Potapov. 2010. Multiscale satellite and spatial information and analysis framework in support of a large-area forest monitoring and inventory update. *Environmental Monitoring and Assessment* 170(1-4): 417–433. doi:10.1007/s10661-009-1243-8.

Yanai, R.D., J.J. Battles, A.D. Richardson, C.A. Blodgett, D.M. Wood, and E.B. Rastetter. 2010. Estimating uncertainty in ecosystem budget calculations. *Ecosystems* 13(2): 239–48. doi:10.1007/s10021-010-9315-8.

Zhang, F., J.M. Chen, Y. Pan, R.A. Birdsey, S. Shen, W. Ju, and L. He. 2012. Attributing carbon changes in conterminous US Forests to disturbance and non-disturbance factors from 1901 to 2010. *Journal of Geophysical Research: Biogeosciences* 117 (G02021): 1–18. doi:10.1029/2011JG001930.

Zhu, Z., and C.E. Woodcock. 2012. Object-based cloud and cloud shadow detection in Landsat imagery. *Remote Sensing of Environment* 118: 83–94. doi:10.1016/j.rse.2011.10.028.